Functional Characterization of the LCMV GP-C Signal Peptide

Sabrina Schrempf

2008

INAUGURAL - DISSERTATION

submitted to the
Combined Faculties for the Natural Sciences and for Mathematics
of the Ruperto-Carola University of Heidelberg
for the degree of
Doctor of Natural Sciences

presented by
Diplom-Biochemikerin Sabrina Schrempf
from Gelnhausen

Date of oral examination: .....

Functional Characterization of the LCMV GP-C Signal Peptide

Referees:
Prof. Dr. Bernhard Dobberstein
Prof. Dr. Irmgard Sinning

Für Oliver,
der mich immer auffängt
und
für meine Eltern,
die mich stets unterstützen.

Abstract

N-terminal signal sequences of secretory and membrane proteins mediate targeting to and translocation across the endoplasmic reticulum (ER) membrane. After membrane insertion, signal sequences are in most cases cleaved from the precursor protein by signal peptidase (SPase). Signal sequences are usually 15 to 25 amino acid residues in length and have a typical tripartite structure with a central hydrophobic core of about 7 to 10 residues, a polar N-terminal region, and a short C-terminal region which contains the SPase cleavage site.

Insertion of the lymphocytic choriomeningitis virus (LCMV) precursor glycoprotein C (pGP-C) into the membrane of the ER is mediated by an unusual signal sequence. It comprises 58 amino acid residues and contains an extended N-terminal region including a myristoylation consensus site and two hydrophobic regions separated by a lysine residue. After cleavage by SPase, the resulting signal peptide (SP^{GP-C}) accumulates in cells and virus particles.

The aim of this study was to characterize the post-targeting functions of the LCMV SP^{GP-C}. It could be shown that the LCMV SP^{GP-C} is an essential component of the glycoprotein complex and that different regions of SP^{GP-C} are required for distinct steps in glycoprotein maturation and virus infectivity.

The investigation of SP^{GP-C} deletion mutants showed that one hydrophobic region of LCMV SP^{GP-C} is sufficient for ER membrane insertion of GP-C, while both hydrophobic regions are required for GP-C processing into its subunits and cell surface expression of the glycoprotein complex. The N-terminal region of SP^{GP-C} and its myristoylation are dispensable for these steps in GP-C maturation, however, were found to be essential for viral infection of target cells. The analysis of a possible association of LCMV SP^{GP-C} with GP-C by co-immunoprecipitation revealed that the LCMV SP^{GP-C} is part of the glycoprotein complex and interacts with the membrane-anchored GP-2 subunit. For this non-covalent interaction the hydrophobic regions of SP^{GP-C} are sufficient and essential, whereas the N-terminal region is not required.

As the LCMV SP^{GP-C} possesses two hydrophobic regions, different topologies across the membrane are conceivable. The membrane topology of SP^{GP-C} was investigated using point mutations introducing potential N-glycosylation sites throughout the SP^{GP-C}. It could be shown that unmyristoylated SP^{GP-C} exposes its N-terminal region to the exoplasmic side of the membrane. This SP^{GP-C} can promote GP-C maturation but is defective in viral infection. Myristoylation and SP^{GP-C} membrane topology may thus hold the key to unravel the role of LCMV SP^{GP-C} in GP-C complex assembly and function.

Zusammenfassung

N-terminale Signalsequenzen von sekretorischen Proteinen und von Membranproteinen vermitteln den zielgerichteten Transport zum endoplasmatischen Retikulum (ER) und die Translokation der Proteine durch die ER-Membran. In den meisten Fällen wird die Signalsequenz nach der Membraninsertion durch die Signalpeptidase (SPase) vom Präprotein abgespalten. Signalsequenzen besitzen üblicherweise eine Gesamtlänge von 15 bis 25 Aminosäuren und sind in drei Regionen unterteilt: einen zentralen hydrophoben Kern bestehend aus 7 bis 10 Aminosäuren, einer polaren N-terminalen Region und einer kurzen C-terminalen Region, die die SPase Spaltstelle beinhaltet.

Die Insertion des lymphozytären Choriomeningitis Virus (LCMV) Glykoproteins (pGP-C) in die Membran des ER wird durch eine ungewöhnliche Signalsequenz vermittelt. Diese Signalsequenz besteht aus 58 Aminosäuren und besitzt eine erweiterte N-terminale Region einschließlich einer Konsensussequenz für Myristoylierung und zwei hydrophobe Regionen, die durch ein Lysin getrennt sind. Nach der Abspaltung durch die SPase akkumuliert das resultierende Signalpeptid (SP^{GP-C}) in Zellen und in Viruspartikeln.
Ziel der vorliegenden Arbeit war die Charakterisierung der Funktionen des LCMV SP^{GP-C} über den zielgerichteten Transport hinaus. Es konnte gezeigt werden, dass das LCMV SP^{GP-C} ein essentieller Bestandteil des Glykoproteinkomplexes ist und dass die unterschiedlichen Regionen des SP^{GP-C} für verschiedene Schritte während der GP-C-Reifung und für die Infektiosität des Virus benötigt werden.
Die Untersuchung von SP^{GP-C} Deletionsmutanten zeigte, dass eine hydrophobe Region des LCMV SP^{GP-C} für die Insertion von GP-C in die ER-Membran genügt, wohingegen beide hydrophobe Regionen für die Prozessierung von GP-C in seine Untereinheiten und für den Transport des Glykoproteinkomplexes zur Zelloberfläche benötigt werden. Die N-terminale Region des SP^{GP-C} und dessen Myristoylierung werden für diese Schritte der GP-C-Reifung nicht benötigt, sind jedoch essentiell für die virale Infektion von Zielzellen.
Die Analyse einer möglichen Assoziierung des SP^{GP-C} mit GP-C durch Koimmunopräzipitation zeigte, dass das LCMV SP^{GP-C} ein Bestandteil des Glykoproteinkomplexes ist und dass es mit der membranverankerten GP-2 Untereinheit interagiert. Die hydrophoben Regionen des SP^{GP-C} sind für diese nichtkovalente Interaktion ausreichend und essentiell, wohingegen die N-terminale Region nicht benötigt wird.
Aufgrund der zwei hydrophoben Regionen des LCMV SP^{GP-C} sind verschiedene Topologien in der Membran vorstellbar. Zur Untersuchung wurden potenzielle N-Glykosylierungsstellen durch Punktmutationen in SP^{GP-C} eingefügt. Es konnte gezeigt werden, dass sich die N-terminale Region des nicht-myristoylierten SP^{GP-C} auf der exoplasmatischen Seite der Membran befindet. Dieses SP^{GP-C} ist fähig die GP-C-Reifung zu begünstigen, verhindert jedoch die virale Infektion. Die Myristoylierung und die Topologie des SP^{GP-C} könnten daher den Schlüssel zur Funktion des SP^{GP-C} innerhalb des Glykoproteinkomplexes darstellen.

Contents

1 Introduction

1.1 Signal sequences

1.1.1 Protein sorting in eukaryotic cells

A typical eukaryotic cell is compartmentalized into functionally distinct, membrane-enclosed organelles, like the nucleus, the endoplasmic reticulum (ER), the Golgi apparatus, mitochondria, chloroplasts, peroxisomes, and lysosomes. All of these organelles contain a characteristic set of proteins in order to fulfill their specific functions. Almost all of these proteins are synthesized on cytosolic ribosomes and have to cross at least one membrane to reach their final destination in the cell (Blobel, 1980; Verner and Schatz, 1988; Schatz and Dobberstein, 1996). Proteins that are destined for a certain compartment in the cell are targeted to these compartments by specific sorting signals that are recognized by complementary receptor proteins (Gierasch, 1989). Proteins that do not have a sorting signal remain in the cytosol.

After synthesized in the cytosol, nuclear proteins are selectively imported into the nucleus through the nuclear pore complexes which function as selective gates between topologically equivalent spaces. The selectivity of this nuclear import process resides in nuclear localization signals. In many nuclear proteins these signals consist of one or two short amino acid sequences that are rich in the positively charged amino acids lysine and arginine (Görlich and Kutay, 1999; Kalderon et al., 1984; Lanford and Butel, 1984).

Protein import into mitochondria, chloroplasts, peroxisomes and into the ER involves membrane-bound protein translocators that transport proteins across a membrane. Most of the mitochondrial and chloroplast proteins have an N-terminal signal that is recognized by cytosolic chaperones which prevent proteins from aggregation or folding and guide the proteins to their respective organelle. Peroxisomal proteins contain short signal sequences and are selectively imported in a fully folded conformation (Alberts et al., 2002; Dalbey and von Heijne, 2003). Proteins targeted to the mitochondria, chloroplasts or peroxisomes are synthesized on free ribosomes in the cytosol before being post-translationally translocated into their target organelle. In contrast, proteins targeted to the ER can be translocated co-translationally, i.e. during synthesis on ER membrane-bound ribosomes, or post-translationally (Rapoport, 2007; Rapoport et al., 1999). The proteins initially targeted to the ER include secretory proteins and proteins destined for the ER, Golgi apparatus, lysosomes, or the plasma membrane. The co-translational translocation of proteins into the ER through the translocon, formed by the Sec61 complex, is usually

mediated by an N-terminal signal sequence that is recognized by the signal recognition particle (SRP) (Johnson and van Waes, 1999; Rapoport, 2007; Walter and Blobel, 1981; Walter and Johnson, 1994). While the polypeptide chain passes through the translocon, the N-terminal signal sequences of soluble proteins and type I membrane proteins are cleaved by signal peptidase (SPase) (Blobel and Dobberstein, 1975; Paetzel et al., 2002). Protein targeting to the ER is not exclusively done by N-terminal signal sequences. Membrane proteins can also be targeted to the ER by internal signal sequences. These internal signal sequences are also recognized by SRP and inserted into the translocon but in contrast to N-terminal signal sequences they are not cleaved by SPase. Like a transmembrane domain, the internal signal sequences exit the translocon laterally thereby anchoring the protein in the ER membrane (Johnson and van Waes, 1999; Martoglio et al., 1995).
From the ER, proteins are transported in vesicles to the Golgi apparatus, where they are sorted for transport to lysosomes, the plasma membrane, or secretion from the cell. Proteins that function within the ER or the Golgi apparatus were retained in the respective organelle (Alberts et al., 2002; Cooper, 2000).

1.1.2 Protein translocation across the ER membrane

In mammalian cells, most proteins translocate into the ER in a co-translational and SRP-dependent manner. The co-translational translocation is initiated by binding of SRP to the signal sequence of a growing polypeptide chain emerging from the ribosome (Luirink and Sinning, 2004). SRP is a ribonucleoprotein consisting of a single small RNA molecule (7S RNA) and six different polypeptides (Keenan et al., 2001; Walter and Blobel, 1982). The signal sequence recognition is mediated by the SRP54 subunit of SRP. Formation of the ribosome-nascent-chain-SRP complex leads to an elongation arrest mediated by binding of the SRP Alu domain at the ribosomal subunit interface (Terzi et al., 2004). The entire complex is targeted to the rough ER via interaction with the SRP receptor (Gilmore et al., 1982; Meyer and Dobberstein, 1980). The SRP receptor is composed of a peripheral (SRα) and a membrane-anchored subunit (SRβ) (Tajima et al., 1986). The GTP-dependent interaction of SRP with the SRP receptor results in the release of SRP and transfer of the ribosome-nascent-chain complex to the translocon (Connolly and Gilmore, 1989; Pool et al., 2002). This allows translation to resume and translocation of the elongating nascent chain through the channel across the ER membrane (Johnson and van Waes, 1999; Pool, 2003). Co-translationally the signal sequence is usually cleaved from the preprotein by SPase (Paetzel et al., 2002) and the growing polypeptide chain can get glycosylated at asparagine residues in the consensus sequence N-X-T/S by the oligosaccharyl transferase in the ER lumen. As translation proceeds and after the release of the polypeptide chain into the ER lumen, the polypeptide is folded in its three-dimensional conformation with the help of molecular chaperones like

BiP and the protein disulfide isomerase which catalyzes the formation of disulfide bonds. In addition to protein folding, the assembly of multisubunit proteins takes place within the ER lumen. Correctly folded proteins are subsequently exported from the ER, further modified in the Golgi apparatus and transported in vesicles to their final destination (Alberts et al., 2002; Cooper, 2000; Ellgaard and Helenius, 2003). ER resident proteins contain an ER retention or retrieval signal to ensure their proper localization (Michelsen et al., 2005; Nilsson and Warren, 1994).

Membrane proteins are only partially translocated across the ER membrane having one or more transmembrane regions that span the phospholipid bilayer and hydrophilic regions exposed to the ER lumen and to the cytosol. Co-translationally inserted membrane proteins are targeting to the ER either by N-terminal or internal signal sequences in a SRP-dependent manner as described above (Rapoport, 2007). Membrane proteins with an N-terminal signal sequence are anchored in the lipid bilayer by a so-called stop-transfer sequence after the signal sequence has been cleaved. By a lateral gating mechanism the stop-transfer sequence exits the translocation channel leaving the N-terminus of the polypeptide chain in the ER lumen while the C-terminus is exposed to the cytosol (type I membrane protein) (Martoglio et al., 1995). Proteins that are anchored in the membrane by an internal signal sequence can adopt two different topologies in the lipid bilayer with either the N-terminus or the C-terminus facing the cytosol. The topology of the proteins in the membrane is determined by the orientation of the internal signal sequence within the translocon which depends on the distribution of charged amino acid residues in proximity to the membrane anchor. Positively charged amino acids are indicators for a cytosolic localization of segments flanking the transmembrane anchor ("positive-inside rule") (Sipos and von Heijne, 1993; Goder et al., 2004). The membrane insertion of multispanning membrane proteins is thought to be mediated by an alternating series of internal signal sequences and stop-transfer sequences (High and Dobberstein, 1992; Higy et al., 2004; Rapoport et al., 2004).

Not all proteins enter the ER co-translationally. Some proteins are synthesized in the cytosol, targeted to the ER independent of SRP and are post-translationally translocated across the ER membrane (Rapoport et al., 1999). Post-translational protein translocation is known for many yeast proteins but only for a few mammalian proteins. After synthesis of these proteins in the cytosol, chaperones are needed to maintain the polypeptide chain in an unfolded conformation. Targeting to the ER is mediated by a moderately hydrophobic signal sequence that is recognized by the Sec62/63 complex which is associated with the translocation channel in the ER membrane (Meyer et al., 2000). Translocation of the polypeptide chain is thought to be driven by cycles of binding and release of the ER lumenal chaperone BiP (Lyman and Schekman, 1997; Matlack et al., 1999; Sanders et al., 1992).

1.1.3 The structure of N-terminal ER signal sequences

N-terminal signal sequences that target secretory and membrane proteins to the ER show great variations in their amino acid sequence and overall length (Martoglio and Dobberstein, 1998). In general, they consist of about 15 to 25 amino acid residues and have a tripartite structure with a central hydrophobic core that is flanked by a polar N-terminal region and a short C-terminal region (Figure 1.1) (von Heijne, 1990). The hydrophobic core is the most characteristic feature of N-terminal signal sequences and is about 7 to 10 amino acid residues in length. This so-called h-region is the recognition site for SRP and essential for ER targeting and membrane translocation (von Heijne, 1985). The region N-terminally of the hydrophobic core, the n-region, is extremely variable in its length and amino acid composition, but usually has a positive net charge. On its C-terminal side, the h-region is flanked by the short c-region that contains the consensus sequence for SPase cleavage. The c-region usually consists of about 2 to 9 amino acids and often contains helix breaking proline and glycine residues. The SPase cleavage site is determined by small, uncharged amino acid residues at the -3 and -1 positions relative to the cleavage site. A proline residue at the +1 position is not tolerated (von Heijne, 1983).

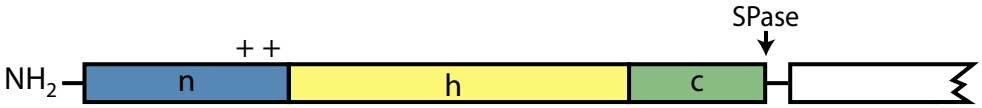

Figure 1.1: Schematic representation of an N-terminal signal sequence for ER targeting
N-terminal ER signal sequences have a typical tripartite structure with a polar N-terminal region (n-region), a central hydrophobic region (h-region), and a short C-terminal region (c-region). The overall length of a typical signal sequence is about 15 - 25 amino acid residues containing an h-region of about 7 - 10 residues. The SPase cleavage site and the positive net charge of the n-region (+) are indicated.

After the N-terminal signal sequence emerges from the ribosome, SRP binds to the h-region and translation is stopped (Walter and Blobel, 1981). Upon binding to the SRP receptor, the ribosome-nascent-chain complex is transferred to the translocon and translation resumes (Johnson and van Waes, 1999). Membrane insertion in the translocating channel is thought to occur in a loop-like fashion such that the N-terminus of the signal sequence is exposed on the cytoplasmic side and the cleavage site for SPase on the lumenal side of the ER membrane (Walter et al., 1984). The SPase of mammalian cells consists of five different subunits with the active site located near the membrane surface on the lumenal side of the ER membrane (Dalbey and von Heijne, 1992; Paetzel et al., 2002). After co-translational cleavage of the signal sequence by SPase, the N-terminus of the resulting signal peptide (SP) thus would face the cytosol while the c-region remains in the ER lumen.

1.1.4 Functions of signal sequences beyond ER targeting

Cleavage of N-terminal ER signal sequences by SPase results in the release of the so-called signal peptides (SPs) which are supposed to be directly degraded by a yet unknown mechanism. A growing number of signal peptides, however, are found not to be degraded but to stay membrane-inserted, to be liberated from the ER membrane or to be further processed by an intramembrane cleaving protease, which results in the release of SP fragments from the lipid bilayer (Martoglio, 2003). These released SP fragments as well as membrane-inserted or liberated full length signal peptides are known to have diverse functions beyond ER targeting (Hegde and Bernstein, 2006).

Signal peptide processing and the release of bioactive signal peptide fragments

After the initial cleavage by SPase, signal peptides can undergo intramembrane proteolysis. This processing is mediated by the signal peptide peptidase (SPP) which belongs to the family of intramembrane cleaving proteases (I-Clip) (Weihofen et al., 2002). SPP cleavage within the transmembrane region of signal peptides results in the release of SP fragments from the ER membrane (Lemberg and Martoglio, 2002). Some of these released SP fragments are known to have post-targeting functions and thus act as so-called bioactive peptides (Martoglio, 2003; Weihofen and Martoglio, 2003).

The first known process that depends on SPP processing is the generation of HLA-E epitopes in humans (Lemberg et al., 2001). The signal sequences of the MHC class I molecules HLA-A, -B, -C, and -G contain a highly conserved segment within their N-terminal portion, which serves as an epitope for the presentation by the non-classical antigen presenting molecule HLA-E (Braud et al., 1997). During biosynthesis of MHC class I molecules the signal sequence is first cleaved by SPase and then further processed by SPP. The generated epitope-containing N-terminal fragment is subsequently released from the ER membrane into the cytosol and after further trimming transported into the ER lumen via the TAP transporter where it is loaded on to the HLA-E molecules (Lemberg et al., 2001). The presentation of peptide-loaded HLA-E molecules on the cell surface serves as an inhibitory signal to natural killer cells reporting proper biosynthesis of MHC class I molecules (Braud et al., 1998).
Another well characterized substrate for SPP is the signal peptide of prolactin, a peptide hormone. Upon processing by SPP, the N-terminal SP fragment is released into the cytosol where it binds to calmodulin in a calcium-dependent manner *in vitro* (Lyko et al., 1995; Martoglio et al., 1997). Similar to prolactin, a SP fragment derived from the human immunodeficiency virus 1 (HIV-1) envelope protein gp160 interacts with calmodulin after release from the ER membrane (Martoglio et al., 1997).

A further example for SPP processing is the maturation of the hepatitis C virus (HCV) core protein. The core protein is synthesized as the most N-terminal component of the HCV polyprotein and is followed by the signal sequence of the envelope glycoprotein. This signal sequence targets the polyprotein to the ER and is subsequently cleaved by SPase leaving the core protein anchored in the ER membrane by the signal peptide. Further processing by SPP results in the release of the mature core protein from the ER membrane (McLauchlan et al., 2002).

So far the physiological role of SPP is not completely understood (Crawshaw et al., 2004; Loureiro et al., 2006; Weihofen et al., 2002). It is conceivable that the major function of SPP is the release of bioactive peptides from the ER membrane (Martoglio, 2003; Weihofen and Martoglio, 2003). However, one cannot exclude a role for SPP in signal peptide and membrane protein degradation (Loureiro et al., 2006).

Further functions of full length signal peptides

Besides the post-targeting role of signal peptides after SPP processing, some signal peptides remain membrane-inserted or are liberated from the ER membrane without further processing to promote their post-targeting functions. In this context mainly signal peptides of viral proteins are so far found to have functions beyond ER targeting.

The signal peptide of the envelope protein of the mouse mammary tumor virus (MMTV), for example, was found to accumulate in nucleoli (Hoch Marchaim et al., 2003). The MMTV envelope signal peptide comprises 98 amino acid residues and contains a nuclear localization signal within its extended n-region. After ER insertion and SPase cleavage, the signal peptide initially accumulates in the ER membrane and is subsequently released into the cytosol in an SPP-independent manner (Dultz et al., 2008). Due to the nuclear localization signal, the signal peptide of the MMTV envelope protein is able to enter the nucleus and was shown to be sufficient to mediate the export of intron-containing RNA transcripts (Mertz et al., 2005).

Other viral signal peptides mediate post-targeting functions that are essential for the viral life cycle as membrane-inserted signal peptides. The signal peptide of the foamy virus envelope glycoprotein, for example, is an essential component of infectious viral particles and is required for particle budding (Lindemann et al., 2001). The need for the signal peptide during foamy virus morphogenesis is due to an interaction between the signal peptide n-region with the N-terminal region of the viral capsid protein Gag (Wilk et al., 2001). While the N-terminus of the extended signal peptide n-region mediates the interaction with the foamy virus capsid, it is dispensable for ER targeting of the envelope glycoprotein (Lindemann et al., 2001).

The unusually long signal peptides of several arenaviral glycoproteins (LCMV, Lassa and Junín virus) also remain membrane-inserted after SPase cleavage and mediate post-targeting functions (Eichler et al., 2003b; Froeschke et al., 2003; York et al., 2004). These highly conserved signal peptides contain an extended n-region with a myristoylation consensus site and two h-regions separated by basic amino acid residues. The signal peptide of the Lassa virus glycoprotein, for example, was shown to be essential for proteolytic maturation of the glycoprotein and performs this function even in *trans* (Eichler et al., 2003a). For the signal peptide of the lymphocytic choriomeningitis virus (LCMV) glycoprotein it was shown that it is actually incorporated into virus particles (Froeschke et al., 2003). The function of the signal peptide in the virus particle as well as the role of the LCMV signal peptide during glycoprotein maturation were not known so far. The post-targeting functions of the signal peptide of the LCMV glycoprotein are subject of this study.

1.2 Viral glycoproteins

Enveloped viruses enter their target cell by fusing the viral membrane with a host cell membrane (Kielian and Rey, 2006; Söllner, 2004). This initial step in the viral replication cycle is mediated by the viral envelope glycoproteins and includes receptor recognition and membrane fusion activity. In addition to the function of the viral glycoproteins during virus entry, they determine for most enveloped viruses the location within the cell at which budding takes place (Garoff et al., 1998; Knipe and Howley, 2001). To achieve the correct localization within a cell, the viral glycoproteins take advantage of the cellular sorting pathways. For this purpose they have adopted many targeting signals found in cellular proteins (Compans et al., 2004).

1.2.1 Trafficking of viral glycoproteins and virus budding

Viral glycoproteins are targeted to the ER by N-terminal or internal signal sequences and are co-translationally inserted into the ER membrane. During synthesis, the polypeptide chain can get glycosylated at asparagine residues in the consensus sequence N-X-T/S by the oligosaccharyl transferase in the ER lumen. Correctly folded and assembled proteins are subsequently transported to the site in the cell where budding occurs (Garoff et al., 1998). This transport may include further protein maturation events, for example, the modification of glycosylation or proteolytic processing. In many cases virus assembly takes place at the plasma membrane, but in others intracellular membranes, e.g. of the ER, the Golgi apparatus or the multivesicular bodies, are the sites where budding is initiated (Compans et al., 2004; Knipe and Howley, 2001).

The glycoproteins of viruses that bud from the plasma membrane travel along the secretory pathway to reach the cell surface. After protein synthesis, folding, and complex assembly, the viral glycoproteins have to pass the quality control in the ER before transit to the Golgi apparatus (Ellgaard and Helenius, 2003). The trafficking between the membrane compartments is mediated by specific transport vesicles. These vesicles are transiently coated with protein complexes that allow the selective transfer of the cargo proteins (Bonifacino and Glick, 2004; Bonifacino and Lippincott Schwartz, 2003; Kirchhausen, 2000). Transport vesicles that bud from the ER membrane are associated with the COP II coat complex, whereas COP I coats are associated with retrograde transport vesicles that bud from the Golgi apparatus membrane (Barlowe et al., 1994; Letourneur et al., 1994; Robinson, 1987). The viral glycoproteins enter the Golgi apparatus at the *cis* Golgi network and are subsequently transported through the Golgi stacks and end up in the *trans* Golgi network where further protein sorting takes place (Keller and Simons, 1997; Matsuura Tokita et al., 2006; Pelham, 2001). As the proteins pass through the Golgi the N-linked oligosaccharides added to the viral glycoproteins in the ER are further modified. In addition, some viral glycoproteins are proteolytically processed before they are transported to the plasma membrane. This processing is crucial for the generation of a functional glycoprotein complex (Kido et al., 1996; Kunz et al., 2003).
Virus assembly at the plasma membrane results in the release of the virus particles directly in the extracellular space. Viruses that bud on intracellular membranes are delivered into the lumen of the respective organelle and finally exit the cell by exocytosis (Compans et al., 2004; Knipe and Howley, 2001). For most enveloped viruses, with the exception of the retroviruses, the efficiency of virus budding depends on the presence of the viral glycoproteins (Klein et al., 2007; Resh, 2005). Budding is driven by the interaction of the viral glycoproteins with internal viral structures, e.g. viral nucleoproteins or matrix proteins, and/or by a lateral interaction between glycoprotein subunits (Garoff et al., 1998).

1.2.2 Membrane fusion mechanisms of viral glycoproteins

Enveloped viruses use different entry pathways to deliver their genome into the cytosol (Marsh and Helenius, 2006). Cell entry is a stepwise process where receptor binding is followed by the fusion of the viral and a host cell membrane. Virus membrane fusion can take place either at the plasma membrane or at intracellular membranes. Membrane fusion at the plasma membrane is triggered by the binding of the viral membrane glycoproteins to a specific cell surface receptor at neutral pH. By contrast, fusion at an intracellular membrane, after virus internalization by receptor-mediated endocytosis, is frequently induced by the low pH within the respective organelle (Jahn et al., 2003; Kielian and Rey, 2006; Söllner, 2004).

So far, two distinct classes of viral fusion proteins have been defined, class I (e.g. influenza and HIV) and class II (e.g. Semliki Forest virus and dengue virus), which differ in key structural features, but follow a similar membrane fusion mechanism. The functions of fusion proteins include pulling the fusing membranes towards one another, dehydrating the membranes, and creating membrane defects that lower the energy barrier for pore formation (Earp et al., 2005).
Class I fusion proteins are synthesized as fusion-inactive precursors that are processed by host-cell proteases. The two generated subunits, a peripheral and a transmembrane subunit, remain associated and are incorporated in the viral membrane as trimeric spikes (Colman and Lawrence, 2003). These prefusion trimers are maintained in a metastable, high-energy state at the virus surface. Upon initiation of membrane fusion the so-called fusion peptide, a critical hydrophobic sequence of the transmembrane subunit, inserts into the target membrane (Epand, 2003). Conformational rearrangements of the fusion protein bring the viral and the host cell membrane in close proximity, which results in membrane fusion (Earp et al., 2005; Eckert and Kim, 2001; Harrison, 2005). In the final lowest-energy form (postfusion form), class I fusion proteins contain six-helix-bundles (Bullough et al., 1994; Carr and Kim, 1993). The postfusion forms are often referred to as "trimers of hairpins" (Eckert and Kim, 2001).
The general structure of class II fusion proteins is quite different from that of class I fusion proteins. Class II fusion proteins exist in their prefusion state as dimers and undergo an oligomeric rearrangement during fusion. In addition, an internal fusion loop instead of a fusion peptide is inserted into the host cell membrane. Insertion of the fusion loop triggers the irreversible trimerization of the fusion proteins. Refolding of the trimers then pulls both membranes towards one another which is followed by membrane fusion (Kielian, 2006; Söllner, 2004).

In general, viral fusion is driven by protein refolding that is triggered by interactions with the target cell and/or by low pH (Earp et al., 2005). The energy needed to pull the fusing lipid bilayers towards one another seems to be stored in the metastable, high-energy state of the prefusion trimers respectively dimers and is released upon protein refolding (Carr et al., 1997; Kielian, 2006; Stiasny et al., 2001). Insertion of the fusion peptides/ loops into the target cell membrane links the two opposite membranes and the protein folding reactions brings the membranes in close proximity. Viral fusion peptides/loops are hydrophobic sequences usually enriched in alanine and glycine residues and have the capacity to destabilize the lipid bilayer (Earp et al., 2005; Epand, 2003; Nieva and Agirre, 2003). As the viral fusion peptides/loops do not penetrate the lipid bilayer it is thought that a fusion intermediate, the hemifusion stalk, is formed as a transition to the fusion pore (Söllner, 2004). The fusion peptide may not only be needed for anchoring the fusion protein to the target membrane but also assist in creating the hemifusion stalk and function in fusion pore opening (Tamm and Han, 2000).

1.3 The lymphocytic choriomeningitis virus

The lymphocytic choriomeningitis virus (LCMV) belongs to the very large family of arenaviruses which are rodent-borne, enveloped RNA viruses. The arenavirus family is subdivided into two major groups, the Old World species (e.g. LCMV and Lassa virus) and the New World species (e.g. Junín virus and Pichinde virus) (Clegg, 2002). Arenaviruses cause, usually asymptomatic, persistent infections of their natural rodent hosts. Infections of humans after contact with infected rodents are common and in some cases cause hemorrhagic fever syndromes (Buchmeier, 2002; Knipe and Howley, 2001).

1.3.1 Genome organization and structure of the viral particle

The arenavirus genome consists of two single-stranded RNA molecules, the S and L segment (Figure 1.2). Each segment is arranged in an ambisense orientation which directs the synthesis of two polypeptides in opposite orientation. The S RNA encodes the nucleocapsid protein (NP) in negative sense at the 3′-end and the viral glycoprotein C (GP-C) in genomic sense at the 5′-end (Auperin et al., 1984; Southern et al., 1987). Post-translational processing of GP-C yields the viral glycoproteins GP-1 and GP-2. The L RNA encodes the viral RNA-dependent RNA polymerase (L) in negative sense and a zinc-binding RING finger protein (Z) in genomic sense (Iapalucci et al., 1989; Salvato et al., 1989). The two proteins on each segment are separated by a non-coding intergenic region (IGR) which has the potential to form relatively stable stem-loop structures (Knipe and Howley, 2001).

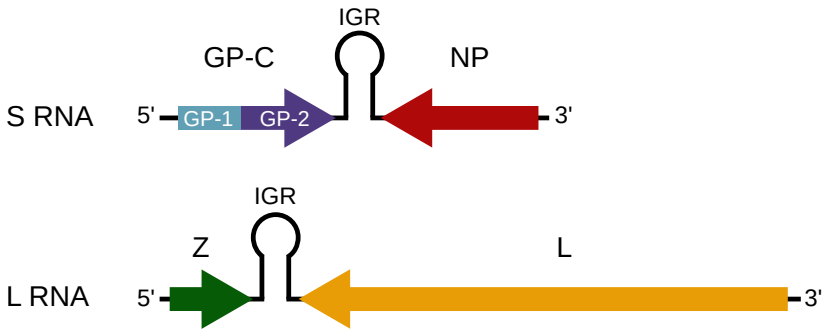

Figure 1.2: Arenavirus genome organization
The arenaviral S RNA encodes the glycoprotein (GP-C) and the nucleocapsid protein (NP); the L RNA encodes the Z protein and the RNA polymerase (L). The proteins on each RNA segment are separated by a non-coding intergenic region (IGR).

Arenaviral particles are composed of a nucleocapsid which is surrounded by a lipid envelope (Figure 1.3 A and B). The particles were observed to have a roughly spherical appearance with great variations in size (Neuman et al., 2005). The spikes that decorate

the surface of the viral particles are formed by GP-1/GP-2 oligomers that mediate the interaction with host cell receptors and virus membrane fusion (Rojek and Kunz, 2008). The Z protein, which interacts with the viral glycoproteins, is located just below the lipid envelope and is thought to act as a matrix protein (Capul et al., 2007; Perez et al., 2003). The genomic RNA is associated with the nucleocapsid proteins (NP) in form of ribonucleoprotein (RNP) complexes (Buchmeier, 2002). The viral polymerase (L) is a minor component of these RNP complexes.

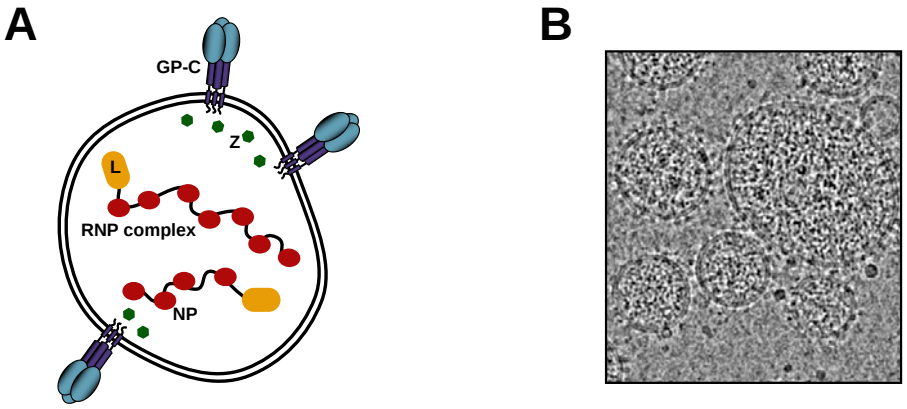

Figure 1.3: Structure of the arenavirus particle
(A) Schematic representation of an arenaviral particle. The nucleocapsid is surrounded by a lipid envelope containing the viral glycoprotein spikes. The genomic RNA, the NP and L proteins form the ribonucleoprotein (RNP) complex. The Z protein is located just below the viral envelope. **(B)** Electron cryomicroscopy of LCMV particles (Neuman et al., 2005).

1.3.2 The LCMV infection cycle

The entry of LCMV particles into target cells is initiated by binding of GP-1, the peripheral component of the viral glycoprotein spikes, to α-dystroglycan, a ubiquitously expressed cell surface receptor for extracellular matrix proteins (Borrow and Oldstone, 1992; Cao et al., 1998). α-dystroglycan is non-covalently associated with the membrane-anchored β-dystroglycan, which binds to a variety of cytoskeletal proteins and signal transduction molecules (Barresi and Campbell, 2006). Docking of the viral particles to the cell is followed by endocytosis into smooth-walled vesicles (Borrow and Oldstone, 1994). LCMV does not appear to use the clathrin-mediated endocytosis and cellular entry was shown to be sensitive to cholesterol depletion (Rojek et al., 2008; Shah et al., 2006). In addition, LCMV entry seems to be independent of caveolin and does not require the GTPase dynamin or the actin cytoskeleton (Borrow and Oldstone, 1994; Rojek et al., 2008). The detailed entry pathway of LCMV, however, is not known until now. Release of the viral RNA into the cell cytoplasm occurs after pH-dependent membrane fusion mediated

by the viral glycoproteins upon an acid-induced conformational change (Borrow and Oldstone, 1994; Di Simone et al., 1994). The pH at which membrane fusion occurs (5.3 to 5.5) suggests delivery of the LCMV particles to late endosomes. Membrane fusion is promoted by structural rearrangements in the transmembrane-containing GP-2 subunit forming a six-helix-bundle characteristic for class I viral fusion proteins (Eschli et al., 2006; Gallaher et al., 2001). After unpacking of the viral RNA in the cytoplasm, replication and transcription is initiated. Newly synthesized viral RNAs, nucleocapsid proteins, and viral polymerases are subsequently assembled into ribonucleoprotein complexes, which are incorporated into budding viral particles. The main driving force for LCMV budding is the myristoylated Z protein, which is thought to function as a matrix protein (Perez et al., 2004). Budding of LCMV particles takes place at the cell surface of infected cells and requires the interaction of the Z protein with the viral glycoprotein spikes that are localized to the plasma membrane (Capul et al., 2007; Knipe and Howley, 2001).

1.3.3 Synthesis and function of the LCMV glycoprotein C

The LCMV glycoprotein C is synthesized as a precursor protein (pGP-C) with an N-terminal signal sequence that targets the protein to the ER (Buchmeier and Parekh, 1987) (Figure 1.4). After pGP-C insertion into the ER membrane the signal sequence is cleaved off by SPase. The cleaved signal sequence is called signal peptide (SP^{GP-C}). After cleavage of SP^{GP-C}, GP-C undergoes extensive N-linked glycosylation and is thought to oligomerize within the ER before being further processed in a late-Golgi or post-Golgi compartment (Wright et al., 1990). Proteolytic processing of GP-C is mediated by the cellular subtilase SKI-1/S1P (subtilisin-kexin isoenzyme 1/ site 1 protease) and yields the glycoprotein subunits GP-1 and GP-2 (Beyer et al., 2003; Borrow and Oldstone, 1992).

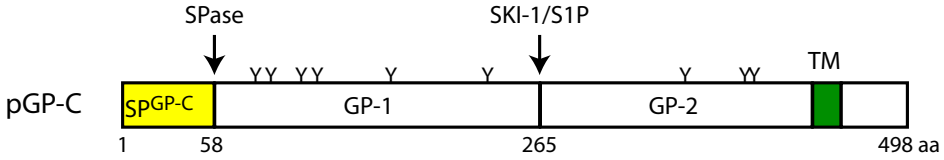

Figure 1.4: The LCMV precursor glycoprotein C
The LCMV pGP-C is composed of a signal sequence (SP^{GP-C}; aa 1-58), the GP-1 subunit (aa 59-265), and the GP-2 subunit containing the transmembrane (TM) region (aa 266-498). Putative N-glycosylation sites (Y), the SPase and SKI-1/S1P cleavage sites are indicated.

GP-1 is a highly glycosylated peripheral protein that is non-covalently attached to the membrane-anchored GP-2 (Burns and Buchmeier, 1991). Together they build up the glycoprotein (GP) spikes in the viral membrane (Figure 1.3). Each GP spike is build of three GP-1/GP-2 heterodimers (Eschli et al., 2006). The GP-1 subunit forms the globular head of the GP complex and mediates the interaction with the cellular receptor α-dystroglycan

(Cao et al., 1998; Neuman et al., 2005). The stem of the LCMV glycoprotein spike is formed by the membrane-spanning GP-2 subunit. In the current model, the GP-2 ectodomain is thought to be composed of two α-helices separated by a disulfide-bonded loop and a hydrophobic N-terminus (Eschli et al., 2006; Gallaher et al., 2001). Whereas the C-terminal half of GP-2 is believed to build up the surface exposed stalk region observed by cryo-EM (Neuman et al., 2005), the N-terminal half, including a coiled-coil core and the N-terminal hydrophobic region, is buried in the interior of the GP complex (Eschli et al., 2006). Exposure to low pH (5.3 to 5.5) triggers GP-1 dissociation from GP-2 and induces irreversible conformational rearrangements in the GP-2 subunit (Di Simone and Buchmeier, 1995; Di Simone et al., 1994). As a consequence it is thought, that the hydrophobic N-terminus of GP-2, the so-called fusion peptide (Glushakova et al., 1990), is inserted into the target cell membrane. The conformational rearrangements in GP-2 presumably lead to the formation of a six-helix bundle, thereby pulling the viral and host cell membranes together giving rise to the fusion pore. Although the LCMV glycoproteins share most of the characteristics of class I fusion proteins (Eschli et al., 2006; Gallaher et al., 2001), further work is needed to understand the detailed mechanism for LCMV glycoprotein-mediated membrane fusion.

1.3.4 The signal peptide of the LCMV glycoprotein C

Insertion of the LCMV precursor glycoprotein C into the ER membrane is mediated by an unusual signal sequence (Froeschke et al., 2003). The LCMV signal sequence is longer than average signal sequences comprising 58 amino acid residues. After cleavage by SPase, the resulting signal peptide, SP^{GP-C}, was found to accumulate in cells and virus particles and therefore proposed to have further functions in the virus life cycle (Froeschke et al., 2003). SP^{GP-C} contains an extended hydrophilic N-terminal region (n-region) including a myristoylation consensus site and two hydrophobic regions (h1- and h2-region) separated by a basic amino acid residue (Figure 1.5).

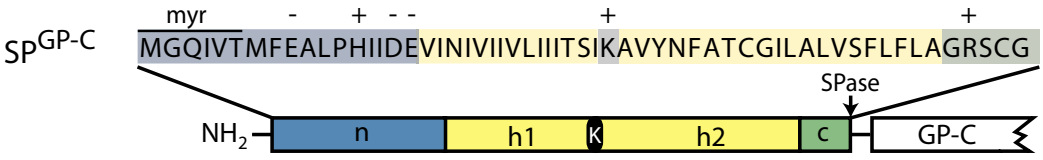

Figure 1.5: The signal peptide of LCMV GP-C
The LCMV signal peptide (SP^{GP-C}) is depicted as amino acid sequence in one-letter code and as schematic outline of the SP^{GP-C} regions. SP^{GP-C} comprises a hydrophilic N-terminal region (n), two hydrophobic regions (h1 and h2) and a C-terminal region (c) containing the SPase cleavage site. The N-terminal amino acid residues of SP^{GP-C} match the myristoylation consensus sequence MGxxxT/S indicated by a line (myr). Charged amino acid residues are marked.

The amino acid sequence of the LCMV SP^{GP-C} shows a high level of conservation among the precursor glycoproteins of arenaviruses. For the Old World Lassa arenavirus it was shown that SP^{GP-C} cleavage is a prerequisite for GP-C processing into GP-1 and GP-2 by SKI-1/S1P (Eichler et al., 2003b; Lenz et al., 2001). Furthermore, the proteolytic processing of GP-C was abolished by substitution of SP^{GP-C} with an unrelated signal sequence or by deletion of the SP^{GP-C} N-terminus including the first hydrophobic region (Eichler et al., 2003a, 2004). Whereas both hydrophobic regions of the Lassa virus SP^{GP-C} were needed for proteolytic processing, each hydrophobic region alone was shown to have the potential to mediate insertion of pGP-C into the ER membrane (Eichler et al., 2004). As the Lassa virus SP^{GP-C} is essential for GP-C processing and was shown to perform this function even in *trans*, SP^{GP-C} was proposed to be a maturation factor for GP-C (Eichler et al., 2003a). Likewise, the New World Junín arenavirus SP^{GP-C} was found to be N-terminally myristoylated and required for pH-dependent cell-cell fusion (York et al., 2004). So far, the responsible mechanisms and the functional regions required for the distinct roles of the arenaviral SPs^{GP-C} are mostly unknown.

1.4 Aim of this work

The aim of this work was to discover and analyze the post-targeting functions of LCMV SP^{GP-C}. More precisely, to investigate SP^{GP-C} requirements for ER membrane insertion, processing and cell surface expression of LCMV GP-C and the role of SP^{GP-C} in virus infection. Furthermore, the question whether SP^{GP-C} is part of the GP complex and the topology of SP^{GP-C} in the membrane were addressed.
In order to determine possible functions of the different SP^{GP-C} regions, SP^{GP-C} deletion mutants were analyzed for their ability to target LCMV pGP-C to the ER membrane and to promote processing and intracellular transport of the GP complex in transiently transfected cells. To understand the function of SP^{GP-C}, it is also important to know the orientation of SP^{GP-C} in the membrane. As the LCMV SP^{GP-C} has two h-regions, of which one or both might span the membrane, the topology of SP^{GP-C} was analyzed by using potential N-glycosylation sites introduced throughout the SP^{GP-C}. The potential involvement of SP^{GP-C} myristoylation in SP^{GP-C} function was investigated by using a SP^{GP-C} mutant in which the N-terminal myristoylation consensus sequence was disrupted. To study a possible complex formation of SP^{GP-C} with GP-C a co-immunoprecipitation protocol was established. The role of SP^{GP-C} in virus infection was investigated using LCMV pseudoviruses, where the LCMV GP complex (wild type or mutant) is embedded in the membrane of a replication-deficient retrovirus encoding eGFP.

2 Materials and Methods

2.1 Materials

2.1.1 Chemicals

All standard chemicals were purchased from Sigma (Taufkirchen), Merck (Darmstadt), Serva (Heidelberg) or Roche (Mannheim) unless otherwise indicated. The source of specific chemicals is mentioned at the corresponding position.

The radiochemical ^{35}S-Met/Cys (cell labeling mix) was purchased from Amersham-Pharmarcia (Braunschweig).

2.1.2 Standard stock solutions and buffers

Solution/ Buffers	Composition
10x PBS	27 mM KCl 14 mM KH_2PO_4 1.37 M NaCl 78 mM Na_2HPO_4
10x TBS	1.37 M NaCl 0.25 M Tris/HCl pH 7.4
TBST	1x TBS 0.05 % (v/v) Tween 20

Other used solutions and buffers are mentioned together with the corresponding method in section 2.2. If necessary sterilization was carried out by autoclaving at 121°C for 20 min or by filtering through a 0.22 μm filter (Millipore, Schwalbach).

2.1.3 DNA and protein standards

A 100 bp DNA standard for estimation of the molecular size of DNA fragments was purchased from New England Biolabs (Schwalbach). The 1 kb molecular size DNA standard was obtained from Invitrogen (Karlsruhe).

For Western blotting the prestained broad range protein marker (6 - 175 kDa) purchased from New England Biolabs (Schwalbach) was used. The radioactive labeled ^{14}C molecular weight markers (MW) for low MW range (2.35 - 30 kDa) and high MW range (14.3 - 200 kDa) were obtained from Amersham-Pharmarcia (Braunschweig).

2.1.4 Oligonucleotides

All oligonucleotides were purchased from MWG-Biotech (Ebersberg).

Name	**Sequence** ($5' \rightarrow 3'$)	**Annotation**
5′-pHCMV-EcoRI	atcattttggcaaagaattcctcg	pHCMV primer
3′-pHCMV-EcoRI	gcacctgaggagtgaattcctcg	pHCMV primer
3′-ΔC	cggatccttatcatctatgtgttggtatc	pGP-C/ΔC primer
3′-HA	agcgtaatctggaacatcgtatgg	sequencing
5′-GP-2	gctggtaggtcctgtggcggcacattcacctggacc	overlap PCR
3′-GP-2	ggtccaggtgaatgtgccgccacaggacctaccagc	overlap PCR
5′-ΔTM-mut	gacaagggagtactcctttagccttaatggattacc	mutagenesis
3′-ΔTM-mut	ggtaatccattaaggctaaaggagtactcccttgtc	mutagenesis
5′-SP^{VSV-G}-mut	cgatgcccaatgcgtgctcagccaacaactc	mutagenesis
3′-SP^{VSV-G}-mut	gagttgttggctgagcacgcattgggcatcg	mutagenesis

2.1.5 Enzymes

Restriction enzymes were purchased from New England Biolabs (NEB) (Schwalbach) or Roche (Mannheim). The deglycosylation enzyme peptide-N-glycosidase F (PNGase F) was obtained from NEB. Further enzymes purchased from Roche are the calf intestine phosphatase (CIP), the Taq-Polymerase, and the T4-DNA-Ligase. The Pfu-Turbo DNA polymerase was obtained from Stratagene (La Jolly, USA).

2.1.6 Plasmids

Plasmids used in this study are listed below.

Name	Features	Reference
pGP-C-HA	LCMV pGP-C	M. Fröschke
pGP-C/ΔC	deletion of cytoplasmic region	this thesis
pGP-C-HA/ΔTMC	deletion of cytoplasmic and TM region	M. Fröschke
SP^{GP-C}-VSV-G-HA	LCMV SP^{GP-C} fused to VSV-G	M. Fröschke
SP^{VSV-G}-GP-C-HA	SP^{VSV-G} fused to LCMV GP-C	M. Fröschke
SP^{VSV-G}-GP-C/ΔC	deletion of cytoplasmic region	this thesis
SP^{VSV-G}-GP-C-HA/ΔTMC	deletion of cytoplasmic and TM region	this thesis
SP^{GP-C} deletion mutants:		M. Fröschke/Schrempf et al. (2007)
ΔnME, ΔnMK	deletion of the SP^{GP-C} n-region with Glu (E) or Lys (K) in front of the h1-region	
Δh1	deletion of the SP^{GP-C} h1-region	
Δh2	deletion of the SP^{GP-C} h2-region	
SP^{GP-C} glycosylation mutants:		M. Fröschke/Schrempf et al. (2007)
I4N	in SP^{GP-C} n-region	
V22T, I29N	in SP^{GP-C} h1-region	
A39T, L46N	in SP^{GP-C} h2-region	
G54N	in SP^{GP-C} c-region	
SP^{GP-C} myristoylation mutants:		M. Fröschke/Schrempf et al. (2007)
G2A	prevention of myristoylation	
G2A/I4N	combined mutant	

Name	Features	Reference
SP^{GP-C}	LCMV SP^{GP-C}	Froeschke et al. (2003)
pGP-C-HA(WE)	LCMV GP-C mutant	M. Fröschke/Beyer et al. (2001)
pGP-1-HA	LCMV GP-1 subunit	M. Fröschke
pGP-2-HA	LCMV GP-2 subunit	this thesis
pMP71-eGFP-pre	retroviral expression vector encoding eGFP	Beyer et al. (2002)
pSV-Mo-MLVgagpol	MLV Gag-Pol	Beyer et al. (2002)
MLV Gag-YFP	MLV Gag C-terminally YFP tagged	Sherer et al. (2003)

The LCMV pGP-C was derived from the cDNA sequence of the recloned GP(WE-HPI) (accession number AJ297484) (Beyer et al., 2001). The coding regions of the constructs obtained from M. Fröschke were recloned in the pHCMV expression vector (Yee et al., 1994) and contain the LCMV GP-C 5′UTR. Plasmids generated in this thesis descend from these constructs. All proteins expressed from the listed plasmids are C-terminally HA tagged except of pGP-C/ΔC, SP^{VSV-G}-GP-C/ΔC, SP^{GP-C}, pMP71-eGFP-pre, pSV-Mo-MLVgagpol and MLV Gag-YFP. Point mutations in SP^{VSV-G}-GP-C-HA and pGP-C-HA/ΔTMC were mutagenized to the GP-C wild type sequence using the Stratagene Mutagenesis Kit. Sequencing was performed at 4base lab (Reutlingen) or MWG-Biolabs (Ebersberg).

2.1.7 Bacteria culture

The *E. coli* strains used in this study are DH5α and TOP10 (Invitrogen, Karlsruhe). Bacteria were cultivated in standard LB-medium (1 % (w/v) Bacto tryptone, 0.5 % (w/v) yeast extract, 1 % (w/v) NaCl) containing 100 μg/ml ampicillin. LB plates additionally contained 1.5 % (w/v) agar.

2.1.8 Cell culture

Cell lines

In this study the following mammalian cell lines were used:

- HeLa: human cervix carcinoma (DSMZ No. ACC 57)
- HEK 293T: human embryonic kidney (ATCC No. CRL-11268)
- TE671: human rhabdomyosarcoma (DSMZ No. ACC 263)

Cell culture media

HeLa cells were grown in DMEM supplemented with 10 % fetal calf serum (FCS), 2 mM glutamine and 1 mM pyruvate. Cultivation of HEK 293T cells was done in DMEM/F-12 supplemented with 10 % FCS and 2 mM glutamine. Cells cultivated at the Georg-Speyer-Haus (GSH, Frankfurt a.M.) in the research group of D. von Laer: HEK 293T cells were grown in DMEM with 4 mM glutamine, 10 % FCS and penicillin-streptomycin; TE671 were grown in DMEM supplemented with 10 % FCS. All media, supplements and Trypsin-EDTA were obtained from Gibco (Invitrogen, Karlsruhe).

2.1.9 Antibodies

Primary antibodies:

Antibody	Properties	Reference
anti-HA	rabbit, polyclonal detection of HA-tag	Santa Cruz Biotechnology (USA)
anti-SP7	rabbit, polyclonal detection of LCMV SP^{GP-C}	Froeschke et al. (2003)
KL25	mouse, monoclonal detection of LCMV GP-1	Bruns et al. (1983)
anti-B23	rabbit, polyclonal detection of B23	Santa Cruz Biotechnology (USA)

Anti-B23 was used as an unrelated control antibody for co-immunoprecipitations.

Secondary antibodies:

Antibody	Properties	Reference
anti-rabbit IgG	goat, HRPO-conjugated	Dianova (Hamburg)
anti-mouse IgG	goat, phycoerythrin-conjugated	Dianova (Hamburg)
anti-mouse IgG	goat, Alexa Fluor 488	Molecular Probes (Karlsruhe)

2.1.10 Kits

- QIAprep Spin Miniprep Kit (QIAGEN, Hilden)
- QIAquick Gel Extraction Kit (QIAGEN, Hilden)
- QIAquick PCR-Purification Kit (QIAGEN, Hilden)
- Nucleobond AX Plasmid-Purification-Kit (Machery-Nagel, Düren)
- ECL Western-Blot Detection-Kit (Roche, Mannheim)
- TOPO TA Cloning® Kit (Invitrogen, Karlsruhe)
- *in vitro* Mutagenesis Kit (Stratagene, La Jolly, USA)

2.1.11 Computer software

Figure editing was done with Adobe Photoshop and figure labeling with Adobe Illustrator. ImageJ was used for the quantification of Western blots. The bar diagrams were prepared with Microsoft Excel. Autoradiography analyses were accomplished using MacBas2.0 software for Fuji BAS1000 phosphoimager (Fuji, Japan) or the FLA-3000 phosphoimager (Fuji, Japan). Construction of plasmid maps and analysis of nucleic acid and protein sequences were done with the Gene Construction Kit (Textco, USA).

2.2 Methods

2.2.1 Biomolecular methods

General cloning strategy

DNA fragments destined for cloning were either cut out of existing plasmids and ligated directly with the target vector or amplified from plasmids by polymerase chain reaction (PCR). PCR products were digested by the appropriate enzymes and subsequently ligated with a vector backbone. Existing and generated plasmids are listed in section 2.1.6.

Polymerase chain reaction

The principal of the polymerase chain reaction (PCR) is the enzymatic amplification of defined DNA sequences between two oligonucleotide primers. The primers contain complementary sequences to both ends of the DNA template. After heat denaturation of the double-stranded DNA, the primers anneal to the DNA template during cooling of the reaction. The primer hybridization is followed by the DNA synthesis catalyzed by a heat-stable DNA polymerase, such as Taq or Pfu polymerase. The elongation time needed to synthesize a new DNA strand complementary to the DNA template depends both on the DNA polymerase used and the length of the DNA fragment to be amplified. Various rounds of denaturation, annealing and elongation lead to an exponential amplification of the DNA template.

A typical 50 μl PCR reaction contained:

- 10 ng DNA template
- 0.2 μM of each primer
- 0.2 mM ever dATP, dCTP, dGTP, dTTP
- 5 μl polymerase buffer (10x)
- 1 U Taq DNA polymerase (Roche, Mannheim)

As starting basis for the optimization of the PCR conditions the following PCR procedure was used:

steps	**time**	**temperature**
1. denaturation	3 min	94°C
2. denaturation	30 s	94°C
3. annealing	30 s	58°C
4. elongation	2 min	72°C
5. final elongation	10 min	72°C
pause	→	4°C

The steps 2 - 4 were repeated 29 times. The annealing temperature and the elongation time were adapted to the used primers and the expected length of the PCR product. The PCR reaction was done in the T3 Thermocycler (Biometra, Göttingen). Purification of the PCR products was done with the QIAquick PCR-Purification Kit (QIAGEN, Hilden).

Site-directed mutagenesis

The site-directed mutagenesis can be used to insert or eliminate specific mutations in a DNA sequence. If a plasmid contains a mutation in the coding region the sequence can be changed by using two complementary oligonucleotides containing the desired sequence. The used primers should be between 25 - 45 base pairs in length, have a melting temperature above 78°C and should contain the sequence change in the center. After successive PCR cycles the primer-based strand outnumbers the mutated template plasmid. The remaining template DNA is eliminated by digestion with DpnI, a restriction enzyme which cleaves specifically the methylated template DNA.

A typical 50 μl reaction contained:

- 20 ng DNA template
- 125 nM of each primer
- 0.2 mM ever dATP, dCTP, dGTP, dTTP
- 5 μl polymerase buffer (10x)
- 2.5 U Pfu-Turbo DNA polymerase (Stratagene, La Jolly, USA)

The PCR reaction was done with the protocol described below. The steps 2 - 4 were repeated 18 times. After the addition of 10 U DpnI (Stratagene, La Jolly, USA) the PCR reaction was incubated at 37°C for 1 h.

steps	**time**	**temperature**
1. denaturation	90 s	95°C
2. denaturation	30 s	95°C
3. annealing	1 min	55°C
4. elongation	7 min (1 min/kb)	68°C
5. final elongation	10 min	68°C
pause	→	4°C

Overlap extension PCR

The overlap extension PCR is a method to link two defined DNA fragments independent of their sequence without using restriction endonucleases or DNA ligases. The two DNA fragments designated for fusion were amplified in separate PCR reactions using the Pfu

polymerase to avoid the addition of adenine on the 3′ ends of the PCR products (see Figure 2.1). The primers b and c covering the fusion sites were designed such that the joining ends contain complementary sequences. The PCR products were purified and quantified by an agarose gel and 100 ng of both fragments diluted in water were mixed in an Eppendorf cup and put in boiling water for denaturation. After cooling of the water bath to room temperature, 5 μl polymerase buffer (10x), 0.2 mM of each dNTP and 2.5 U Pfu-Turbo DNA polymerase were added and an elongation reaction of 10 min was done using the T3 Thermocycler. At last the primers a and d (0.1 μM of each), already used in the first PCR reaction, were added and the second PCR was performed.

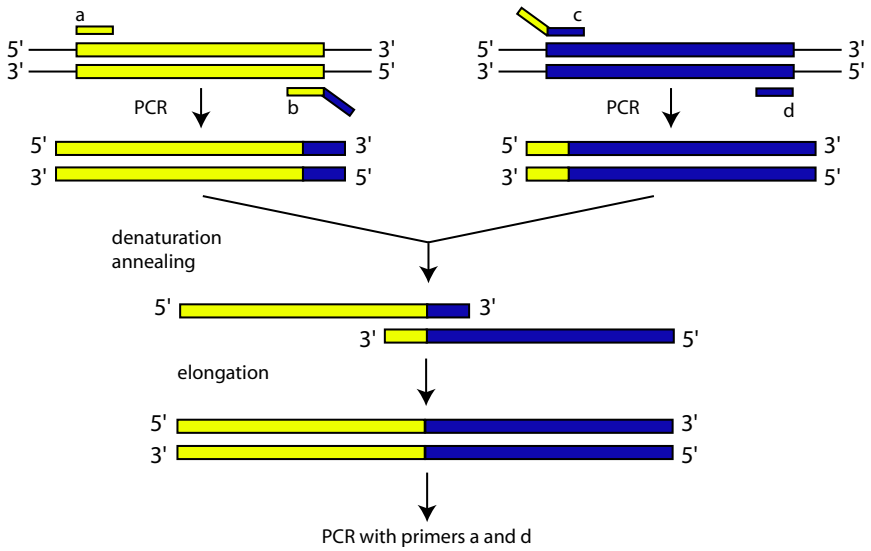

Figure 2.1: Overlap extension PCR
Two DNA fragments were amplified in separate PCR reactions with the indicated primers. The primers b and c are complementary to each other. After denaturation of the PCR products, annealing and elongation, a second PCR with the primers a and d is performed.

Restriction digest

All restriction digests were done with the buffers recommended by the manufacturer. In a standard 50 μl reaction for a preparative digest, 5 μg DNA were mixed with 5 μl 10x buffer and 5 μl restriction enzyme and incubated at 37°C for 1 - 2 h. To prevent religation of the vector backbone the 5′-ends were dephosphorylated with the calf intestine phosphatase (CIP) (Roche, Mannheim) at 37°C for 30 min.

Agarose gel electrophoresis

To analyze and purify PCR products and digestion reactions typically a 1 % agarose gel was used. For a 1 % agarose gel 3 g Agarose were heated in 300 ml TAE buffer until a clear solution was gained. Before pouring the gel, ethidium bromide was added to an end concentration of 1 μg/ml. When the gel had cooled down and become solid it was covered with TAE buffer. The DNA samples were mixed with the DNA loading buffer in a 1/10 ratio and injected into the slots. As size markers a 1 kb or 500 bp DNA latter was used. For documentation the stained DNA was visualized with a UV transilluminator (366 nm). Purification of DNA fragments was done with the QIAquick Gel Extraction Kit (QIAGEN, Hilden).

TAE:	90 mM Tris-acetate, 2 mM EDTA
DNA loading buffer: (10x)	0.1 % (w/v) bromphenol blue, 50 % (v/v) glycerol in 1x TAE

Ligation

The relative amounts of the DNA fragments destined for ligation were quantified by agarose gel electrophoresis. In general, a four fold molar excess of the insert compared to the vector was used. A typical 10 μl ligation reaction contained 1 μl dephosphorylated vector, 4 μl insert, 1 μl 10 x T4 DNA ligase buffer, and 0.5 μl T4 DNA ligase. The reaction was incubated at 16°C for 2 h. If the pCRII-Topo-vector from the Topo TA Cloning® Kit from Invitrogen was used, 4 μl insert were incubated with 1 μl salt solution and 1 μl Topo-vector for 5 min at room temperature.

Transformation of chemical competent cells

To produce chemical competent cells a single colony of the *E. coli* strain DH5α was inoculated into LB-medium and grown to OD_{600} of 0.4 - 0.5 at 37°C. After incubation of the cell suspension on ice for 10 min the cells were pelleted at 2100 $\times$g for 10 min at 4°C and resuspended in ice-cold calcium chloride solution (100 mM $CaCl_2$, 15 % glycerol). After two rounds of centrifugation, resuspension in $CaCl_2$ solution and incubation on ice for 30 min for the first round and 60 min for the second round, aliquots of 100 μl were snap freeze in liquid nitrogen and stored at -80°C.
For transformation 50 μl chemical competent DH5α were incubated with 5 μl ligation reaction on ice for 30 min followed by a heat shock at 42°C for 45 s. Directly after the heat shock the cells were placed on ice for at least 2 min. Afterwards 200 μl of LB-medium without antibiotics were added and the cell suspension was incubated at 37°C for 30 min.

At last the cell suspension was plated on a LB agar plate with ampicillin and incubated over night at 37°C. If the Topo TA Cloning® Kit was used, the whole ligation reaction was incubated with TOP10 chemical competent cells for 30 min on ice followed by a heat shock at 42°C for 30 s. Immediately after the heat shock the tubes were transferred onto ice. After the addition of 250 μl S.O.C medium (Invitrogen, Karlsruhe) and incubation at 37°C for 1 h the cells were spread on a selective plate with X-Gal and incubated over night at 37°C.

Amplification and isolation of plasmid DNA from *E. coli*

For plasmid amplification a single colony of transformed cells was inoculated into LB-medium containing 100 μg/ml ampicillin and grown over night at 37°C. To store the transformed cells 850 μl of an overnight culture were mixed with 150 μl 87 % glycerol and stored at -80°C. Purification of large amounts of plasmid DNA (100 - 500 μg) from 500 ml *E. coli* culture was done with the Nucleobond Plasmid-Purification-Kit (Machery-Nagel, Düren) according to the instruction manual. For plasmid isolation from cultures up to a volume of 5 ml the QIAprep Spin Miniprep Kit (QIAGEN, Hilden) was used. The purified plasmid DNA was dissolved in water, adjusted to a concentration of 1 μg/μl and stored at -20°C.

2.2.2 Cell culture techniques

Cultivation of eukaryotic cell lines

Mammalian cells were cultivated in their appropriate medium (see 2.1.8) at 37°C in a 5 % CO_2 atmosphere with a high air humidity in a Heraeus incubator. At regular intervals the adherent cell monolayers were detached from the cell culture dish and seeded in a new plate under sterile working conditions. To detach the cells the medium was removed and the cells were washed with PBS followed by an incubation with Trypsin-EDTA at 37°C. Trypsin is a proteolytic enzyme that cleaves proteins on the cell surface that mediate cell-cell interaction and the contact to the bottom of the dish. As some cell adhesion molecules (for example the cadherins) depend on calcium ions to function, the calcium chelator EDTA together with trypsin make the cells detach from the bottom of the dish. Detached cells were resuspended in fresh media and seeded into a new culture dish in a particular dilution depending on the growing behavior of the cells.

Freezing and thawing of cells

Cultivated cell lines can be stored frozen for many years using cryoprotective agents such as DMSO (dimethylsulphoxide). For that purpose adherent cells were washed with PBS, trypsinized, resuspended in fresh medium, and pelleted at 200 ×g for 2 min. After aspiration of the supernatant the cell pellet was gently resuspended in freezing medium (10 % DMSO / 90 % FCS). 1 ml aliquots of the cell suspension were distributed in cryo-tubes and placed over night in the -80°C freezer. For long time storage the cryo-tubes were transferred to liquid nitrogen.
Unfreezing of cells was done at 37°C in a water bath. When the cells were almost thawed, the cell suspension was gently resuspended in the appropriate culture medium and centrifuged at 200 ×g for 2 min. The cell pellet was again resuspended in fresh medium and transferred into a culture dish.

Transient transfection with calcium phosphate

For Western blot and pulse-chase, cells were transiently transfected using the calcium phosphate precipitation method. If DNA is mixed with a solution of $CaCl_2$ the negatively charged phosphate groups of the DNA interact with the positively charged calcium ions. With the addition of a phosphate-buffered solution, calcium phosphate co-precipitates with the DNA. The insoluble precipitates attach to the plasma membrane of cells and are taken up into the cells by endocytosis. After several cell divisions the DNA gets lost because of the lack of a centrosome in the transfected DNA. For that reason the highest expression level is achieved after 48 - 72 hours of transfection.
For transfection 2.5×10^5 HeLa cells in 2 ml medium were seeded in a 6 cm dish. After 20 - 24 h the cells were washed two times with PBS to remove dead cells and 4.5 ml fresh medium was added. To generate the calcium phosphate precipitates, 7.5 μg DNA (3 μg plasmid DNA and 4.5 μg carrier DNA (herring sperm DNA)) were mixed with 25 μl $CaCl_2$ solution (2.5 M stock solution) and adjusted to 250 μl with dH_2O. This $CaCl_2$/DNA solution was dropwise added to 250 μl HeBS solution on a vortexer within 30 s. After incubation at room temperature for 20 - 30 min, the transfection mixture was slowly pipetted onto the cells. Transfected cells were cultivated at 37°C for 20 h, washed twice with PBS and supplemented with fresh medium. 24 hours later the cells were harvested.

HeBS solution:	280 mM NaCl, 50 mM HEPES, 1.48 mM Na_2HPO_4, adjusted to pH 7.05 with NaOH

Transient transfection with Lipofectamine 2000

Lipofectamine 2000 from Invitrogen is a cationic lipid-based transfection reagent with a very high transfection efficiency and little toxicity to cells. This transfection method was used to investigate the cell surface expression of LCMV GP-C in HEK 293T cells. For transfection, cells were seeded in a 6 well plate in 1 ml medium (1/3 DMEM/F-12 and 2/3 DMEM) per well so that the cells will be 90 - 95 % confluent at the time of transfection. For each transfection sample 4 μg DNA were diluted in 250 μl serum-free medium. In a separate Eppendorf cup 6 μl Lipofectamine 2000 were diluted in 250 μl serum-free medium and incubated for 5 min at room temperature. Afterwards the Lipofectamine solution was added to the DNA solution, incubated for 20 min and pipetted onto the cells. After incubation of the cells at 37°C for 5 h, the medium was changed to the growth medium (DMEM/F-12). Cells were harvested 24 h later.
Cell surface expression of the LCMV SP^{GP-C} mutants was analyzed in cooperation with the research group of D. von Laer (GSH, Frankfurt a.M.) using 800 ng plasmid DNA per well (24-well plate) for the transient transfection with Lipofectamine 2000.

2.2.3 Metabolic labeling / Pulse-chase

40 h after transfection, HeLa cells were washed with PBS and starved for 2 h at 37°C with depletion medium lacking methionine and cysteine, which was supplemented with 2 mM glutamine and 10 % amino acid free FCS (dialyzed). Metabolic labeling (pulse) was performed with 72 μCi/ml ^{35}S-Met/Cys for 30 min. Subsequently, cells were washed with PBS and lysed directly or were incubated in normal growth medium for the indicated time periods (chase). After cell lysis, proteins of interest were immunoprecipitated, separated by SDS-PAGE and analyzed by autoradiography.

Cell lysis for immunoprecipitation

Cell lysis was performed directly after the metabolic labeling or after the chase. For lysis, cells were washed two times with ice-cold PBS, covered with PBS containing protease inhibitors (1 mM PMSF; 10 ng/μl aprotinin), scraped from the cell culture dish and transferred in an Eppendorf cup. Cells were pelleted by centrifugation at 1000 ×g for 4 min at 4°C. The cell pellet was resuspended in 200 μl ice-cold lysis buffer supplemented with protease inhibitors (1 mM PMSF; Complete Protease Inhibitor Cocktail Tablets (Roche, Mannheim)) and incubated for the appropriate time period on ice (indicated below the respective lysis buffer). After cell lysis, un-soluble cell debris was removed by centrifugation (16000 ×g; 5 min; 4°C). If not otherwise indicated the 1 % Triton lysis buffer with 150 mM NaCl was used. For co-immunoprecipitations a 2 % digitonin lysis buffer with 150 mM NaCl (Co-IP lysis buffer) was used.

Digitonin lysis buffer: (lysis: 20 min on ice)	10 % glycerol, 1.5 mM $MgCl_2$, 50 mM HEPES pH 7.5, 150 mM or 500 mM NaCl, 1 mM EGTA, 0.2 - 2 % digitonin
Triton lysis buffer: (lysis: 10 min on ice)	10 % glycerol, 1.5 mM $MgCl_2$, 50 mM HEPES pH 7.5, 150 mM or 500 mM NaCl, 1 mM EGTA, 0.5 - 2 % Triton X-100
ODG lysis buffer: (lysis: 10 min on ice)	5 % glycerol, 50 mM Tris/HCl pH 8, 150 mM NaCl, 1 mM EGTA, 2 % Octyl-β-D-glucopyranoside (Calbiochem, Darmstadt)
RIPA lysis buffer: (lysis: 10 min on ice)	50 mM Tris/HCl pH 8, 150 mM NaCl, 0.1 % SDS, 0.5 % deoxycholate, 1 % Triton X-100

Immunoprecipitation

Immunoprecipitation (IP) of proteins from cell lysates (200 μl) was carried out in lysis buffer with 30 μl of a 1:1 slurry protein A-sepharose (Amersham-Pharmarcia (Braunschweig) and the indicated antibody over night at 4°C. After centrifugation at 3500 $\times$g for 2 min at 4°C, the sedimented protein A-sepharose with the bound proteins were washed to remove unspecifically bound proteins. In general, immunoprecipitated samples were washed two times in 1 ml IP-buffer A, two times in IP-buffer B and two times in IP-buffer C. The washing buffers used for the test of different lysing conditions for co-immunoprecipitation are listed below. Where indicated, the immunoprecipitated proteins were deglycosylated with peptide-N-glycosidase F (PNGase F) as described by the manufacturer. After the deglycosylation or directly after the last IP washing step, 30 - 40 μl Schägger loading buffer was added to the sample followed by an incubation for 10 min at 95°C before loading onto a Schägger gradient gel.

Antibody amounts:	4 μl anti-HA 4 μl anti-SP7 (1:1 diluted with glycerol) 2 μl KL25 4 μl B23 (unrelated control antibody for Co-IP)
IP-buffer A:	150 mM NaCl, 10 mM Tris/HCl (pH 7.5), 2 mM EDTA, 0.4 % Triton X-100
IP-buffer B:	500 mM NaCl, 10 mM Tris/HCl (pH 7.5), 2 mM EDTA, 0.2 % NP-40
IP-buffer C:	10 mM Tris/HCl (pH 7.5)

Lysis buffer:	**Washing buffer:**
Digitonin low salt:	IP-buffer A without detergent
Digitonin high salt:	IP-buffer A and B without detergent
Triton low salt:	IP-buffer A and C
Triton high salt:	IP-buffer A, B and C
ODG:	ODG lysis buffer
RIPA:	IP-buffer A and C

2.2.4 SDS-PAGE

SDS-PAGE is the abbreviation for Sodium dodecyl sulfate (SDS) polyacrylamide gel electrophoresis (PAGE) and is used to separate proteins according to their electrophoretic mobility. To better separate proteins between 2 - 30 kDa the SDS-PAGE as described by Schägger and von Jagow (1987) was used in this thesis. Gels were poured in 20 cm × 20 cm format or 15 cm × 30 cm format between two glass plates separated by spacers (0.75 mm) and sealed with a rubber tube. The separating gel was poured as a 10 % - 16 % gradient gel with the help of a mixing chamber on top of a pure 16 % gel. After polymerization of the separating gel, a 5 cm high stacking gel was layered on top. The acrylamide used was purchased from AppliChem (Darmstadt). SDS-PAGE was performed in vertical electrophoresis chambers with Schägger anode and cathode buffer. Samples were incubated for 10 min at 95°C in Schägger loading buffer before loading onto a gel. Gels were run over night at 30 mA for 20 cm × 20 cm gradient gels or at 50 mA with the voltage limited to 130 V for 15 cm × 30 cm gels.

Schägger loading buffer: (2x)	24 % (v/v) glycerol, 8 % (w/v) SDS, 0.02 % Serva Blue G, 150 mM Tris/HCl pH 6.8, 200 mM DTT (freshly added)
Schägger gel buffer:	3 M Tris/HCl pH 8.45, 0.3 % (w/v) SDS
Schägger anode buffer: (10x)	2 M Tris/HCl pH 8.9
Schägger cathode buffer: (10x)	1 M tricine, 1 M Tris, 1 % (w/v) SDS

Schägger gradient gel 20 cm × 20 cm / 15 cm × 30 cm	**10 %** **separating gel**	**16 %** **separating gel**	**4 %** **stacking gel**
H_2O	4.14 ml / 6.2 ml	2.52 ml / 3.8 ml	5 ml / 10 ml
Schägger gel buffer	3 ml / 4.5 ml	6 ml / 9 ml	1.8 ml / 3.6 ml
49.5 % acrylamide (acrylamide/bisacrylamide)	1.8 ml/ 2.7 ml (48:1.5)	6.36 ml / 9.5 ml (46.5:3)	0.6 ml / 1.2 ml (48:1.5)
glycerol (80 %)	-	3 ml / 4.5 ml	-
TEMED (gradient + pure gel)	3 μl / 4.5 μl	2.5 μl + 3 μl / 3.8 μl + 4.5 μl	6.25 μl / 12.5 μl
10 % APS (gradient + pure gel)	45 μl / 67.5 μl	37.5 μl + 45 μl / 56.5 μl + 67.5 μl	75 μl / 150 μl

7.5 ml / 12 ml of the 16 % separating gel were used as a pure 16 % gel and 9 ml / 13.5 ml were used for the gradient.

Gels with radioactively labeled proteins were fixed in Fix-Mix for 45 min and subsequently dried for 2.5 h under vacuum on a Whatman paper at 70°C. Dried gels were exposed on phosphoimager plates (Fuji, Japan) for at least 24 h. The read out of the plates was done with a Fuji BAS1000 phosphoimager (Fuji, Japan) or the FLA-3000 phosphoimager (Fuji, Japan). Non-radioactive gels were analyzed by Western blotting.

Fix-Mix: 40 % (v/v) methanol, 10 % (v/v) acetic acid

2.2.5 Western blotting

Western blotting is a method to detect a specific protein after separation of the proteins in a given sample using SDS-PAGE and transfer onto a membrane, by probing the membrane with an antibody specific to the target protein.
40 - 48 h after transfection, cells were washed two times with ice-cold PBS, covered with PBS containing protease inhibitors (1 mM PMSF; 10 ng/μl aprotinin), transferred in an Eppendorf cup and pelleted by centrifugation at 1000 ×g for 4 min at 4°C. For whole cell lysates the pellets were resuspended in 1x Schägger loading buffer containing 100 mM DTT if not otherwise indicated, followed by an incubation for 10 min at 95°C, 15 min sonification and a further incubation for 5 min at 95°C. If the proteins were destined for deglycosylated with peptide-N-glycosidase F (PNGase F) the cells were lysed in 100 μl of the 1 % Triton lysis buffer containing 150 mM NaCl for 10 min on ice, followed by centrifugation (16000 ×g; 5 min; 4°C) to remove un-soluble cell debris. One half of the Triton lysate was subsequently treated with PNGase F, while the other half was left untreated.

Deglycosylation was performed as described by the manufacturer. After the addition of Schägger loading buffer the samples were incubated for 10 min at 95°C.
Proteins of whole cell lysates or Triton lysates were separated using a Schägger gradient gel. To transfer the proteins from the gel onto the nitrocellulose membrane (Protran®, Schleicher & Schuell, Dassel) a semi-dry blotting device (Schleicher & Schuell) was used. For blotting, three Whatman papers (3 mm) soaked in anode buffer II and three Whatman papers soaked in anode buffer I were placed onto the anode of the blotting device followed by the nitrocellulose membrane, the gel and three Whatman papers soaked in cathode buffer. Gel and membrane were soaked in anode buffer I before put onto the stack of Whatman papers. Electrotransfer was conducted for 2 h under constant current of 1 mA/cm^2 and a maximum of 20 V. To verify uniform blotting the membrane was incubated in Ponceau red followed by destaining in TBST. The membrane was blocked in blocking buffer for 1 h at RT. After incubation with the primary antibody for 1 h at RT, unbound antibodies were removed by washing three times 5 min with TBST. Incubation with the secondary antibody conjugated to horseradish peroxidase (HRPO) was carried out for 1 h at RT followed by four washing steps with TBST for 5 min each. The blot was developed with BM chemiluminscence blotting substrate (Roche, Mannheim) according to the manufacturer and exposed on Super RX films (Fuji, Japan).

Anode buffer II:	300 mM Tris, 20 % (v/v) methanol
Anode buffer I:	30 mM Tris, 20 % (v/v) methanol
Cathode buffer:	40 mM 6-Aminohexanoic acid, 25 mM Tris, 0.01 % (w/v) SDS, 20 % (v/v) methanol
Ponceau red:	2 % acetic acid, 0.4% PonceauS
TBS: (10x)	1.37 M NaCl, 0.25 M Tris/HCl pH 7.4
TBST:	1x TBS, 0.05 % (v/v) Tween 20
Block buffer:	10 % powdered milk, 0.5 % (v/v) Tween 20 in 1x TBS
Primary antibody:	block buffer diluted 1:5 with 1x TBS, anti-HA 1:2500 or anti-SP7 1:1000
Secondary antibody:	2 % powdered milk in TBST HRPO-conjugated anti-rabbit IgG 1:10000

2.2.6 Analysis of cell surface expression by flow cytometry

Flow cytometry is a technique for counting and examining fluorescently labeled cells suspended in a stream of fluid. To investigate the cell surface expression of LCMV GP-C, HEK 293T cells were transiently transfected with one of the GP-C expression plasmids listed in section 2.1.6 using Lipofectamine 2000 or mock treated. After 48 h, transfected cells were washed two times with PBS, resuspended in PBS/3 % FCS and incubated for 1 h at RT with the KL25 antibody, which recognizes an epitope in the LCMV GP-1 subunit. To remove the primary antibody the cells were pelleted at 400 ×g for 2 min at 4°C and washed three times with ice-cold PBS/3 % FCS. After washing, the cells were incubated with the secondary antibody for 30 - 60 min at RT in the dark. If not otherwise indicated, the secondary antibody used was the Alexa Fluor 488 goat anti-mouse IgG. In experiments done in cooperation with the research group of D. von Laer (GSH, Frankfurt a.M.) the antibody incubation was done at 4°C and the phycoerythrin (PE)-conjugated goat anti-mouse IgG was used as secondary antibody. After incubation with the secondary antibody the cells were pelleted and washed four times with PBS/3 % FCS and analyzed subsequently by flow cytometry on a FACS-Scan (Becton Dickinson, USA) or a FACS-Calibur (Becton Dickinson, USA). To distinguish between living cells and dead cells, 1 μl/ml propidium iodide (Invitrogen, Karlsruhe) was added to each sample.

Primary antibody:	KL25 1:100
Secondary antibody:	Alexa Fluor 488 goat anti-mouse IgG 1:400
	PE-conjugated goat anti-mouse IgG 1:40

2.2.7 Production and analysis of LCMV pseudoviruses

MLV-based LCMV pseudoviruses

For the transient production of LCMV GP-C pseudoviruses, one 10 cm dish of subconfluently grown HEK 293T cells was transfected with 7.5 μg of pMP71-eGFP, 12.5 μg pSV-Mo-MLVgagpol, and 2 μg of LCMV pGP-C-HA (wt or mutant) using a calcium phosphate transfection kit (Sigma, Taufkirchen). The medium was replaced 6 to 8 hours after transfection. The supernatants containing the LCMV GP-C pseudoviral particles were harvested 39 and 48 hours after transfection, filtered through a 0.45 μm Millex-HV filter (Millipore, Schwalbach), and used for transduction of target cells and Western blot analysis of GP-C.
For Western blotting, purified pseudoviruses were obtained by ultracentrifugation of 10 ml supernatant of transfected cells through 1.5 ml of a 20 % sucrose cushion in a SW41 Beckman rotor (2 h, 25000 rpm, 4°C). Pelleted pseudoviruses were lysed in Schägger loading

buffer and analyzed by Western blot. Glycoprotein amounts were quantified using the ImageJ software (National Institute of Health).
The infectivity of pseudoviral particles was determined by flow cytometry of transduced TE671 cells. TE671 cells were seeded at a density of 5×10^4 cells in 24-well plates and incubated over night. Dilutions of supernatants were added to the cells and plates were centrifuged at 1000 ×g for 1 h. 24 h later, supernatants were removed and the cells were cultivated in normal growth medium. The percentage of eGFP positive cells was determined 72 h post transduction with a FACS-Calibur (Becton Dickinson, USA). Infectivity of pseudoviral particles was normalized to the amount of LCMV GP-C quantified from the Western blot of virus lysates.

Fluorescently labeled LCMV pseudoviruses

To generate fluorescently labeled LCMV pseudoviruses, one 10 cm dish of subconfluently grown HEK 293T cells was transfected with 4 μg LCMV pGP-C-HA (wt or mutant), 3 μg pSV-Mo-MLVgagpol, 1 μg MLV Gag-YFP, 4 μg pMP71-eGFP, and 8 μg carrier DNA using Lipofectamine 2000. Viral particles lacking a glycoprotein in the viral membrane were produced without LCMV pGP-C-HA. For transfection, the DNA was diluted in 1.25 ml serum-free medium. In a separate Eppendorf cup 30 μl Lipofectamine 2000 was mixed with 1.25 ml serum-free medium, incubated for 5 min and added to the DNA solution. After 20 min incubation, the mixture was pipetted onto the cells. The medium was changed to the growth medium (DMEM/F-12) after incubation of the cells at 37°C for 5 hours. Produced pseudoviruses released into the cell culture supernatant were collected 48 hours after transfection and filtered through a 0.45 μm Millex-HA filter (Millipore, Schwalbach). For transduction of target cells, the collected cell culture supernatant was added to HeLa cells grown on a coverslip in a 12-well plate.
To analyze the binding and uptake of the fluorescently labeled pseudoviruses, HeLa cells were incubated with the pseudovirus containing supernatant at 37°C for 1 hour. After extensive washing with PBS, the cells were fixed with 4 % formaldehyde (EM grade, methanol free, Polysciences, Eppelheim). Coverslips with fixed cells were mounted with Mowiol mounting medium containing 0.1 μg/ml DAPI.
In order to analyze the infectivity of the produced pseudoviruses, HeLa cells were incubated with the collected supernatant of transfected HEK 293T cells over night at 37°C. After removal of the pseudovirus containing supernatant, the cells were cultivated in normal growth medium for 3 to 4 days to allow for eGFP expression, fixed with 4 % formaldehyde and mounted with Mowiol mounting medium containing 0.1 μg/ml DAPI.

Immunofluorescence microscopy was performed on a Leica DM IRE2 microscope (Leica, Bensheim) with a 100 × oil immersion objective (HCX PL APO CS 100/1,4 0,7, Leica,

Bensheim). Pictures were taken with an ORCA ER digital camera (Hamamatsu Photonics, Herrsching am Ammersee) using Openlab 5.0.2 (Improvision, Heidelberg). The used filter cubes were purchased from AHF Analysentechnik (Tübingen) or Leica (Bensheim).

Mowiol mounting medium: 6 g water free glycerol, 2.4 g Mowiol 40-88, 6 ml H_2O, 12 ml 0.2 M Tris/HCl pH 8.5

Filter	**Exciter**	**Beamsplitter**	**Emitter**
YFP (AHF: F31-040)	D 510/20	530 DCLP	D 560/40
EGFP (AHF: F41-017)	HQ 470/40	Q 495 LP	HQ 525/50
DAPI (Leica: A)	BP 340-380	LP 400	LP 425

3 Results

3.1 The LCMV $SP^{GP\text{-}C}$ is essential for GP-C processing and transport to the cell surface

Most secretory and membrane proteins are synthesized as preproteins with an N-terminal signal sequence that targets the protein to the ER. Signal sequences are usually 15 to 25 amino acid residues in length and contain a central hydrophobic core. The signal sequences of the arenavirus precursor glycoproteins (pGP-Cs) are longer than average signal sequences and share several well-conserved features, like an extended N-terminal region and two hydrophobic regions. After pGP-C insertion into the membrane of the ER the signal sequence is cleaved off by the ER resident signal peptidase (SPase). For the lymphocytic choriomeningitis virus (LCMV), the prototypic arenavirus, it was shown that the resulting signal peptide, called SP^{GP-C}, accumulates in cells and virus particles (Froeschke et al., 2003). After co-translational cleavage of SP^{GP-C}, GP-C is further processed into GP-1 and GP-2 while transported to the cell surface. Together the peripheral protein GP-1 and the membrane-anchored GP-2 build up the viral glycoprotein (GP) complex. For the Lassa virus, a further member of the arenavirus family, it has been shown that the cleaved signal peptide of GP-C is needed for the processing of the glycoprotein into its subunits (Eichler et al., 2003a).
In order to investigate whether the LCMV SP^{GP-C} is essential for GP-C processing and transport of the GP complex to the cell surface, the SP^{GP-C} was replaced by the signal sequence of the vesicular stomatitis virus glycoprotein precursor (pVSV-G) (Figure 3.1). The pVSV-G signal sequence contains the characteristic short N-terminal region and one central hydrophobic core of a minimal signal sequence for ER targeting (von Heijne, 1985). To allow for immunodetection the constructs were C-terminally HA-tagged.

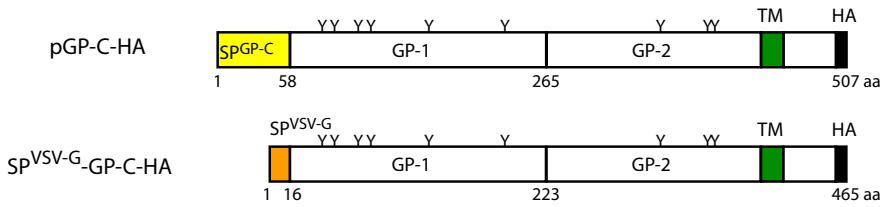

Figure 3.1: Substitution of SP^{GP-C} with SP^{VSV-G}
Schematic representation of LCMV pGP-C-HA and GP-C-HA fused to the signal sequence of the VSV glycoprotein (SP^{VSV-G}-GP-C-HA). The SP^{GP-C} (58 amino acids (aa)), the SP^{VSV-G} (16 aa), and the GP-C subunits (GP-1 and GP-2) are indicated. Putative N-glycosylation sites (Y), the transmembrane region (TM), and the HA-tag are marked.

To determine the effect of the SP^{GP-C} substitution on GP-C maturation, the proteins were expressed in HeLa cells and analyzed by Western blot. After cell lysis in a Triton lysis buffer, the proteins were treated with the peptide-N-glycosidase F (PNGase F) to remove N-linked oligosaccharide side chains or left untreated. Soluble proteins were separated by SDS polyacrylamide gel electrophoresis (PAGE) using a Tris-Tricine gradient gel. After transfer onto nitrocellulose, the membrane was probed with the anti-HA antibody. For pGP-C-HA and SP^{VSV-G}-GP-C-HA, the glycosylated GP-C-HA of about 70 kDa and, after PNGase F treatment, its unglycosylated lower-molecular-mass form, GP-C-HA*, of about 49 kDa were detected (Figure 3.2 A). As glycosylation requires membrane translocation of GP-C-HA, the VSV-G signal sequence is able to target GP-C-HA to the ER, leading to membrane insertion of the glycoprotein. In addition to the full length protein, the glycosylated GP-2-HA (about 36 kDa) and, after PNGase F treatment, the unglycosylated form (about 27 kDa) were detected for pGP-C-HA but not for SP^{VSV-G}-GP-C-HA expressing cells. Thus, an unrelated signal sequence still promotes insertion of LCMV GP-C into the ER membrane, but proteolytic processing of GP-C into GP-1 and GP-2 depends on the presence of the authentic SP^{GP-C}.

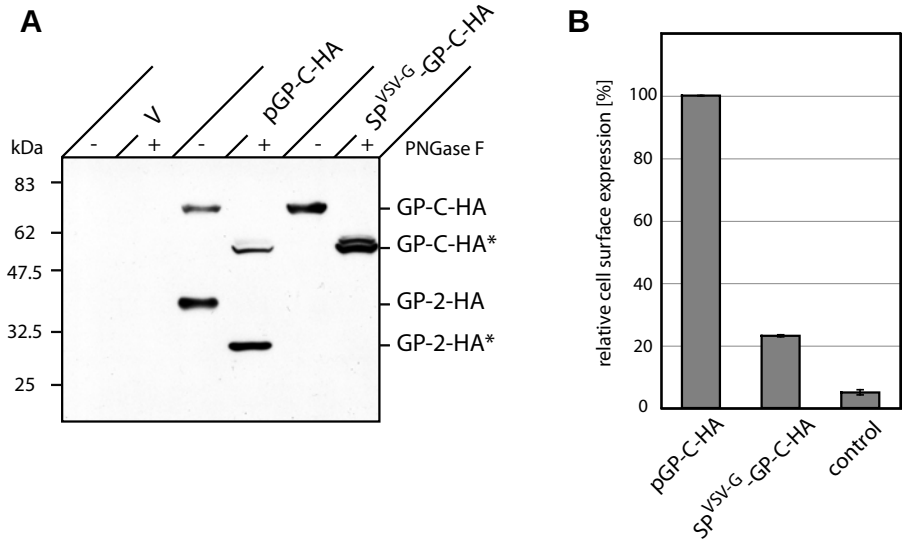

Figure 3.2: Effect of SP^{GP-C} substitution with SP^{VSV-G} on GP-C processing and transport
(A) Analysis of ER insertion and processing of GP-C. HeLa cells transfected with pGP-C-HA, SP^{VSV-G}-GP-C-HA or vector control plasmid (V) were lysed with 1% Triton X-100 and analyzed by Western blot using the anti-HA antibody. Where indicated, proteins were deglycosylated with PNGase F to remove all N-linked carbohydrates. Deglycosylated proteins are marked by an asterisk. **(B)** Analysis of cell surface expression. Transfected HEK 293T cells expressing pGP-C-HA or SP^{VSV-G}-GP-C-HA as well as untransfected control cells were analyzed by flow cytometry with the GP-1-specific KL25 antibody. The GP amount detected for pGP-C-HA expressing cells was set to 100 %. Data represent three independent experiments (± standard deviation).

Processing of the LCMV GP-C into GP-1 and GP-2 is not a prerequisite for cell surface expression of the GP complex (Beyer et al., 2003; Kunz et al., 2003). To investigate the

influence of the SP^{GP-C} substitution on transport of the glycoprotein, the GP amount on the cell surface of transfected cells was determined by flow cytometry using the KL25 antibody, which recognizes an epitope in the GP-1 subunit (Bruns et al., 1983). After transient transfection of HEK 293T cells with pGP-C-HA or SP^{VSV-G}-GP-C-HA, intact cells were incubated with the KL25 antibody and subsequently with a fluorescently labeled secondary antibody. Cell surface expression of the GPs was detected for pGP-C-HA expressing cells and was set to 100 % (Figure 3.2 B). The detected amount of GP-C-HA on the cell surface derived from the SP^{VSV-G}-containing precursor protein was drastically reduced compared to the amount seen with pGP-C-HA. Thus, the LCMV SP^{GP-C} is required for the cell surface expression of the GP complex. Substitution with the VSV-G signal sequence results in an intracellular accumulation of the glycoprotein.

3.2 Effects of C-terminal truncations of LCMV GP-C on GP-C processing and transport

Assembly of oligomeric complexes typically takes place in the endoplasmic reticulum (Hurtley and Helenius, 1989). To ensure that only fully assembled complexes are transported to their destination, transmembrane proteins often encode specific ER localization signals within the cytoplasmic domain (Ellgaard and Helenius, 2003; Teasdale and Jackson, 1996). The deletion of the cytoplasmic domains of viral glycoproteins was also shown to have profound effects on ectodomain structure and function (Edwards et al., 2002; Krzyzaniak et al., 2007; de Zarate et al., 2004). In order to investigate the role of the cytoplasmic domain of LCMV GP-C in glycoprotein maturation, the C-terminus of GP-C was truncated leaving 6 amino acids after the transmembrane region (pGP-C/ΔC) (Figure 3.3 A). As the substitution of SP^{GP-C} with SP^{VSV-G} resulted in an intracellular accumulation of the glycoprotein, a ΔC deletion mutant of SP^{VSV-G}-GP-C was also analyzed.

In order to determine the effect of the deletion on GP-C processing, HeLa cells expressing pGP-C-HA or one of the GP-C ΔC deletion mutants were metabolically labeled for 30 min with ^{35}S-Met/Cys (pulse) and lysed directly or chased for 3 hours in non-radioactive medium to allow for transport and processing of GP-C. Lysed proteins were immunoprecipitated using the KL25 antibody and analyzed by SDS-PAGE and autoradiography. To show ER membrane insertion by glycosylation of the proteins and to better resolve the GP-1 and GP-2 subunits, proteins were deglycosylated with PNGase F or left untreated. Directly after the pulse, the glycosylated GP-C-HA was detected for the pGP-C-HA expressing cells and the glycosylated shorter GP-C/ΔC (about 65 kDa) for the pGP-C/ΔC and the SP^{VSV-G}-GP-C/ΔC deletion mutants (Figure 3.3 B). The double banding pattern in case of the pGP-C-HA and the pGP-C/ΔC might be due to inefficient cleavage of the SP^{GP-C} (Froeschke et al., 2003). Expression of pGP-C-HA and a chase of 3 hours resulted in the immunoprecipitation of two additional diffuse bands which resolve into

distinct bands after PNGase F treatment (lanes 7 and 8). These bands represent GP-1* (about 23 kDa (lane 8)) and the co-immunoprecipitated GP-2-HA* (about 27 kDa). For the pGP-C/ΔC and SP^{VSV-G}-GP-C/ΔC mutants only a weak band was detected in addition to the full length GP-C/ΔC in the PNGase F treated samples after the 3 hours chase (lanes 12 and 16). As the expected molecular weight of the truncated GP-2 subunit, GP-2/ΔC* (about 22 kDa), and the GP-1 subunit differ by only 1 kDa, both subunits overlap leading to only one additional band. In the untreated sample the band might be to diffuse to be detected. For pGP-C-HA and, to a lower amount, for pGP-C/ΔC expressing cells a further protein of about 6 kDa was detected (arrow). Due to the molecular weight, this band most likely represents the cleaved SP^{GP-C} (see section 3.5). Taken together, the deletion of the cytoplasmic domain of LCMV GP-C drastically effects processing of GP-C into GP-1 and GP-2. This effect is independent of the type of signal sequence that mediates GP-C insertion into the ER membrane.

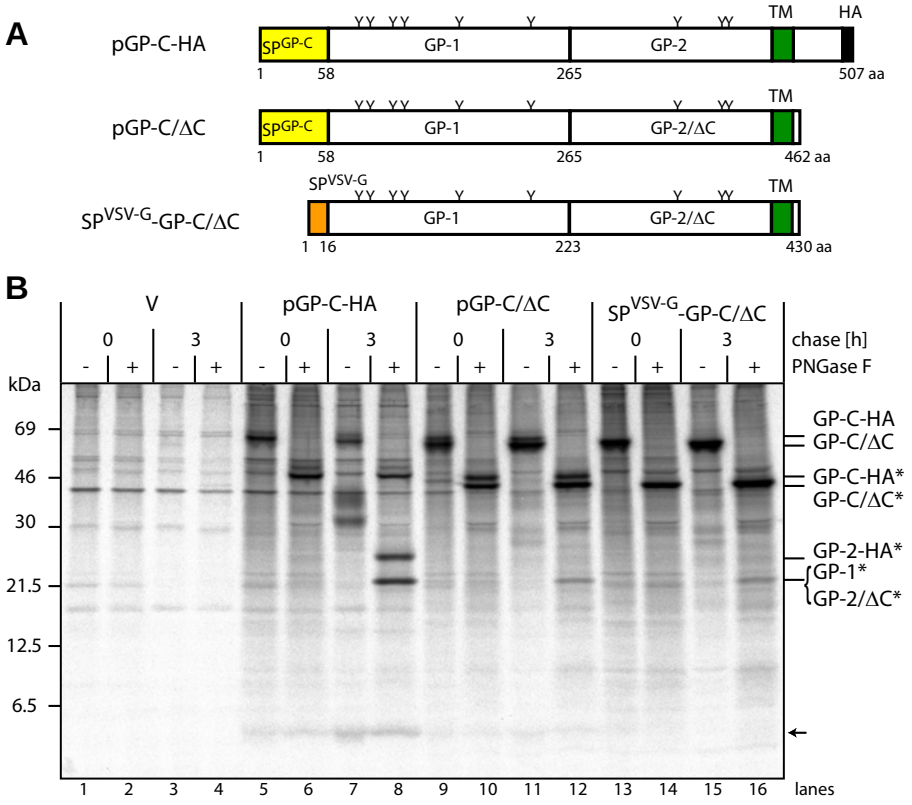

Figure 3.3: ER insertion and processing of the GP-C ΔC deletion mutants
(A) Schematic representation of pGP-C-HA, pGP-C/ΔC and SP^{VSV-G}-GP-C/ΔC. In both ΔC deletion mutants the GP-C C-terminus was deleted 6 amino acids after the transmembrane region (TM). The putative N-glycosylation sites (Y) are indicated. **(B)** HeLa cells expressing pGP-C-HA, pGP-C/ΔC, SP^{VSV-G}-GP-C/ΔC or mock treated cells (V) were metabolically labeled (pulse) and chased for the indicated time periods. After solubilization with 1 % Triton X-100, proteins were immunoprecipitation with the KL25 antibody and where indicated deglycosylated with PNGase F. Deglycosylated proteins are marked by an asterisk. The position of an additional 6 kDa band is marked by an arrow.

To see whether the deletion of the cytoplasmic domain of GP-C effects the intracellular transport of the glycoprotein, the cell surface expression of the GP-C ΔC deletion mutants was analyzed by flow cytometry using the KL25 antibody. Cell surface expression was detected for pGP-C-HA, pGP-C/ΔC and to a very low extent for SP^{VSV-G}-GP-C/ΔC expressing cells (Figure 3.4). The detected amount for pGP-C/ΔC, however, was reduced compared to pGP-C-HA. The reduction of cell surface expression was even stronger in SP^{VSV-G}-GP-C/ΔC expressing cells. Thus, deletion of the cytoplasmic domain of LCMV GP-C has an influence on the transport efficiency of the glycoprotein to the cell surface. The substitution of SP^{GP-C} with SP^{VSV-G} further decreased the amount of the glycoprotein detected on the plasma membrane. Hence, SP^{GP-C} is still required for the cell surface expression of LCMV GP-C when the cytoplasmic domain of GP-C is deleted.

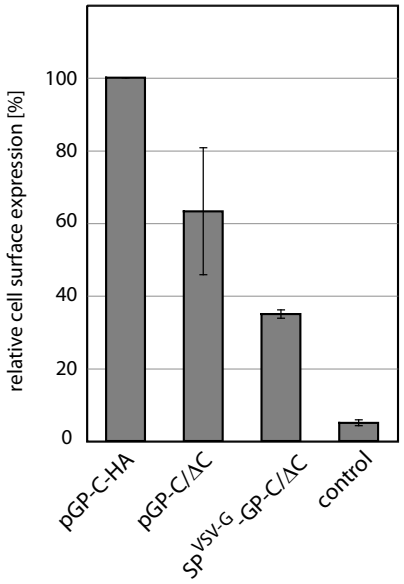

Figure 3.4: Cell surface expression of the GP-C ΔC deletion mutants
Transfected HEK 293T cells expressing pGP-C-HA, pGP-C/ΔC or SP^{VSV-G}-GP-C/ΔC as well as untransfected control cells were analyzed by flow cytometry using the KL25 antibody. Data represent cell surface expression of the glycoproteins normalized to the amount detected for pGP-C-HA expressing cells (set to 100 %) from three independent experiments (± standard deviation).

Analysis of a secretory form of GP-C

To further analyze the requirements for a SP^{GP-C}-dependent transport of GP-C to the cell surface, the transmembrane region of GP-C was deleted in addition to the cytoplasmic domain, generating the GP-C ΔTMC deletion mutants shown in Figure 3.5 A. Again the signal sequence of LCMV pGP-C or that of pVSV-G was used to target the now secretory form of GP-C to the ER.

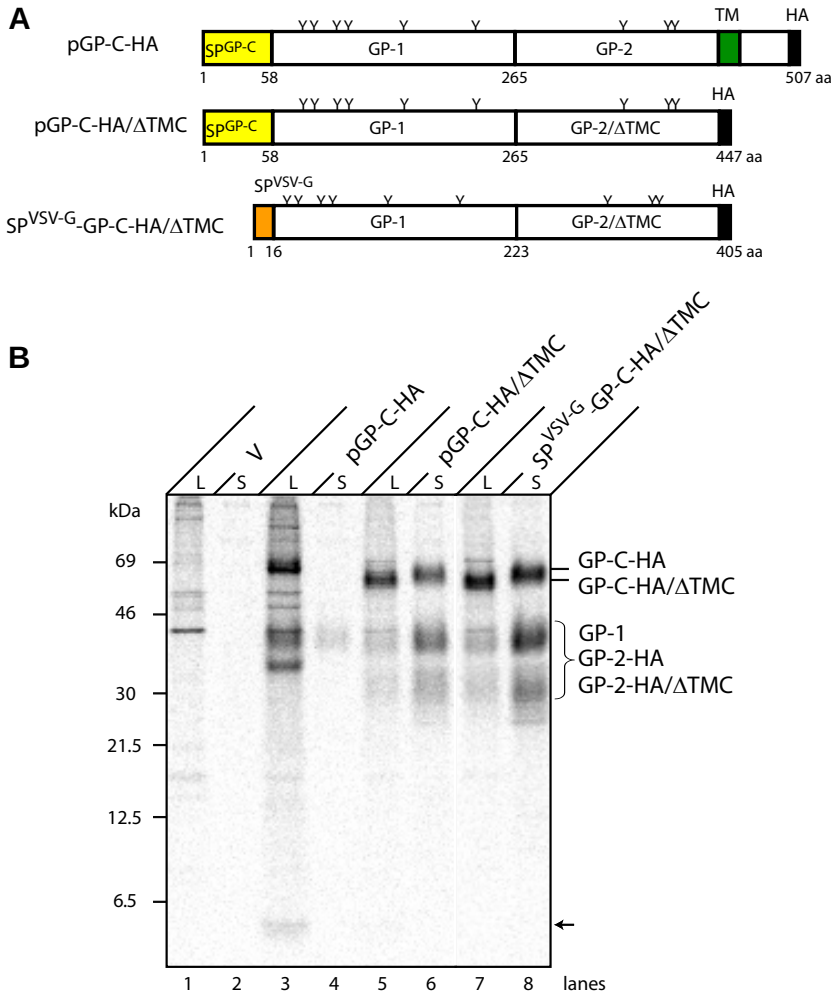

Figure 3.5: Expression and secretion of the GP-C ΔTMC deletion mutants
(A) Schematic representation of pGP-C-HA, pGP-C-HA/ΔTMC, and SP^{VSV-G}-GP-C-HA/ΔTMC. The C-terminal truncations include the cytoplasmic and the transmembrane (TM) region of GP-2. All constructs are C-terminally HA-tagged. **(B)** Pulse-chase analysis of the GP-C ΔTMC deletion mutants. HeLa cells transfected with pGP-C-HA, pGP-C-HA/ΔTMC, SP^{VSV-G}-GP-C-HA/ΔTMC or vector control plasmid (V) were metabolically labeled (pulse) and chased for 3 hours. The cell culture supernatant (S) as well as the cell lysate (L) were used for immunoprecipitation with the KL25 antibody. The full length glycoproteins (GP-C-HA and GP-C-HA/ΔTMC), the subunits and an additional 6 kDa protein (arrow) are indicated.

HeLa cells expressing pGP-C-HA or one of the GP-C ΔTMC deletion mutants were metabolically labeled (pulse) and chased in non-radioactive medium for 3 hours to allow for protein transport. Due to the lack of the transmembrane region, the truncated proteins will be secreted into the medium instead of being expressed on the cell surface if they were transported through the secretory pathway. To detect the secreted glycoproteins, the cell culture supernatant was collected before cell lysis. Both, cell lysate and cell culture supernatant, were subjected to immunoprecipitation with the KL25 antibody (Figure 3.5 B). In the cell lysate (L) of pGP-C-HA expressing cells the glycosylated GP-C-HA, the GP-1 and GP-2-HA subunits and a protein of about 6 kDa (arrow;

see section 3.5) were detected (lane 3). The diffuse banding pattern for the GP-C subunits is due to the glycosylation of the proteins. In the cell culture supernatant (S) only one diffuse band was detected (lane 4). It most likely corresponds to GP-1 released by shedding from the non-covalently associated GP complex on the cell surface. For cells expressing the pGP-C-HA/ΔTMC or the SP^{VSV-G}-GP-C-HA/ΔTMC deletion mutant, GP-C-HA/ΔTMC (about 64 kDa) was detected in the cell lysate and the cell culture supernatant. A 6 kDa protein was not detected. The processing products, GP-1 and the truncated form of GP-2-HA (GP-2-HA/ΔTMC), were for both GP-C deletion mutants mainly found in the cell supernatant (lanes 6 and 8). Thus, transport and processing of GP-C lacking the cytoplasmic domain and the transmembrane region (ΔTMC) to the cell surface is independent of the type of signal sequence that targets the protein to the ER.

3.3 The SP^{GP-C} h-regions are required for distinct steps in LCMV GP-C maturation

Signal sequences have a typical tripartite structure with one central hydrophobic core (h-region), a polar N-terminal region (n-region) that is usually positively charged, and a short C-terminal region (c-region) containing the SPase cleavage site (von Heijne, 1985). The signal sequence of the LCMV pGP-C, however, contains two h-regions separated by a lysine residue and an overall negatively charged n-region (Figure 3.6). In order to investigate possible functions of the two h-regions either of them was deleted (Δh1 and Δh2) and membrane insertion of pGP-C, processing into GP-1 and GP-2 and intracellular transport of the GP complex was analyzed. To identify a possible contribution of the SP^{GP-C} n-region to these processes, the n-region was deleted leaving the initiating methionine and the negatively charged glutamic acid in front of the h1-region (ΔnME) as in wild type (wt) SP^{GP-C}, or replaced the glutamic acid by a positively charged lysine residue (ΔnMK).

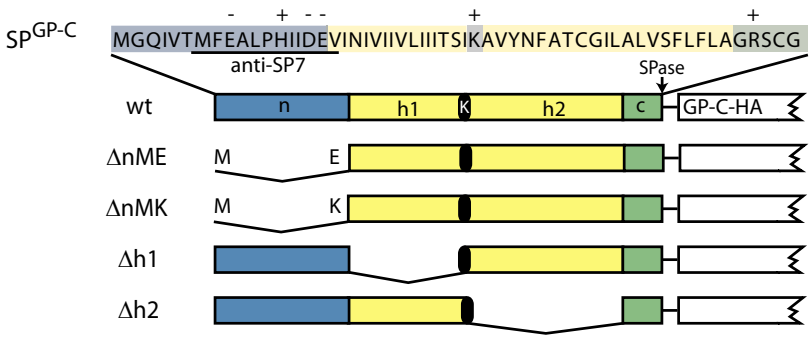

Figure 3.6: Outline of SP^{GP-C} deletion mutants
On top the sequence of wt SP^{GP-C} in one-letter amino acid code is shown. In the schematic representation of SP^{GP-C} (wt) and the SP^{GP-C} deletion mutants, the N-terminal (n), hydrophobic (h1 and h2), and C-terminal (c) regions are indicated. The region to which the SP^{GP-C} antibody was raised (anti-SP7) (Froeschke et al., 2003) and the SPase cleavage site are marked. Charged amino acid residues are indicated.

3.3.1 One SP^{GP-C} h-region is sufficient for ER membrane insertion of pGP-C while both are required for GP-C processing

HeLa cells expressing pGP-C-HA (wt) or one of the SP^{GP-C} deletion mutants (ΔnME, ΔnMK, Δh1, Δh2) were lysed in a Triton lysis buffer and soluble proteins were treated with PNGase F to remove N-linked oligosaccharide side chains or left untreated. After transfer of the proteins onto nitrocellulose, the membrane was probed with the anti-HA antibody (Figure 3.7). For the wt and all SP^{GP-C} deletion mutants the glycosylated GP-C-HA and, after PNGase F treatment, its unglycosylated smaller-molecular-mass form, GP-C-HA*, were detected. The expression levels of the SP^{GP-C} deletion mutants were comparable to those of the wt, with the exception of Δh2, where a reduced amount of GP-C-HA was detected. As glycosylation requires membrane translocation of GP-C-HA, the results show that only one SP^{GP-C} h-region is required for ER membrane insertion of pGP-C-HA. The detected double banding pattern of the PNGase F treated samples might be due to inefficient deglycosylation of GP-C-HA. Processing of GP-C-HA into GP-1 and GP-2-HA, indicated by the appearance of glycosylated GP-2-HA, was only detected for the wt and the ΔnME mutant (Figure 3.7, lanes 2-5) but was not detected for the other deletion mutants (lanes 6-11). Thus, both h-regions and a negatively charged amino acid in front of the h1-region are required for processing of GP-C into its subunits. A positively charged amino acid in the same position prevents GP-C processing.

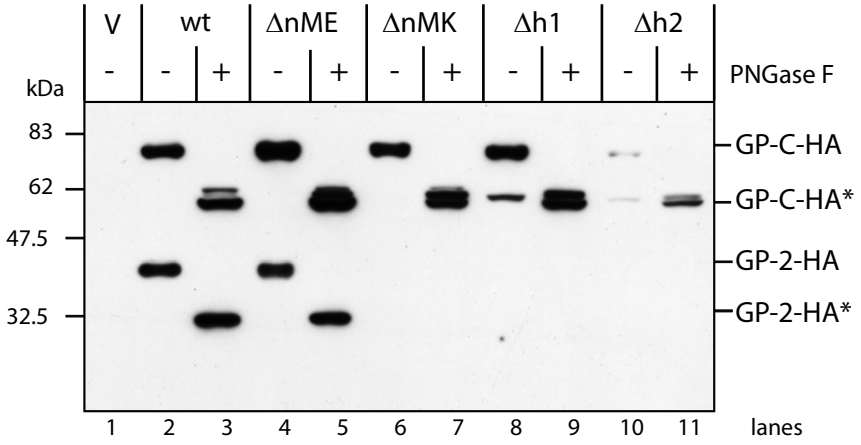

Figure 3.7: Effects of SP^{GP-C} deletions on ER membrane insertion and processing of GP-C
HeLa cells transfected with vector control plasmid (V) or expression plasmids encoding for pGP-C-HA (wt) or one of the SP^{GP-C} deletion mutants were solubilized with 1 % Triton X-100 and analyzed by Western blot using the anti-HA antibody. Where indicated, proteins were deglycosylated with PNGase F. The glycosylated GP-C-HA and GP-2-HA as well as the deglycosylated proteins, marked by an asterisk, are indicated.

The possible effect of the deletions on SP^{GP-C} stability was subsequently investigated. As the epitope that is recognized by the anti-SP7 antibody is deleted in case of the Δn SP^{GP-C}, it was only possible to analyze the Δh1 and Δh2 deletion mutants. HeLa

cells expressing pGP-C-HA (wt) or one of the SP^{GP-C} h-region deletion mutants were metabolically labeled (pulse) and lysed directly or chased for 3 hours. Proteins were immunoprecipitated using the anti-SP7 antibody and analyzed by SDS-PAGE and autoradiography (Figure 3.8). For both time points the cleaved SP^{GP-C} was detected for the wt (lanes 1 and 2) and the shorter Δh2 SP^{GP-C} for the Δh2 deletion mutant (lanes 5 and 6). From cells expressing the SP^{GP-C} Δh1 deletion mutant, no Δh1 SP^{GP-C} was immunoprecipitated (lanes 3 and 4). As no precursor glycoprotein was found for any of the SP^{GP-C} deletion mutants using the anti-SP7 antibody in a Western blot (data not shown), it is most likely that the Δh1 SP^{GP-C} is rapidly degraded after cleavage from the preprotein.

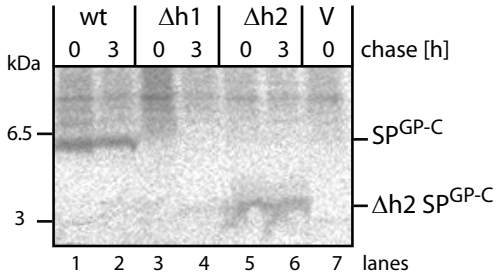

Figure 3.8: SP^{GP-C} stability of the h-region deletion mutants
HeLa cells transfected with vector control plasmid (V) or plasmids expressing pGP-C-HA (wt) or one of the SP^{GP-C} h-region deletion mutants (Δh1 or Δh2) were metabolically labeled (pulse) and chased for the times indicated. After cell lysis, antigens were immunoprecipitated using the anti-SP7 antibody. The positions of the SP^{GP-C} and the Δh2 SP^{GP-C} are indicated.

3.3.2 Both SP^{GP-C} h-regions are needed for cell surface expression of the GP complex

To investigate whether deletion of one of the SP^{GP-C} regions influences the cell surface expression of the GPs, transfected cells were analyzed by flow cytometry. These experiments were done in cooperation with T. Giroglou (research group of D. von Laer, GSH, Frankfurt a.M.) (Schrempf et al., 2007). To monitor cell surface localization of the GPs, transfected HEK 293T cells were incubated with the GP-1-specific KL25 antibody and subsequently labeled with a PE-conjugated secondary antibody. Efficient cell surface expression was detected for the wt and the ΔnME mutant (Figure 3.9). For the other deletion mutants (ΔnMK, Δh1 and Δh2) very low or no surface expression was detected. The latter SP^{GP-C} deletion mutants did also not promote processing of GP-C into GP-1 and GP-2 (see Figure 3.7). Thus, both h-regions of SP^{GP-C} are required for the cell surface expression of the GP complex, while the SP^{GP-C} n-region is dispensable. The positively charged lysine residue in front of the h1-region in the ΔnMK deletion mutant negatively influences the cell surface expression.

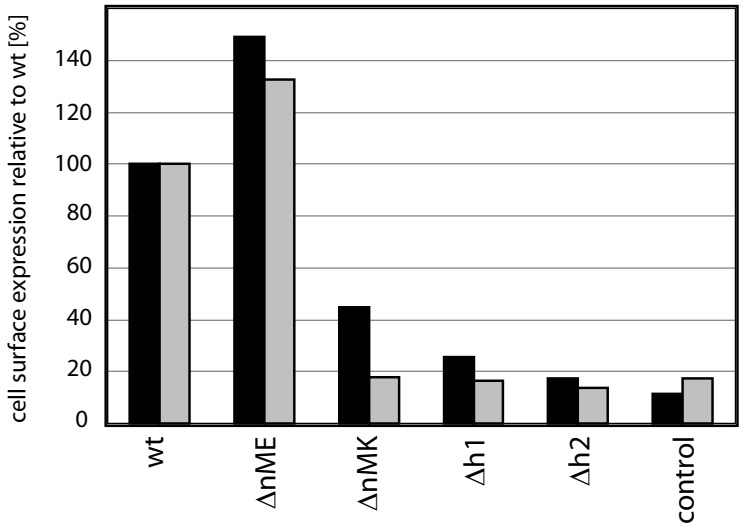

Figure 3.9: Cell surface expression of SP^{GP-C} deletion mutants
Untransfected HEK 293T cells (control) or cells expressing pGP-C-HA (wt) or one of the SP^{GP-C} deletion mutants were analyzed by flow cytometry. Cell surface expression of the GP complex was detected with the KL25 antibody directed against the GP-1 subunit. Different shaded bars represent independent experiments. Cell surface expression of wt was set to 100 %.

3.4 Use of SP^{GP-C} point mutants to investigate SP^{GP-C} membrane topology and effects on SP^{GP-C} stability and GP-C maturation

ER membrane insertion is thought to occur in a loop-like fashion such that the signal sequence spans the membrane exposing the N-terminus to the cytosol and the C-terminus with the SPase cleavage site to the ER lumen (Walter et al., 1984). In such a topology the signal sequence can get co-translationally cleaved by the ER resident SPase. Minimal signal sequences contain only a single h-region and the SPase cleavage typically occurs 5 to 6 amino acids C-terminally of this region (von Heijne, 1985). As SP^{GP-C} has two h-regions it is unclear whether one or both of them span the membrane with the N-terminus exposed on the cytosolic or the lumenal side of the ER membrane. In general, it is possible that the N-terminus of the cleaved signal peptide is translocated into the lumen of the ER (von Heijne, 1989). To analyze the topology of SP^{GP-C}, potential N-glycosylation sites were introduced throughout the signal peptide. The mutations were chosen such that the overall properties of the different SP^{GP-C} regions remained essentially unchanged (Figure 3.10 A). Glycosylation of SP^{GP-C} bearing one of the mutations would indicate that the corresponding N-glycosylation consensus site is exposed on the lumenal side of the ER membrane. In the next two sections the SP^{GP-C} glycosylation mutants were used to investigate the topology of SP^{GP-C}. In addition, the influence of these point mutations on SP^{GP-C} stability and GP-C maturation was analyzed.

3.4.1 Point mutations introduced in SP^{GP-C} did not lead to SP^{GP-C} glycosylation but influence SP^{GP-C} stability and GP-C maturation

In order to investigate the topology of SP^{GP-C}, the SP^{GP-C} point mutants as well as pGP-C-HA (wt) were expressed in HeLa cells and analyzed by Western blot (Figure 3.10 B). Probing the membrane with the anti-HA antibody (top panel) showed that for each point mutant the glycosylated 70 kDa GP-C-HA was detected, indicating insertion into the ER. Processing of GP-C-HA into GP-1 and GP-2-HA was seen for the wt and the I4N, V22T, and A39T point mutants, however not for the I29N, L46N, and G54N point mutants.
To analyze SP^{GP-C} glycosylation and stability, the Western blot membrane was probed with the anti-SP7 antibody (bottom panel). Accumulation of SP^{GP-C} was seen for the wt and the I4N, V22T, and A39T point mutants, the same mutants that showed processing into GP-1 and GP-2-HA. Very small amounts of SP^{GP-C} were detected for the I29N, L46N, and G54N point mutants. For none of the SP^{GP-C} point mutants a 3-kDa-higher-molecular-mass form of SP^{GP-C}, indicative for glycosylation, was detected. Taken together, even minor changes in the amino acid sequence of SP^{GP-C} can result in drastic effects on SP^{GP-C} accumulation and GP-C processing. As for none of the investigated SP^{GP-C} point mutants a glycosylated form of SP^{GP-C} was detected, no conclusion can be drawn regarding the topology of SP^{GP-C}.

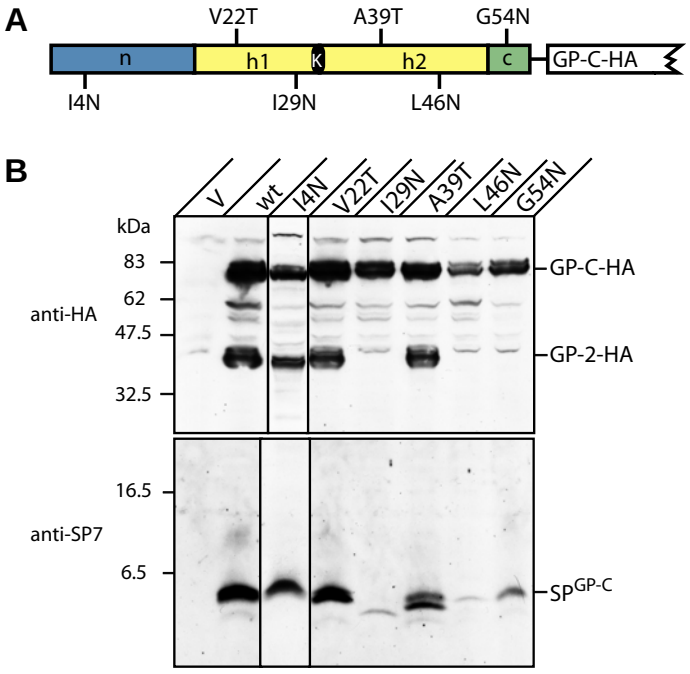

Figure 3.10: Analysis of SP^{GP-C} point mutants by Western blot
(A) Schematic outline of SP^{GP-C} with introduced point mutations to generate potential N-glycosylation sites. **(B)** Western blot analysis of HeLa cells expressing pGP-C-HA (wt) or one of the SP^{GP-C} point mutants. Proteins of whole cell lysates were separated by SDS-PAGE and identified using the anti-HA (top panel) or anti-SP7 antibody (bottom panel). Lane 3 derives from a different experiment.

The Western blot of the SP^{GP-C} point mutants showed that the detected amounts of SP^{GP-C} are very low for the I29N, L46N, and G54N point mutants. Therefore, the question arises, whether these SPs^{GP-C} are not generated or are instable and become degraded. In order to answer this question, HeLa cells expressing the SP^{GP-C} point mutants were metabolically labeled for 30 min with ^{35}S-Met/Cys and lysed directly. After cell lysis, proteins were immunoprecipitated using the anti-SP7 antibody and analyzed by SDS-PAGE and autoradiography. The cleaved SPs^{GP-C} were detected for all SP^{GP-C} point mutants (Figure 3.11). A glycosylated, 3-kDa-higher-molecular-mass form of SP^{GP-C} was detected for none of the mutants. Thus, the introduced N-glycosylation sites in SP^{GP-C} were either not exposed to the ER lumen or are not accessible to the oligosaccharyl transferase. As cleavage of SP^{GP-C} from the preprotein was detected for all SP^{GP-C} point mutants, the reduced amount of SP^{GP-C} detected in the Western blot is most likely due to SP^{GP-C} degradation.

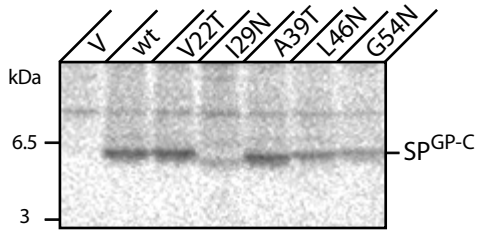

Figure 3.11: Identification of mutant SPs^{GP-C} after metabolic labeling
HeLa cells transfected with vector control plasmid (V) or plasmids expressing pGP-C-HA (wt) or one of the SP^{GP-C} point mutants were metabolically labeled and lysed directly. Antigens were immunoprecipitated with the anti-SP7 antibody. The cleaved SPs^{GP-C} are indicated.

The SP^{GP-C} point mutants that showed SP^{GP-C} degradation (I29N, L46N, and G54N) were also not processed into GP-1 and GP-2-HA. To investigate whether GP-C expressed from the different SP^{GP-C} point mutants is still transported to the plasma membrane, the cell surface expression of the GPs were analyzed by flow cytometry (done in cooperation with the research group of D. von Laer). Transfected HEK 293T cells were incubated with the KL25 antibody and subsequently with the appropriate secondary antibody. Cell surface expression of the GPs was detected for the I4N, V22T, and A39T point mutants (Figure 3.12). These mutants were also processed into GP-1 and GP-2-HA. The detected amounts on the cell surface were comparable to those detected for the wt or even higher. The I29N, L46N, and G54N point mutants were not or only in a very low amount expressed on the plasma membrane. Thus, the SP^{GP-C} point mutants that were not processed into GP-1 and GP-2 and show SP^{GP-C} degradation were mainly not transported to the cell surface.

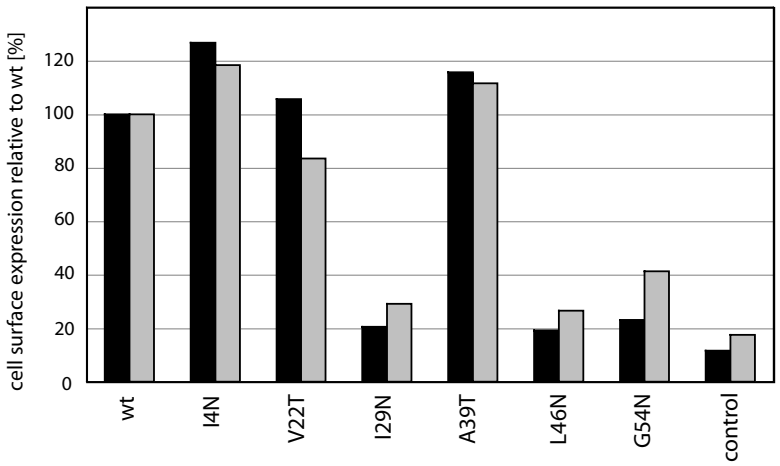

Figure 3.12: Cell surface expression of SP^{GP-C} point mutants
Transfected HEK 293T cells expressing pGP-C-HA (wt) or one of the SP^{GP-C} point mutants were analyzed by flow cytometry with the KL25 antibody. Different shaded bars represent independent experiments. Data show percent cell surface expression relative to the wt (set to 100 %).

3.4.2 The unmyristoylated SP^{GP-C} n-region is exposed to the ER lumen

The N-terminal amino acid sequence of the LCMV SP^{GP-C} match the myristoylation consensus sequence (MGxxxT/S) (Figure 3.13). This motif is conserved among all signal sequences of arenavirus pGP-Cs (York et al., 2004). Myristoylation is a co-translational event occurring after the initiating methionine has been removed. Myristate is then linked to the glycine residue via an amide bond (Resh, 1999).

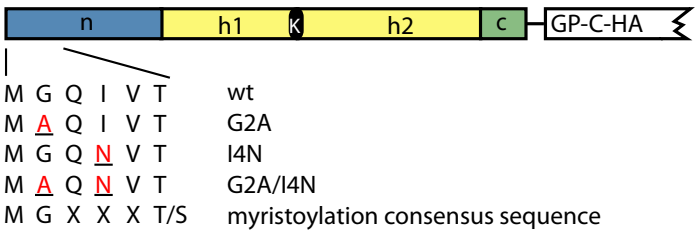

Figure 3.13: Schematic representation of SP^{GP-C} myristoylation mutants
Sequence of the extreme N-terminus of SP^{GP-C} and outline of the myristoylation consensus site in one letter amino acid code. Point mutations to prevent SP^{GP-C} myristoylation (G2A) and to allow N-glycosylation (I4N) are indicated.

Myristoylation of the LCMV SP^{GP-C} was shown by M. Fröschke, a former member of our group. He determined SP^{GP-C} myristoylation after incubation of transfected HeLa cells with ^{3}H-myristic acid and immunoprecipitation of soluble proteins with the anti-SP7 antibody. When myristoylation was inhibited by 2-Hydroxy myristic acid the amount of myristoylated SP^{GP-C} was drastically reduced. In addition, M. Fröschke showed that mutation of the glycine residue in position 2 to alanine (G2A) completely abolished SP^{GP-C}

myristoylation. These results are published in Schrempf et al. (2007). Myristoylation was also reported for SP^{GP-C} of the New World Junín arenavirus (York et al., 2004).

In this thesis the LCMV SP^{GP-C} G2A mutant was used to determine whether myristoylation of SP^{GP-C} is a prerequisite for proteolytic processing and transport of the GP complex to the plasma membrane. In order to analyze the effect of myristoylation on the orientation of the SP^{GP-C} n-region, a double mutant (G2A/I4N) combining the G2A myristoylation mutant and the I4N glycosylation mutant was investigated (Figure 3.13). This G2A/I4N double mutant cannot be myristoylated, but the n-region of SP^{GP-C} can be N-glycosylated at the asparagine residue in position 4 if it is exposed to the ER lumen.

HeLa cells transfected with a plasmid encoding pGP-C-HA (wt), G2A, I4N or the G2A/I4N double mutant were lysed and soluble proteins were analyzed by Western blot using the anti-HA antibody (Figure 3.14, top panel). For the wt and all mutants, the glycosylated, ER inserted GP-C-HA and the processing product GP-2-HA were detected. Probing the membrane with the anti-SP7 antibody revealed SP^{GP-C} accumulation for the G2A and I4N mutants in an amount comparable to the wt (bottom panel). For the G2A/I4N double mutant, a low amount of SP^{GP-C} and, in addition, a 3-kDa-higher-molecular-mass form of SP^{GP-C} (gSP^{GP-C}) were detected. This higher-molecular-mass form was identified as glycosylated SP^{GP-C} as it disappeared at the expense of wt-sized SP^{GP-C} after deglycosylation with PNGase F or Endo H (M. Fröschke, Schrempf et al. (2007)).

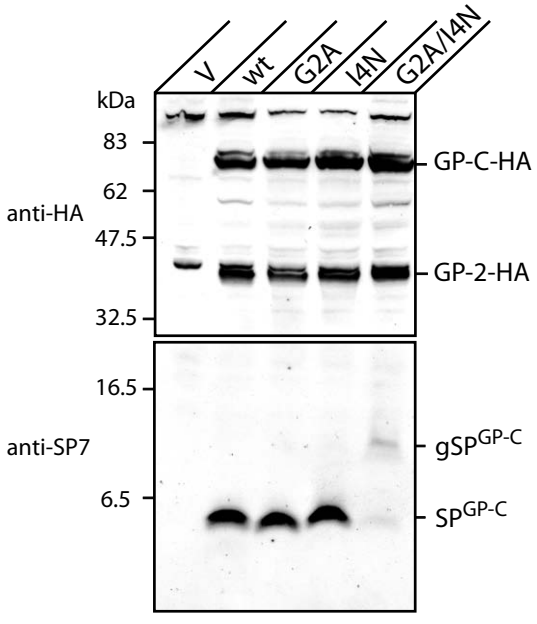

Figure 3.14: Analysis of SP^{GP-C} myristoylation mutants by Western blot
Whole cell lysates of HeLa cells transfected with pGP-C-HA (wt), the I4N glycosylation mutant or one of the SP^{GP-C} myristoylation mutants (G2A or G2A/I4N) were separated by SDS-PAGE and analyzed by Western blot with the anti-HA (top panel) or anti-SP7 antibody (bottom panel). gSP^{GP-C} indicates the glycosylated 3-kDa-higher-molecular-mass form of SP^{GP-C}.

In order to determine whether the SP^{GP-C} myristoylation mutants were transported to the plasma membrane, HEK 293T cells were transfected with plasmids encoding pGP-C-HA (wt), the G2A mutant or the G2A/I4N double mutant. Cell surface expression of the GPs was analyzed by flow cytometry using the KL25 antibody (done in cooperation with the research group of D. von Laer). For the G2A as well as for the G2A/I4N expressing cells, the GP complex was detected on the cell surface in an amount comparable to the amount detected for the wt (Figure 3.15).

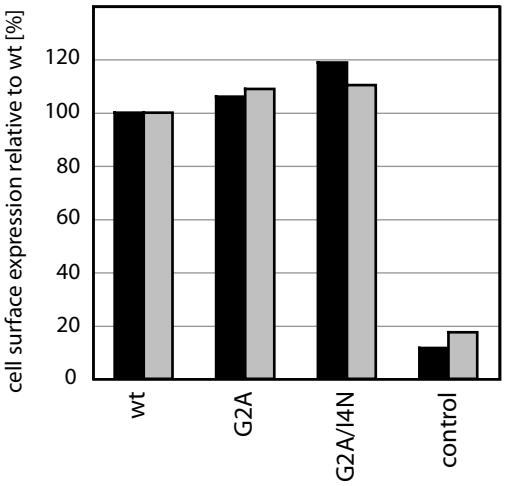

Figure 3.15: Cell surface expression of SP^{GP-C} myristoylation mutants
Transfected HEK 293T cells expressing pGP-C-HA (wt), the G2A or the G2A/I4N myristoylation mutant were analyzed by flow cytometry using the KL25 antibody. Different shaded bars represent cell surface expression from two independent experiments.

Taken together, the results show that the SP^{GP-C} n-region can become glycosylated and thus exposed to the ER lumen when myristoylation is prevented by the G2A mutation. Furthermore, prevention of SP^{GP-C} myristoylation and glycosylation at the asparagine residue in position 4 do not interfere with processing of GP-C into GP-1 and GP-2 and transport of the GP complex to the plasma membrane.

3.5 SP^{GP-C} is part of the LCMV GP complex

As SP^{GP-C} is required for LCMV GP-C maturation and was furthermore found to accumulate in LCMV particles (Froeschke et al., 2003), it is likely that it assembles into the particles as part of the GP complex. To investigate a possible interaction, it was tested whether SP^{GP-C} can be co-immunoprecipitated with the GPs.

3.5.1 Co-immunoprecipitation of $SP^{GP\text{-}C}$ with GP-C under different lysing conditions

In order to analyze a possible interaction between the LCMV SP^{GP-C} and the GPs, it is important to determine the conditions under which the proteins can be solubilized and non-covalent protein complexes remain bound. As the forces that are involved in non-covalent protein-protein interactions include electrostatic forces and hydrophobic effects, non-ionic detergents in combination with low and high salt concentrations as well as ionic detergents were used for protein solubilization. The non-ionic detergents used are digitonin, Triton X-100, and Octyl-β-D-glucopyranoside (ODG). ODG is a detergent that is known to efficiently extract proteins from Triton-resistant membranes (Brown and Rose, 1992). In order to solubilize most of the cellular proteins, while not affecting the antibody-antigen interaction, the RIPA lysis buffer containing Triton X-100 and low amounts of the ionic detergents sodium deoxycholate and SDS was used.

Transient transfected HeLa cells expressing pGP-C-HA were metabolically labeled with ^{35}S-Met/Cys for 30 min followed by protein solubilization using different lysis buffers as above-mentioned. After immunoprecipitation with the KL25 antibody, proteins were separated by SDS-PAGE and analyzed by autoradiography. The glycosylated GP-C-HA was detected under all lysing conditions tested (Figure 3.16, top panel). The highest amount of GP-C-HA was detected after lysis with the RIPA buffer. In comparison, cell lysis with ODG, Triton X-100 or digitonin resulted in a slightly reduced amount of immunoprecipitated GP-C-HA. The increase of the salt concentration from 150 mM to 500 mM NaCl in combination with Triton X-100 and digitonin did not much alter the detected amounts of GP-C-HA. Note that even the lowest amount of digitonin (0.2 %) was already sufficient to solubilize GP-C-HA. In addition to GP-C-HA, a protein of about 6 kDa representing SP^{GP-C} was detected in all samples to a different extent. Whereas nearly no SP^{GP-C} was co-immunoprecipitated with GP-C-HA after cell lysis with the RIPA buffer, the highest amount of SP^{GP-C} was detected using a digitonin-containing lysis buffer. The two tested salt concentration combined with Triton X-100 or digitonin showed nearly no difference in the amount of co-immunoprecipitated SP^{GP-C}. Taken together, SP^{GP-C} co-immunoprecipitates with GP-C and cell lysis with digitonin is sufficient to solubilize the GP complex.

To determine the total amount of SP^{GP-C} and to investigate the solubility of SP^{GP-C} under the different lysing conditions, an aliquot of each sample was used for immunoprecipitation with the anti-SP7 antibody. SP^{GP-C} was detected after cell lysis with the RIPA buffer, ODG and Triton X-100 (Figure 3.16, bottom panel). No SP^{GP-C} was immunoprecipitated after protein solubilization with digitonin. The shift of SP^{GP-C} after cell lysis with the ODG buffer is most likely due to an incomplete displacement of the detergent by SDS resulting in an altered mobility in the gel. In addition to SP^{GP-C}, the precursor glycoprotein, pGP-C-HA, was detected in some samples. Comparing the amounts of SP^{GP-C}

detected with the anti-SP7 antibody and the amounts of SP^{GP-C} co-immunoprecipitated with GP-C-HA reveals that a high amount of co-immunoprecipitated SP^{GP-C} correlates with a low amount of immunoprecipitated SP^{GP-C} and the other way around. Thus, interaction of SP^{GP-C} with GP-C-HA seems to impair binding of the anti-SP7 antibody. The high amount of co-immunoprecipitated SP^{GP-C} and the low accessibility of the anti-SP7 antibody in the presence of digitonin, indicates a tight association of the complex. The increased accessibility of the anti-SP7 antibody after cell lysis with Triton X-100 and the lower amount of co-immunoprecipitated SP^{GP-C} suggest a weaker interaction between SP^{GP-C} and GP-C-HA under these conditions.

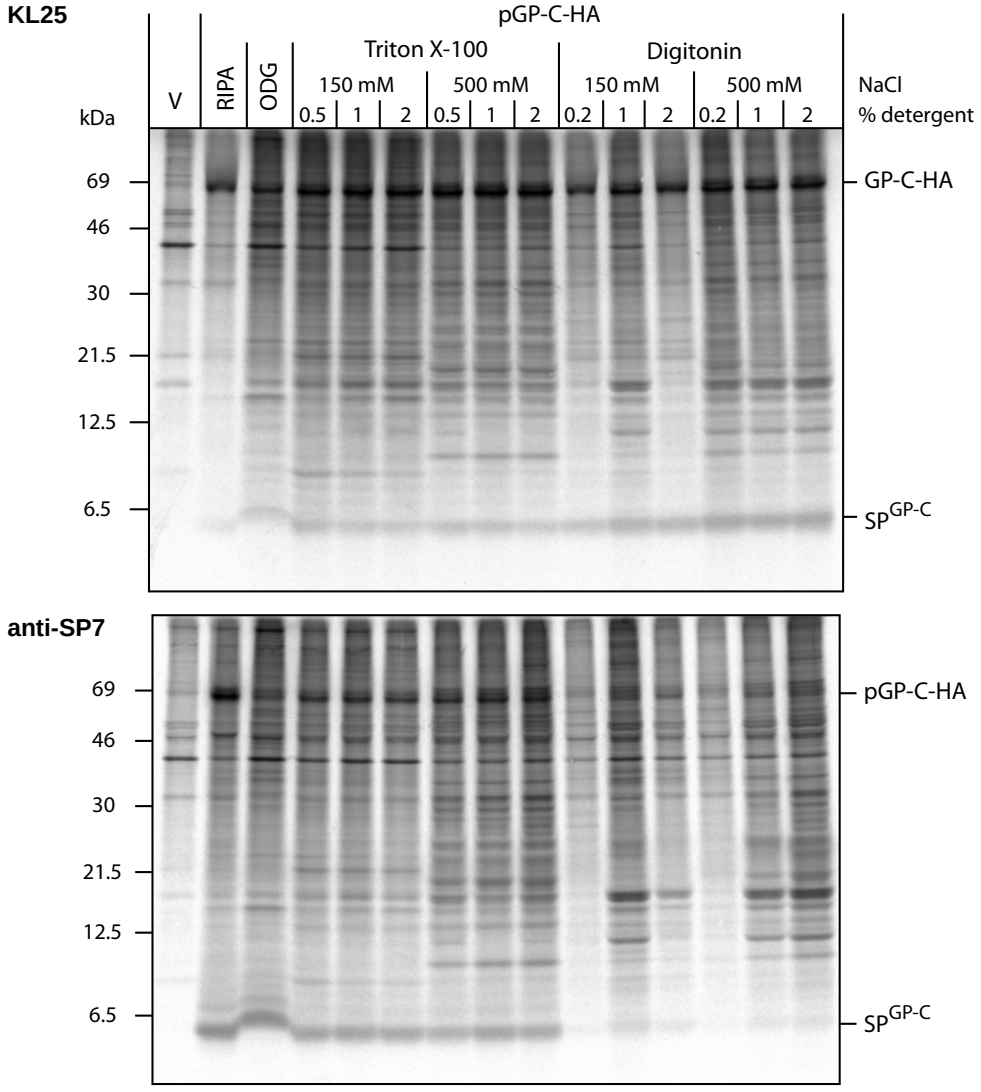

Figure 3.16: Protein solubility and co-immunoprecipitation conditions
HeLa cells expressing pGP-C-HA were metabolically labeled and lysed with different detergents (RIPA lysis buffer, Octyl-β-D-glucopyranoside (ODG), Triton X-100 or digitonin). The percentage of Triton X-100 and digitonin and the used salt concentrations are indicated. Solubilized proteins were immunoprecipitated with the KL25 antibody (top panel) or with the anti-SP7 antibody (bottom panel).

3.5.2 Interaction of $SP^{GP\text{-}C}$ with GP-C during maturation of the GP complex

To analyze the interaction between SP^{GP-C} and GP-C during GP maturation, HeLa cells expressing pGP-C-HA were metabolically labeled (pulse) and chased for 3 or 6 hours to allow for GP-C processing and transport of the GP complex. As the highest amount of co-immunoprecipitated SP^{GP-C} was detected after cell lysis with digitonin, a low salt digitonin lysis buffer (Co-IP lysis buffer) was used for protein solubilization. After anti-HA immunoprecipitation the solubilized proteins were deglycosylated with PNGase F to better resolve the GP-1 and GP-2-HA subunits. Directly after the pulse, the deglycosylated GP-C-HA* and, in addition, SP^{GP-C} were detected (Figure 3.17). The co-immunoprecipitation of SP^{GP-C} was still detectable after chase times of 3 and 6 hours, when a large proportion of GP-C-HA was already processed into GP-1 and GP-2-HA. Thus, the interaction of SP^{GP-C} with the GPs persists during intracellular transport.

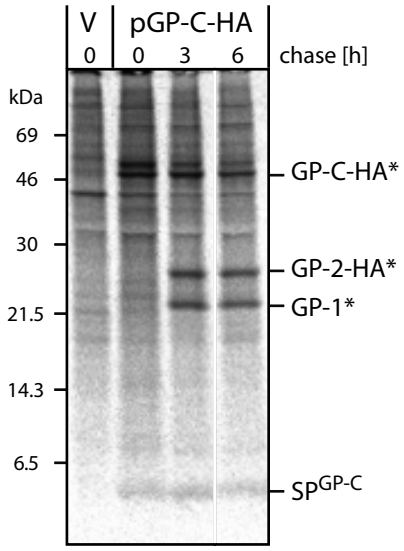

Figure 3.17: Co-immunoprecipitation of SP^{GP-C} with GP-C during GP maturation
Transfected HeLa cells expressing pGP-C-HA were metabolically labeled (pulse) and chased for the times indicated. Proteins were solubilized with 2 % digitonin (Co-IP lysis buffer), immunoprecipitated with the anti-HA antibody, and treated with PNGase F. Deglycosylated proteins are marked by an asterisk.

3.5.3 $SP^{GP\text{-}C}$ requirements for the interaction with GP-C

To determine which parts of SP^{GP-C} are required for the interaction of SP^{GP-C} with GP-C, the SP^{GP-C} deletion and point mutants introduced in section 3.3 and 3.4 were analyzed for their ability to interact with GP-C. Transfected HeLa cells were metabolically labeled and lysed with the Co-IP lysis buffer. Immunoprecipitation was performed either with the KL25 or the anti-HA antibody. To rule out unspecific co-immunoprecipitation

an unrelated control antibody (anti-B23) was used. The KL25 antibody but not the unrelated control antibody efficiently co-immunoprecipitated SP^{GP-C} from cells expressing wt pGP-C-HA (Figure 3.18 A). For ΔnME and ΔnMK expressing cells the Δn SP^{GP-C} was specifically co-immunoprecipitated with GP-C-HA (lanes 4 - 7). The positively charged lysine residue in front of the SP^{GP-C} h1-region (ΔnMK mutant), however, negatively affects the co-immunoprecipitation with GP-C-HA. This mutant also failed to promote GP-C processing and transport to the cell surface (see section 3.3). No specific co-immunoprecipitation was detected for the Δh1 and Δh2 deletion mutants (lanes 8 - 11). This suggests that both SP^{GP-C} h-regions are sufficient and essential for the interaction of SP^{GP-C} with GP-C, whereas the n-region of SP^{GP-C} is not needed.
Co-immunoprecipitation of the SP^{GP-C} point mutants showed that all mutated SPs^{GP-C} interact with GP-C-HA (Figure 3.18 B). Note that even the unmyristoylated and glycosylated SP^{GP-C} (gSP^{GP-C}) of the G2A/I4N double mutant was co-immunoprecipitated with GP-C-HA (lane 5).

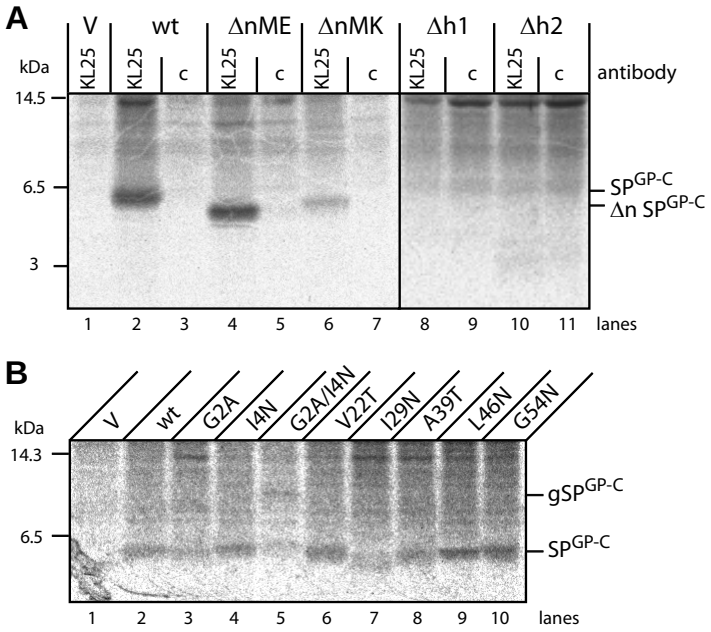

Figure 3.18: Co-immunoprecipitation of SP^{GP-C} mutants with GP-C
(A, B) pGP-C-HA (wt) and the SP^{GP-C} mutants were expressed in HeLa cells. After metabolic labeling and cell lysis with 2 % digitonin (Co-IP lysis buffer), solubilized proteins were immunoprecipitated with the KL25 antibody, an unrelated control antibody (c (anti-B23)) **(A)** or the anti-HA antibody **(B)**. The positions of the co-immunoprecipitated SPs^{GP-C} are indicated. gSP^{GP-C} represents the glycosylated form of SP^{GP-C}. Last lanes in **(A)** derive from a different experiment.

3.5.4 $SP^{GP\text{-}C}$ interacts with the GP-2 subunit

The LCMV GP-C is processed into GP-1 and GP-2 by the cellular subtilase SKI-1/S1P during transport to the cell surface (Beyer et al., 2003). After processing, the peripheral protein GP-1 non-covalently associates with the membrane-anchored GP-2. Together they build up the viral glycoprotein spikes. To examine with which subunit SP^{GP-C} is interacting, constructs containing SP^{GP-C} and only one of the GP-C subunits were generated (Figure 3.19). In case of pGP-1-HA, the GP-2 subunit of pGP-C was deleted and an HA-tag was added to the C-terminus of GP-1. To generate pGP-2-HA the GP-1 subunit was deleted such that SP^{GP-C} is located directly in front of GP-2-HA.

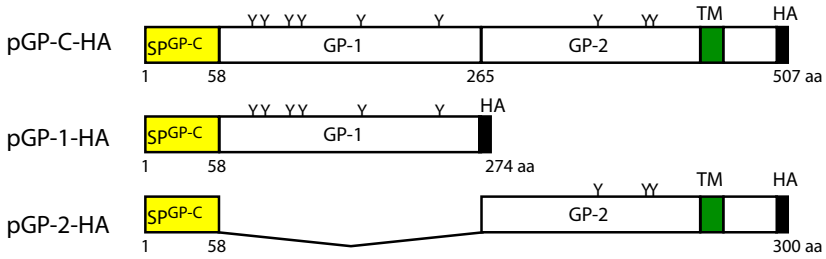

Figure 3.19: Outline of pGP-C subunit deletion mutants
In order to express the GP-1 and GP-2 subunits of pGP-C-HA separately with SP^{GP-C}, constructs where either GP-1 or GP-2 are deleted were generated. To allow for their immunodetection an HA-tag was added to the C-terminus of each construct. Potential N-glycosylation sites (Y) and the transmembrane region (TM) are indicated.

Due to the deletion of GP-1 in the pGP-2-HA construct, the amino acid sequence C-terminally of the SPase cleavage site has changed, which might affect the ER insertion efficiency as well as the efficiency of SP^{GP-C} cleavage. In pGP-1-HA, SP^{GP-C} is still in the same context as in the full length pGP-C-HA. To characterize the pGP-C subunit deletion mutants concerning their ER insertion and SP^{GP-C} cleavage efficiency, pGP-C-HA, pGP-2-HA or pGP-1-HA were expressed in HeLa cells and proteins of whole cell lysates were separated by SDS-PAGE. After transfer onto nitrocellulose the membrane was probed with the anti-HA antibody (Figure 3.20, top panel). For pGP-C-HA expressing cells, the glycosylated full length GP-C-HA of about 70 kDa and the glycosylated GP-2-HA (about 36 kDa) were detected. For pGP-1-HA, one major protein (about 42 kDa) and a low amount of a second protein (about 30 kDa) were detected using the anti-HA antibody. The molecular weight of the detected proteins are consistent with the calculated molecular weights of the glycosylated GP-1-HA and the unglycosylated precursor protein (pGP-1-HA*). Transfection of pGP-2-HA resulted in a low amount of a 36 kDa protein which co-migrates with GP-2-HA generated from pGP-C-HA. In addition to GP-2-HA, one major protein of about 32 kDa was detected in pGP-2-HA expressing cells. Due to the molecular weight, this protein most likely represents the

unglycosylated pGP-2-HA precursor protein (pGP-2-HA*). Accumulation of pGP-2-HA* and pGP-1-HA* was confirmed by probing the membrane with the anti-SP7 antibody (data not shown). Thus, placing the SP^{GP-C} directly in front of the GP-2 subunit reduces the ER insertion efficiency of the preprotein, whereas deletion of GP-2 in the pGP-1-HA construct has only a minor effect.
To analyze the cleavage of SP^{GP-C} from the pGP-C subunit deletion mutants the Western blot membrane was probed with the anti-SP7 antibody (Figure 3.20, bottom panel). Accumulation of SP^{GP-C} was detected for cells expressing pGP-C-HA, pGP-1-HA and pGP-2-HA. The low amount of SP^{GP-C} detected for pGP-2-HA is most likely due to the observed low ER insertion efficiency of pGP-2-HA.

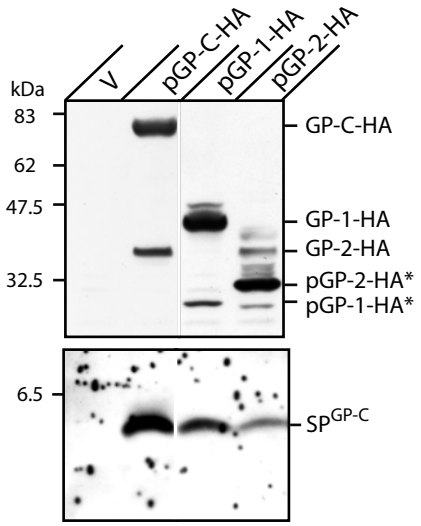

Figure 3.20: Analysis of pGP-1-HA and pGP-2-HA ER insertion and SP^{GP-C} cleavage
HeLa cells expressing pGP-C-HA, pGP-1-HA or pGP-2-HA were lysed and soluble proteins were separated by SDS-PAGE and analyzed by Western blot using the anti-HA (top panel) or anti-SP7 (bottom panel) antibody. Unglycosylated preproteins (p) are marked by an asterisk.

In order to examine with which subunit of GP-C the SP^{GP-C} is interacting, HeLa cells expressing pGP-C-HA, pGP-1-HA or pGP-2-HA were metabolically labeled and lysed with the Co-IP lysis buffer. After immunoprecipitation with the KL25 antibody, the anti-HA antibody or an unrelated control antibody (anti-B23), the proteins were separated by SDS-PAGE and analyzed by autoradiography. SP^{GP-C} was efficiently co-immunoprecipitated with GP-C-HA using the KL25 antibody (Figure 3.21). Essentially no co-immunoprecipitation of SP^{GP-C} was detected with GP-1-HA. In contrast, co-immunoprecipitation of SP^{GP-C} was detected with GP-2-HA. The low amount of co-immunoprecipitated SP^{GP-C} is most likely due to the detected low amount of glycosylated, ER-inserted GP-2-HA. In addition, a high amount of unglycosylated (p)GP-2-HA* was detected. Thus, SP^{GP-C} interacts with the membrane-anchored GP-2 subunit of GP-C.

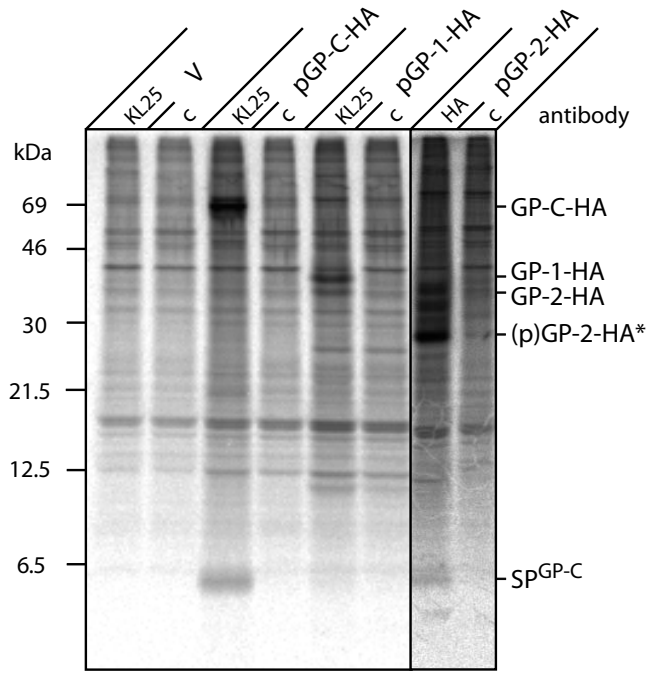

Figure 3.21: Co-immunoprecipitation of SP^{GP-C} with GP-1-HA and GP-2-HA
Metabolically labeled proteins from cells transfected with pGP-C-HA, pGP-1-HA, pGP-2-HA or vector control plasmid (V) were solubilized with 2 % digitonin (Co-IP lysis buffer) and immunoprecipitated with the KL25 antibody or the anti-HA antibody. As a control, an unrelated antibody (c (anti-B23)) was used. Unglycosylated proteins are marked by an asterisk. The last two lanes derive from a different experiment.

3.5.5 The cytoplasmic and transmembrane region of GP-C are not essential for the interaction with SP^{GP-C}

The analysis of the pGP-C subunit deletion mutants, pGP-1-HA and pGP-2-HA, showed that SP^{GP-C} is interacting with GP-2. In order to determine whether the cytoplasmic domain and/or the transmembrane region of GP-2 are needed for the interaction with SP^{GP-C}, the GP-C C-terminal deletion mutants pGP-C/ΔC and pGP-C-HA/ΔTMC were analyzed for their ability to interact with SP^{GP-C}. In the pGP-C/ΔC deletion mutant the cytoplasmic domain of GP-C was truncated leaving 6 amino acids after the transmembrane region. To generate pGP-C-HA/ΔTMC, a secretory form of pGP-C-HA, the C-terminus of GP-C including the transmembrane region was deleted. Expression of pGP-C/ΔC or pGP-C-HA/ΔTMC in HeLa cells showed that both mutants were inserted into the ER and expressed on the cell surface, respectively, secreted into the medium (see section 3.2).
To investigate whether the cytoplasmic and/or the transmembrane region of GP-C are needed for the interaction with SP^{GP-C}, pGP-C-HA or one of the GP-C C-terminal deletion mutants were expressed in HeLa cells and metabolically labeled. After cell lysis with the Co-IP lysis buffer, soluble proteins were immunoprecipitated using the KL25

antibody (Figure 3.22 A). For pGP-C-HA expressing cells, the glycosylated GP-C-HA and the co-immunoprecipitated SP^{GP-C} were detected. Expression of pGP-C/ΔC resulted in the immunoprecipitation of the glycosylated form of GP-C/ΔC with a molecular weight of about 65 kDa. For pGP-C-HA/ΔTMC expressing cells, a protein of about 64 kDa, which corresponds to the calculated molecular weight of the glycosylated GP-C-HA/ΔTMC, was detected. SP^{GP-C} was co-immunoprecipitated with GP-C/ΔC as well as with GP-C-HA/ΔTMC. Unspecific co-immunoprecipitation was ruled out by using an unrelated control antibody (anti-B23). Thus, the cytoplasmic domain and the transmembrane region of GP-C are not essential for the interaction with SP^{GP-C}.
As a control, the total amount of SP^{GP-C} was determined after expression of the GP-C C-terminal deletion mutants in HeLa cells, metabolic labeling and cell lysis. Immunoprecipitation with the anti-SP7 antibody showed that the amount of SP^{GP-C} in pGP-C/ΔC and pGP-C-HA/ΔTMC expressing cells is comparable to the amount detected for pGP-C-HA (Figure 3.22 B).

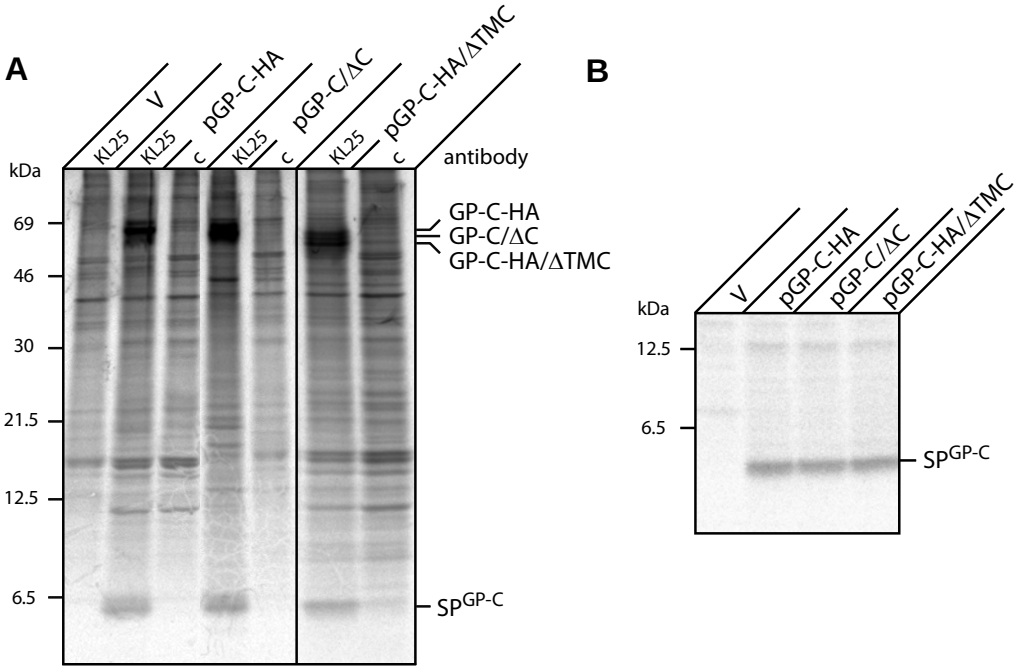

Figure 3.22: Co-immunoprecipitation of SP^{GP-C} with the GP-C C-terminal deletion mutants
(A) Co-immunoprecipitation of SP^{GP-C}. HeLa cells expressing pGP-C-HA, pGP-C/ΔC or pGP-C-HA/ΔTMC were metabolically labeled and lysed with 2 % digitonin (Co-IP lysis buffer). Soluble proteins were immunoprecipitated with the KL25 or an unrelated control antibody (c (anti-B23)). The immunoprecipitated glycoproteins as well as the co-immunoprecipitated SP^{GP-C} are indicated. The last two lanes derive from a different experiment. **(B)** Total amount of SP^{GP-C}. HeLa cells transfected with vector control plasmid (V), pGP-C-HA, pGP-C/ΔC or pGP-C-HA/ΔTMC were metabolically labeled and solubilized with 1 % Triton X-100. Antigens were immunoprecipitated with the anti-SP7 antibody.

3.5.6 SP^{GP-C} is not disulfide linked to GP-C

The LCMV SP^{GP-C} contains two highly conserved cysteine residues. One cysteine residue is located within the h2-region (C41) and the second one is found in the c-region (C57) of SP^{GP-C}. As the LCMV SP^{GP-C} interacts with the GP-2 subunit of GP-C, the question arises whether SP^{GP-C} is linked to GP-C via disulfide bonds. For the Lassa virus SP^{GP-C} it was shown that the C41 is involved in dimerization of SP^{GP-C} via disulfide bond formation if SP^{GP-C} is expressed without GP-C (Eichler et al., 2004). To determine whether the LCMV SP^{GP-C} forms disulfide linked oligomers, SP^{GP-C} was expressed alone or together with GP-C and analyzed under non-reducing and reducing conditions.
HeLa cells expressing pGP-C-HA or SP^{GP-C} alone were lysed under reducing conditions (with DTT (Dithiothreitol)) or under non-reducing conditions (without DTT). Soluble proteins were separated by SDS-PAGE and analyzed by Western blot using the anti-HA antibody. For pGP-C-HA, the glycosylated GP-C-HA and the processing product GP-2-HA were detected under both conditions showing no difference in their migration behavior (Figure 3.23 A). To analyze SP^{GP-C}, the membrane was probed with the anti-SP7 antibody. In pGP-C-HA expressing cells, SP^{GP-C} was detected under reducing and non-reducing conditions as a single peptide of 6 kDa (Figure 3.23 B). Additional bands were not detected. When SP^{GP-C} was expressed alone, in addition to the 6 kDa SP^{GP-C} detected under both conditions, a protein with a molecular weight of about 12 kDa was detected only under non-reducing conditions. This may represent a homodimer of SP^{GP-C} or a crosslink to another small component. Taken together, SP^{GP-C} is not disulfide linked to GP-C and SP^{GP-C} only forms homo- or heterodimers in the absence of GP-C.

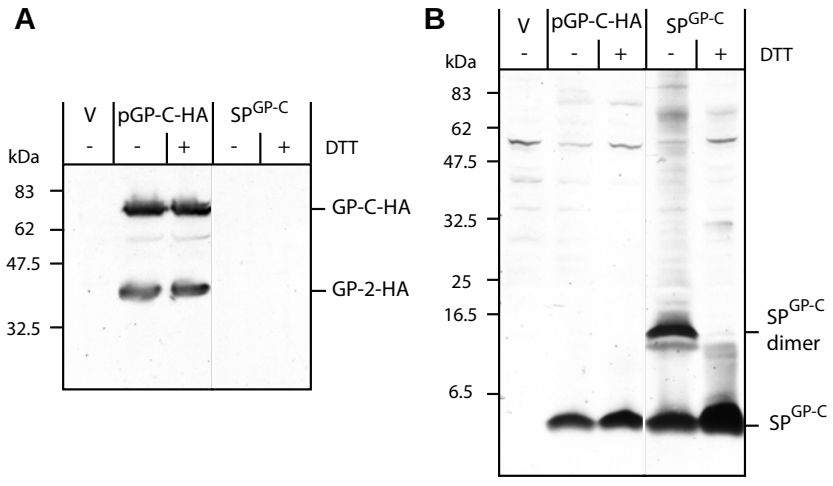

Figure 3.23: Disulfide bond formation of SP^{GP-C}
Transfected HeLa cells expressing pGP-C-HA or SP^{GP-C} alone were lysed under non-reducing conditions (- DTT) or reducing conditions (+ DTT). Soluble proteins were separated by SDS-PAGE and analyzed by Western blot using the anti-HA antibody **(A)** or the anti-SP7 antibody **(B)**.

3.5.7 ER retention of GP-C(WE) is not due to a lack of SP^{GP-C} interaction

Beyer et al. (2001) showed that the protein encoded by the original LCMV(WE) GP-C cDNA (Romanowski et al., 1985) is neither processed into GP-1 and GP-2 nor expressed on the cell surface of transfected cells. Comparison of the amino acid sequence with the GP-C cDNA recloned after LCMV infection, encoding a GP-C that is efficiently processed and transported, revealed 12 mutated amino acids. Mutational analysis showed that the exchange of a single amino acid (L110P) causes the block in GP-C maturation (Beyer et al., 2001). One possible explanation for the maturation defect is that the mutation may influence the correct assembly of the GP complex. As SP^{GP-C} is part of the GP complex and essential for GP-C processing and transport to the cell surface, interaction of SP^{GP-C} with GP-C(WE) was investigated. A schematic representation of pGP-C-HA and pGP-C-HA(WE) is shown in Figure 3.24.

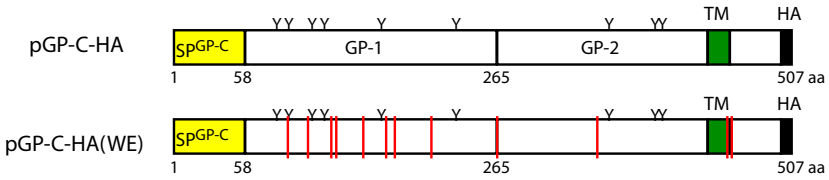

Figure 3.24: Schematic representation of GP-C-HA(WE)
Outline of pGP-C-HA and pGP-C-HA(WE). Mutations in the GP-C(WE) amino acid sequence compared to pGP-C-HA are indicated by lines. Glycosylation sites (Y), the transmembrane region (TM) and the HA-tag are marked.

To investigate whether pGP-C-HA(WE) interacts with SP^{GP-C}, HeLa cells expressing pGP-C-HA or pGP-C-HA(WE) were metabolically labeled and lysed with the Co-IP lysis buffer. Soluble proteins were immunoprecipitated with the anti-HA antibody, separated by SDS-PAGE and analyzed by autoradiography. For pGP-C-HA as well as for pGP-C-HA(WE) expressing cells, the glycosylated 70 kDa GP-C-HA respectively GP-C-HA(WE) was detected (Figure 3.25). SP^{GP-C} was co-immunoprecipitated with both proteins. The amount of co-immunoprecipitated SP^{GP-C} derived from pGP-C-HA(WE) was comparable to the amount of SP^{GP-C} detected in pGP-C-HA expressing cells. This shows that the interaction of SP^{GP-C} with GP-C is not disturbed by the amino acid changes in GP-C-HA(WE). Hence, the ER retention of GP-C(WE) is not due to a lack of SP^{GP-C} interaction.

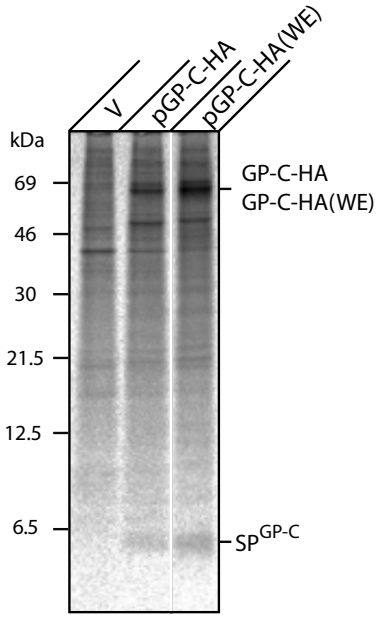

Figure 3.25: Co-immunoprecipitation of SP^{GP-C} with GP-C-HA(WE)
HeLa cells expressing pGP-C-HA or pGP-C-HA(WE) were metabolically labeled and lysed with 2 % digitonin (Co-IP lysis buffer). Solubilized proteins were immunoprecipitated with the anti-HA antibody and analyzed by SDS-PAGE and autoradiography.

3.6 Influence of the interaction with GP-C on SP^{GP-C} stability

For the LCMV SP^{GP-C} a half-life of more than 6 hours was calculated from a pulse-chase of pGP-C expressing cells (Froeschke et al., 2003). In order to investigate the influence of the interaction between SP^{GP-C} and GP-C on SP^{GP-C} stability, SP^{GP-C} was fused to an unrelated glycoprotein; the glycoprotein of the vesicular stomatitis virus (VSV-G) (Figure 3.26).

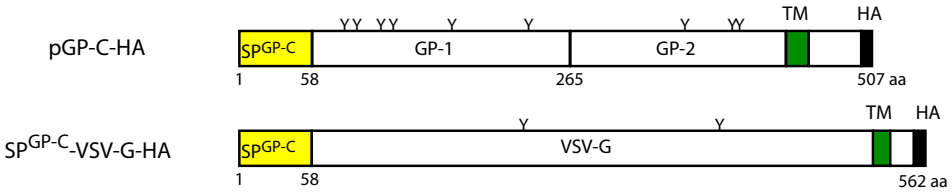

Figure 3.26: LCMV SP^{GP-C} fused to the VSV glycoprotein
Schematic representation of LCMV pGP-C-HA and SP^{GP-C} fused to VSV-G. To allow for immunodetection both constructs are C-terminally HA-tagged. SP^{GP-C} and the glycoproteins with their putative N-glycosylation sites (Y) and transmembrane region (TM) are marked. The two subunits of GP-C-HA, GP-1 and GP-2, are indicated.

HeLa cells expressing pGP-C-HA or SP^{GP-C}-VSV-G-HA were lysed and proteins were separated by SDS-PAGE. After transfer onto nitrocellulose, the membranes were probed with the anti-HA antibody (Figure 3.27 A, top panel) or the anti-SP7 antibody (bottom panel). For pGP-C-HA expressing cells, the glycosylated GP-C-HA, GP-2-HA and SP^{GP-C} were detected. Expression of the SP^{GP-C}-VSV-G-HA fusion protein resulted in the detection of a protein with an estimated molecular weight of about 63 kDa using the anti-HA antibody and a faint band detected with the anti-SP7 antibody, corresponding to SP^{GP-C}. As the expected molecular weight of the SP^{GP-C}-VSV-G-HA precursor protein (about 62 kDa) is the same as for the fully glycosylated and signal-sequence-cleaved VSV-G-HA, the two proteins cannot be distinguished in this Western blot. Thus, it remains unclear whether SP^{GP-C} is not cleaved from the SP^{GP-C}-VSV-G-HA precursor protein or if SP^{GP-C} is degraded after cleavage.

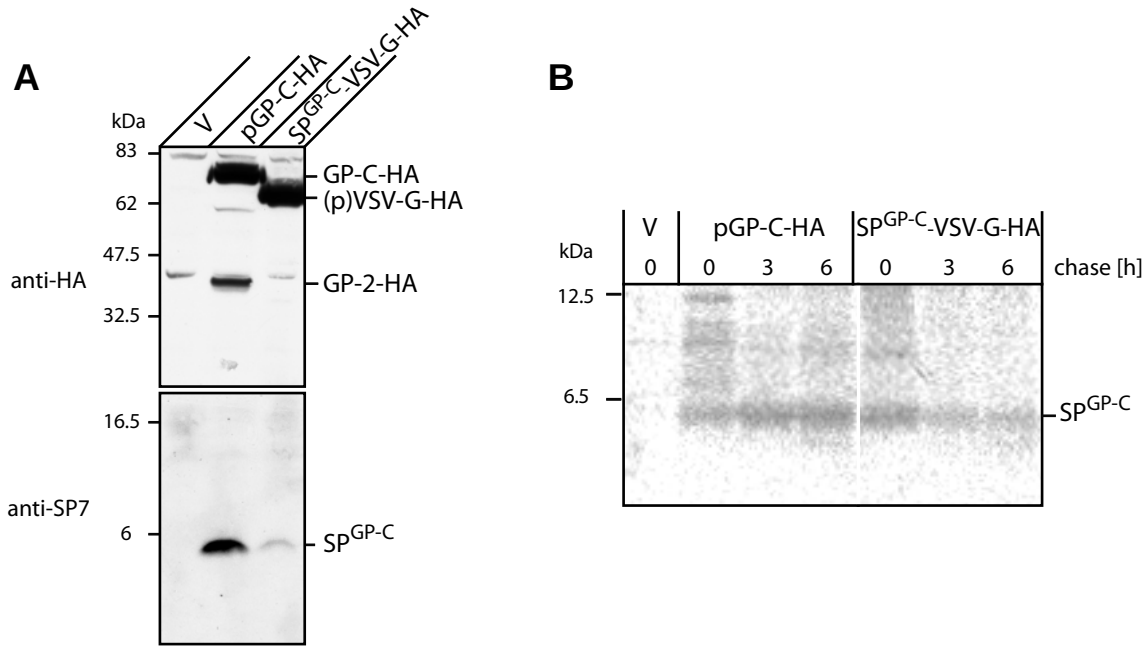

Figure 3.27: Stability of SP^{GP-C} fused to the VSV glycoprotein
HeLa cells transfected with pGP-C-HA, SP^{GP-C}-VSV-G-HA or vector control plasmid (V) were analyzed by Western blot **(A)** or by pulse-chase **(B)**. **(A)** Proteins of whole cell lysates were separated by SDS-PAGE, transferred onto a nitrocellulose membrane and identified with the anti-HA (top panel) or the anti-SP7 antibody (bottom panel). The N-glycosylated GP-C-HA and GP-2-HA as well as (p)VSV-G-HA (precursor (p) and/or glycosylated VSV-G-HA) and the cleaved SP^{GP-C} are indicated. **(B)** HeLa cells expressing pGP-C-HA or SP^{GP-C}-VSV-G-HA were metabolically labeled (pulse) and chased for the indicated time periods. Soluble proteins were immunoprecipitated using the anti-SP7 antibody.

To analyze the signal sequence cleavage from the SP^{GP-C}-VSV-G-HA preprotein and to investigate the stability of SP^{GP-C}, a pulse-chase experiment was performed. Transfected HeLa cells were metabolically labeled (pulse) for 30 min with ^{35}S-Met/Cys followed by a chase for 3 or 6 hours in medium containing unlabeled amino acids. After cell lysis,

proteins were immunoprecipitated using the anti-SP7 antibody, separated by SDS-PAGE and visualized by autoradiography. The SP^{GP-C} was detected for the pGP-C-HA and the SP^{GP-C}-VSV-G-HA fusion protein to all time points (Figure 3.27 B). At time point 0 the detected amounts of SP^{GP-C} were comparable. After a chase of 3 and 6 hours the amount of SP^{GP-C} stayed nearly the same for pGP-C-HA expressing cells, whereas for SP^{GP-C}-VSV-G-HA lower amounts of SP^{GP-C} were detected. Thus, the SP^{GP-C} is able to direct the unrelated VSV-G to the ER where it is cleaved from the preprotein. In comparison to pGP-C-HA, however, the stability of SP^{GP-C} derived from SP^{GP-C}-VSV-G-HA is reduced.

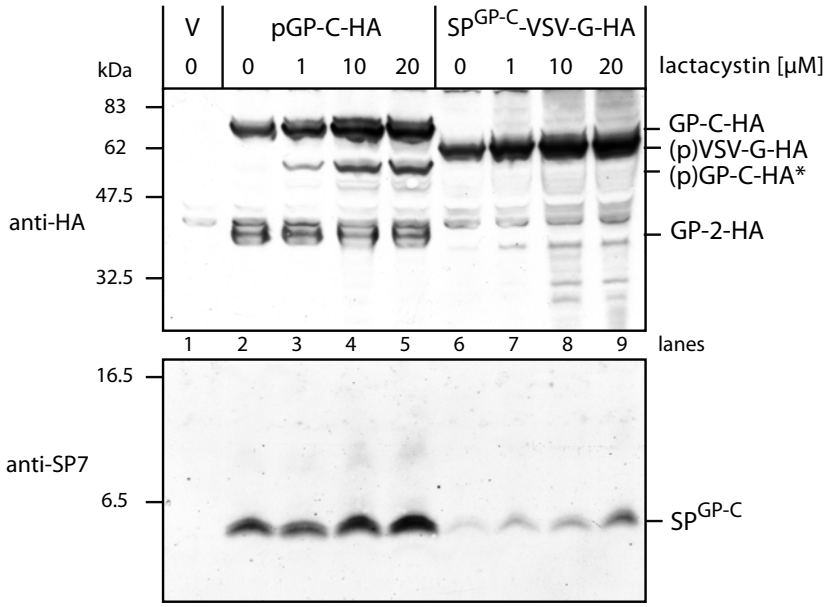

Figure 3.28: Lactacystin treatment of SP^{GP-C}-VSV-G-HA expressing cells
HeLa cells expressing pGP-C-HA or the SP^{GP-C}-VSV-G-HA fusion protein were incubated with different amounts of lactacystin for 13 hours and analyzed by Western blot. Proteins were separated by SDS-PAGE and identified with the anti-HA (top panel) or anti-SP7 antibody (bottom panel). Unglycosylated (p)GP-C-HA is marked by an asterisk. (p)VSV-G-HA indicates the unglycosylated precursor (p) and/or the glycosylated VSV-G-HA.

As the stability of SP^{GP-C} was reduced in cells expressing SP^{GP-C}-VSV-G-HA, the question whether SP^{GP-C} is degraded via the proteasome was addressed. Cells expressing pGP-C-HA or SP^{GP-C}-VSV-G-HA were treated with different concentrations of lactacystin, a specific inhibitor of the 26S proteasome (Fenteany and Schreiber, 1998), for 13 hours. Analysis of whole cell lysates by Western blot with the anti-SP7 antibody revealed that the SP^{GP-C} derived from the SP^{GP-C}-VSV-G-HA fusion protein accumulated with increasing amounts of lactacystin (Figure 3.28, bottom panel). An increase in protein amounts, even though less compared to SP^{GP-C} derived from SP^{GP-C}-VSV-G-HA, was also observed for the expressed glycoproteins, detected with the anti-HA antibody

(top panel), and SP^{GP-C} derived from pGP-C-HA. In addition, the unglycosylated and most likely SP^{GP-C}-containing (p)GP-C-HA* accumulated upon lactacystin treatment (top panel, lanes 3-5). The precursor of the SP^{GP-C}-VSV-G-HA and the fully glycosylated and SP^{GP-C}-cleaved VSV-G-HA cannot be distinguished as both are expected to have a similar molecular weight, as mentioned above. Higher molecular weight forms of the proteins due to ubiquitinylation were not detected.

3.7 The myristoylated SP^{GP-C} n-region is essential for virus infectivity

LCMV particles consist of a nucleocapsid surrounded by a lipid envelope containing the viral glycoprotein spikes (Neuman et al., 2005). Assembly of LCMV particles occurs at the plasma membrane where budding of infectious virions takes place. The LCMV GP complex is an essential component in this assembly process. Furthermore, the GP complex promotes entry of the viral particles into target cells (Borrow and Oldstone, 1994; Lee et al., 2002). Docking of LCMV particles onto target cells is mediated by binding of the GP-1 subunits to cell surface receptors (α-dystroglycan), which is followed by endocytosis of the viral particles (Cao et al., 1998). Acidification of endocytosed vesicles leads to a conformational change of the GP complex and fusion with the vesicular membrane (Di Simone et al., 1994). To study the effect of SP^{GP-C} mutations on viral infectivity, LCMV pseudoviruses were analyzed for their ability to infect target cells.

In cooperation with the research group of D. von Laer (GSH, Frankfurt a.M.), LCMV pseudoviral particles were produced by transfection of HEK 293T cells with plasmids encoding LCMV pGP-C-HA (wt or mutant), murine leukemia virus (MLV) Gag-Pol, and a retroviral vector encoding eGFP (Beyer et al., 2002). The infectivity of LCMV pseudoviral particles released from transfected cells was determined after incubation of the cell culture supernatant with target cells by measuring the green fluorescence of target cells expressing eGFP. As GP-C processing and cell surface expression of the GP complex are prerequisites for the incorporation into budding viral particles to produce infectious LCMV virions (Beyer et al., 2003; Kunz et al., 2003), only those SP^{GP-C} mutants that were processed and transported to the plasma membrane were investigated for pseudovirus formation and infectivity.

To investigate the formation of LCMV pseudoviral particles, the cell culture supernatant of transfected HEK 293T cells was collected and subjected to ultracentrifugation in order to concentrate the produced pseudoviruses. The incorporation of the GP complex into the released pseudoviral particles was analyzed by Western blot of pseudovirus lysates using the anti-HA antibody (Figure 3.29 A). A high amount of GP-2-HA in the pseudovirus lysates was detected for cells expressing pGP-C-HA (wt) and the unmyristoylated G2A mutant (lanes 1 and 3). The other SP^{GP-C} mutants, in particular the n-region mutants (lanes 2, 4 and 5), showed less efficient pseudovirus particle formation.

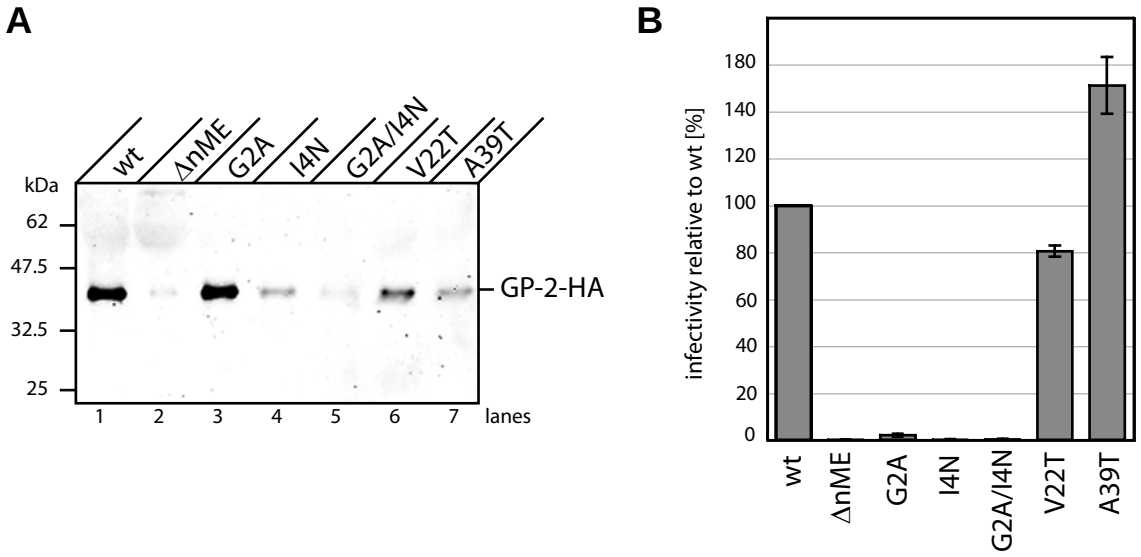

Figure 3.29: Formation and infectivity of LCMV pseudoviruses with SP^{GP-C} mutants
(A) Pseudovirus formation: HEK 293T cells were transfected with plasmids encoding LCMV pGP-C-HA (wt) or one of the indicated SP^{GP-C} mutants, MLV Gag-Pol, and a retroviral vector encoding eGFP. Produced LCMV pseudoviruses were collected from the cell supernatant by ultracentrifugation and lysed in SDS-PAGE sample buffer. Solubilized proteins were separated by SDS-PAGE and analyzed by Western blot using the anti-HA antibody. The amount of GP-2-HA was quantified by ImageJ and used for normalization of pseudovirus infectivity. **(B)** Pseudovirus infectivity: TE671 cells were incubated with the cell culture supernatant of HEK 293T cells producing LCMV pseudovirus. eGFP expression, indicative for pseudovirus infection, was determined 72 hours after transduction by flow cytometry. Data represent mean infectivity of LCMV pseudoviruses normalized to wt amount of GP-2-HA from three independent experiments (± standard deviation). The infectivity of wt pseudoviruses was set to 100 %.

In order to analyze the infectivity of LCMV pseudoviral particles, TE671 cells were incubated with the cell supernatant collected from transfected HEK 293T cells. 72 hours post transduction, the amount of eGFP expressing cells was quantified by flow cytometry. Infectivity of pseudoviral particles was normalized to the amount of GP-2-HA calculated from the Western blot of pseudovirus lysates (Figure 3.29 A). Infection of target cells was detected for LCMV pseudoviruses assembled from GP-C-HA (wt) and the SP^{GP-C} mutants V22T and A39T (Figure 3.29 B). Essentially no infectivity was determined for pseudoviral particles collected from cells expressing the SP^{GP-C} n-region deletion mutant (ΔnME) or SP^{GP-C} carrying a point mutation in the n-region (G2A, I4N or G2A/I4N). Note that despite the high amount in the Western blot, the pseudoviral particles from cells expressing the unmyristoylated G2A SP^{GP-C} mutant showed no infection of target cells. Thus, the SP^{GP-C} n-region and, specifically, its myristoylation are essential for LCMV pseudovirus infectivity.

3.8 Visualization of LCMV pseudoviruses during cell entry

The LCMV pseudovirus system used so far is based on the delivery of the viral RNA encoding eGFP into the target cell to determine the infectivity of the pseudoviruses. This system, however, does not allow to directly follow the LCMV pseudoviruses during cell entry. The visualization of LCMV pseudoviruses during cell entry would allow to identify the intracellular compartments to which the LCMV pseudoviruses (wt and SP^{GP-C} mutants) localize within the target cells using organellar markers. In addition, it would allow identifying the step at which the cell entry of mutant LCMV pseudoviruses that were not able to infect target cells, for example LCMV pseudoviruses produced from cells expressing the unmyristoylated SP^{GP-C} G2A mutant, is blocked. Entry could be blocked e.g. at the initial step of receptor binding or at the step of membrane fusion which would presumably lead to an accumulation of the pseudoviruses in intracellular vesicles.

In order to follow the LCMV pseudoviruses during cell entry, a system was established that allows to visualize the pseudoviruses by using a Gag-YFP (yellow fluorescent protein) fusion protein to fluorescently label the viral capsid (Sherer et al., 2003). To determine the infectivity of the fluorescently labeled LCMV pseudoviruses, a viral RNA encoding eGFP was used. eGFP expression in the target cells indicates delivery of the viral RNA.

Fluorescently labeled LCMV pseudoviral particles were produced by transfection of HEK 293T cells with plasmids encoding LCMV pGP-C-HA (wt or mutant), MLV Gag-Pol, MLV Gag-YFP (Sherer et al., 2003), and a retroviral vector encoding eGFP (Beyer et al., 2002). Because attachment of YFP to Gag truncates Pol expression, the production of infectious fluorescently labeled viruses requires the co-expression of the wild type Gag-Pol precursor protein. A high infectivity of labeled viruses was reported when labeled Gag did not exceed 25 % of all Gag molecules (Sherer et al., 2003).

In order to analyze the infectivity, HeLa cells were incubated with the cell culture supernatant of transfected HEK 293T cells producing LCMV pseudoviruses with GP-C-HA (wt) or with the SP^{GP-C} G2A mutant over night at 37°C. Particles produced without a viral envelope glycoprotein (no GP) were used as a control. After removal of the pseudovirus-containing supernatant, the cells were cultivated in normal growth medium for 3 to 4 days to allow for eGFP expression, fixed and analyzed by immunofluorescence microscopy. eGFP expressing HeLa cells were only detected after incubation with the supernatant of HEK 293T cells producing LCMV pseudoviruses with GP-C-HA (wt) (Figure 3.30). As eGFP expression indicates delivery of the viral RNA into the cell, the LCMV pseudoviruses produced with GP-C-HA (wt) are able to infect target cells. No eGFP positive cells were detected after incubation with the cell culture supernatant of HEK 293T cells producing LCMV pseudoviruses with the unmyristoylated SP^{GP-C} G2A mutant and for particles produced without a viral glycoprotein (no GP).

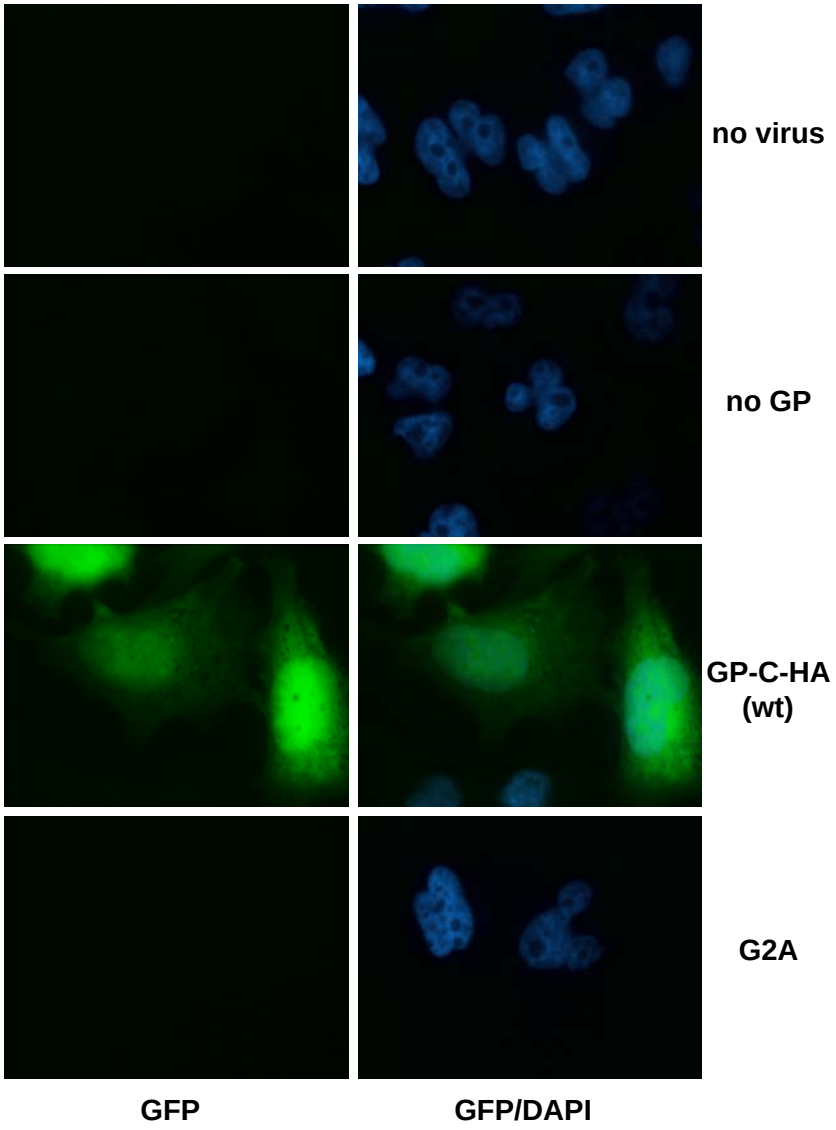

Figure 3.30: Infectivity of fluorescent LCMV pseudoviruses
To analyze the infectivity of the fluorescent LCMV pseudoviruses, HeLa cells were incubated with the cell culture supernatant of transfected HEK 293T cells over night at 37°C. For infection, LCMV pseudoviruses produced with GP-C-HA (wt) or with the SP^{GP-C} G2A mutant and particles produced without a viral glycoprotein (no GP) were used. The cell culture supernatant harvested from untransfected HEK 293T cells was used as control (no virus). Expression of eGFP was analyzed 3 to 4 days after transduction in fixed cells.

In order to determine whether the produced LCMV pseudoviruses are fluorescently labeled and detectable during cell entry, HeLa cells were incubated with the supernatant of transfected HEK 293T cells at 37°C for 1 hour. After extensive washing, the cells were fixed and analyzed by immunofluorescence microscopy. Fluorescent viral particles were detected after the incubation with the supernatant of HEK 293T cells producing YFP-labeled LCMV pseudoviruses with GP-C-HA (wt) and with pseudoviruses containing the

SP^{GP-C} G2A mutant (Figure 3.31). Fluorescently labeled particles produced without a viral glycoprotein (no GP) were also detected. The observed YFP-labeled viral particles represent either particles bound to the cell surface or internalized particles and are found on the cell periphery as well as in the center of the cells.

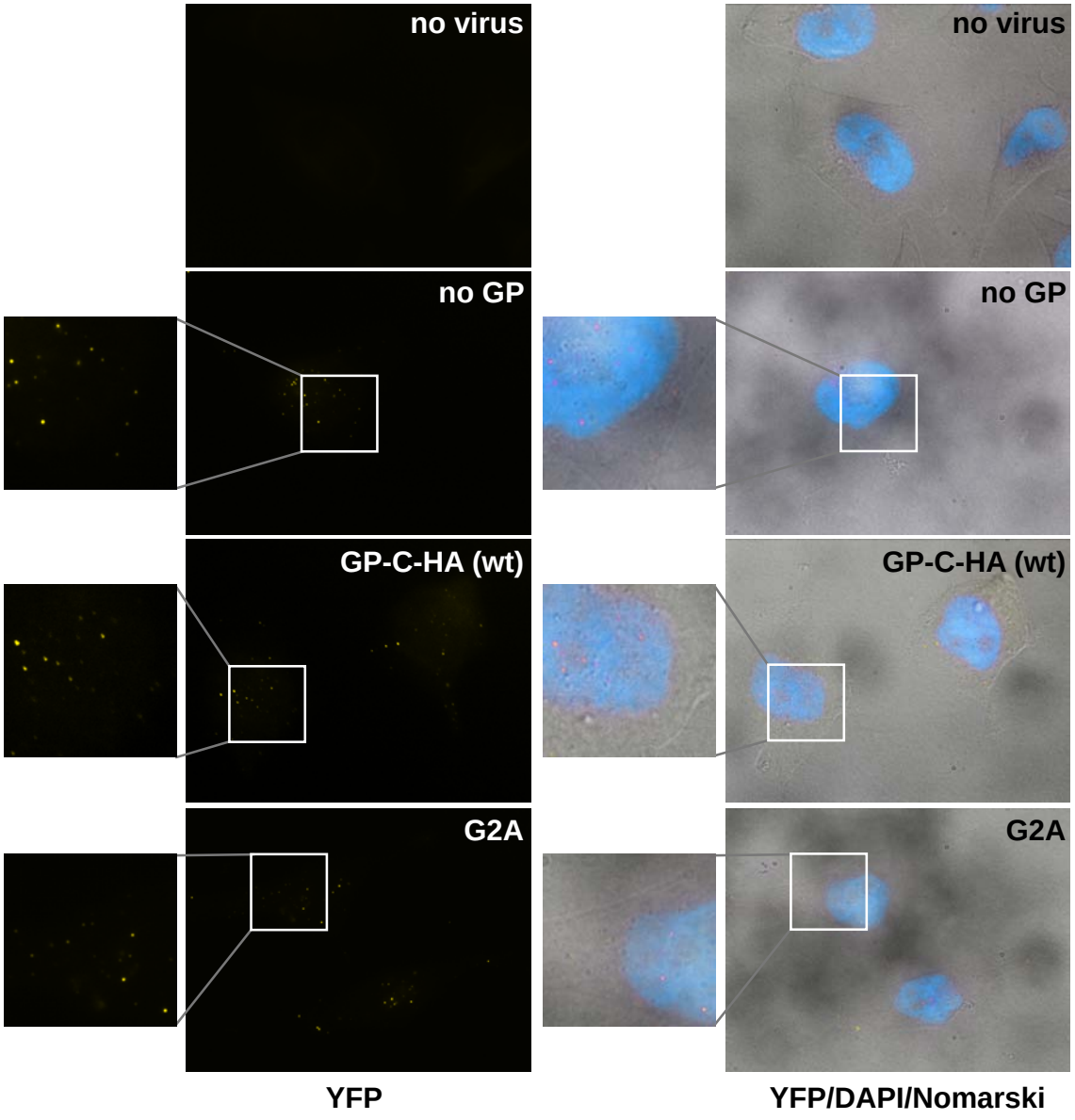

Figure 3.31: Fluorescently labeled viral particles
YFP-labeled LCMV pseudoviruses (GP-C-HA (wt) or SP^{GP-C} G2A mutant) produced from transfected HEK 293T cells or particles produced without a viral glycoprotein (no GP) were added to HeLa cells and incubated at 37°C for 1 hour. As a control, the cell supernatant from untransfected HEK 293T cells was used. After the incubation, HeLa cells were washed extensively, fixed and analyzed by immunofluorescence microscopy.

Taken together, the produced fluorescently labeled LCMV pseudoviruses are able to infect target cells and can be directly visualized by immunofluorescence microscopy. However, fluorescent particles produced without a viral glycoprotein, although not able to infect the target cells, were also detected on, respectively, within the cells.

4 Discussion

The signal sequence of LCMV pGP-C is unusually long, containing an extended n-region and two h-regions. After insertion of pGP-C into the ER membrane, the signal sequence is cleaved by SPase and the resulting signal peptide, SP^{GP-C}, was shown to accumulate in cells and virus particles (Froeschke et al., 2003). LCMV belongs to the arenaviruses, a family of enveloped RNA viruses that includes highly pathogenic members that cause hemorrhagic fever. The amino acid sequence of the LCMV signal sequence is highly conserved among the arenavirus pGP-Cs. This conservation and the high stability of LCMV SP^{GP-C} points to a function of SP^{GP-C} besides ER targeting.

In this work the post-targeting functions of LCMV SP^{GP-C} were analyzed. It could be shown that the LCMV SP^{GP-C} is an essential component of the glycoprotein complex and that different regions of SP^{GP-C} are required for distinct steps in glycoprotein maturation and virus infectivity (summarized in Figure 4.1). Investigation of SP^{GP-C} mutants revealed that one h-region of LCMV SP^{GP-C} is sufficient for membrane insertion of pGP-C, while both h-regions are required for GP-C processing and cell surface expression of the GP complex. The n-region of SP^{GP-C} and its myristoylation were not needed for these steps in GP-C maturation but were found to be essential for pseudovirus formation and viral infectivity. The LCMV SP^{GP-C} mediates these functions as part of the GP complex. For the non-covalent association of SP^{GP-C} with GP-C the h-regions of SP^{GP-C} were shown to be sufficient and essential.

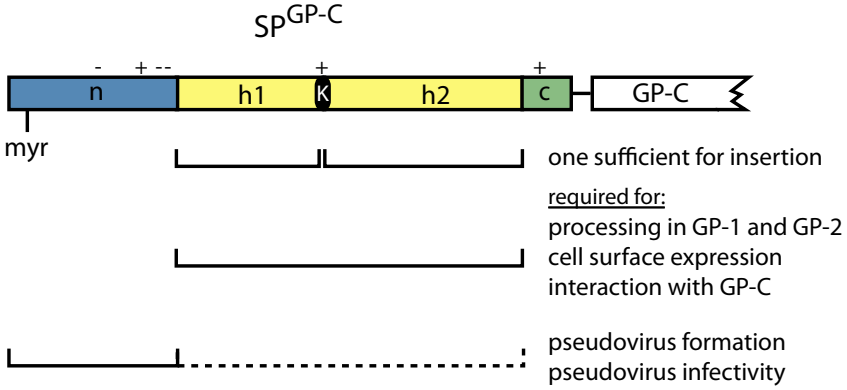

Figure 4.1: Functions of LCMV SP^{GP-C} besides ER targeting
The different regions of LCMV SP^{GP-C} mediate specific functions during GP-C maturation and viral infection. One of the SP^{GP-C} h-regions is sufficient for ER membrane insertion of pGP-C, while both are required for processing of GP-C into GP-1 and GP-2, cell surface expression, and interaction with GP-C. For pseudovirus formation and infectivity, the SP^{GP-C} n-region and, specifically, its myristoylation (myr) are required in addition to the h-regions.

As the LCMV SP^{GP-C} possesses two h-regions, different topologies across the membrane are thinkable. Analysis of the SP^{GP-C} topology revealed that the unmyristoylated SP^{GP-C} exposes its N-terminal region to the exoplasmic side of the membrane. This SP^{GP-C} can promote GP-C processing and transport to the cell surface but is defective in viral infection. Myristoylation and membrane topology of SP^{GP-C} may thus hold an important key to an understanding of the role of SP^{GP-C} in GP-C complex maturation and LCMV infectivity.

4.1 Function of the LCMV SP^{GP-C} during GP-C maturation

4.1.1 SP^{GP-C} is essential for GP-C maturation

Replacing the authentic signal sequence of LCMV pGP-C with the signal sequence of the unrelated vesicular stomatitis virus glycoprotein precursor (pVSV-G) still allows ER membrane insertion of GP-C but prevents processing into GP-1 and GP-2 (Figure 3.2 A). Similarly, the signal sequence of the Old World Lassa arenavirus pGP-C was shown to be essential for proteolytic processing of Lassa GP-C. For the Lassa virus, this deficiency in GP-C processing was reversed by coexpression of the authentic Lassa virus SP^{GP-C} in *trans* (Eichler et al., 2003a).

Processing of the LCMV GP-C by the cellular subtilase SKI-1/S1P takes place during transport to the cell surface (Beyer et al., 2003). The absence of the GP-C processing products, GP-1 and GP-2, upon substitution of the authentic pGP-C signal sequence with the signal sequence of pVSV-G, may be due to ER retention of GP-C caused by incorrect folding or incomplete complex assembly. A further possibility is that SP^{GP-C} is needed to keep GP-C in a conformation that is accessible to the processing enzyme, while transport to the plasma membrane is not impaired. As the cell surface expression of LCMV GP-C derived from the SP^{VSV-G}-containing precursor protein was drastically reduced compared to pGP-C, the authentic LCMV SP^{GP-C} seems to be necessary for the transport of GP-C (Figure 3.2 B). A similar observation was made for the Junín virus GP-C. For this New World arenavirus it was shown that a recombinant pGP-C in which the authentic signal sequence was replaced by the signal sequence of human CD4 was unable to promote efficient GP-C maturation (York et al., 2004). This recombinant pGP-C was found to localize to the ER (Agnihothram et al., 2006). The reason for the intracellular accumulation of the LCMV GP-C in absence of the authentic SP^{GP-C}, might be a folding or assembly defect such that the protein does not pass the quality control mechanisms in the ER (Doms et al., 1993; Ellgaard and Helenius, 2003). The transport competent GP complex might include the SP^{GP-C} as an essential component. Complex formation of LCMV SP^{GP-C} with GP-C is discussed in section 4.3. The dependency of LCMV GP-C maturation on the presence of the authentic SP^{GP-C} clearly shows that the

LCMV SP^{GP-C} has additional functions besides ER targeting.
For the Lassa virus SP^{GP-C} it is assumed that it functions as a chaperone for GP-C, as the association of GP-C with the ER resident chaperone calnexin was prolonged in pGP-C mutants containing an unrelated signal sequence (Eichler et al., 2003a).

4.1.2 Functional significance of the SP^{GP-C} n-region and its myristoylation for GP-C maturation

The analysis of LCMV SP^{GP-C} mutants revealed that the n-region of the LCMV SP^{GP-C} is neither required for ER membrane insertion nor for processing and intracellular transport of GP-C (Figure 4.1). Similarly, deletion of the n-region of the Lassa virus pGP-C signal sequence had no effect on GP-C maturation (Eichler et al., 2004). Even though the n-region of LCMV SP^{GP-C} is not required for GP-C maturation, there are certain requirements with regard to the charged amino acid residues following the initiating methionine. Leaving the negatively charged glutamic acid in front of the h1-region (ΔnME mutant), as in wild type SP^{GP-C}, does not affect pGP-C membrane insertion, GP-C maturation or complex formation with GP-C (summarized in Figure 4.2). Placing a positively charged lysine residue at the same position (ΔnMK mutant) does also not affect ER membrane insertion of pGP-C, however, prevents processing of GP-C into GP-1 and GP-2 and negatively influences the interaction of SP^{GP-C} with GP-C as well as transport of the GP complex to the cell surface. A similar result was recently reported for a LCMV SP^{GP-C} mutant in which both negatively charged amino acid residues in front of the h1-region were replaced by lysine residues (Saunders et al., 2007). This substitution was shown to result in a drastic reduction of GP-C processing and cell surface expression.
N-terminal regions of signal sequences for ER targeting are usually positively charged (von Heijne, 1990), whereas the extended n-region of the LCMV SP^{GP-C} has an overall negative-charge character. Indeed, placing a positively charged amino acid residue in front of the LCMV SP^{GP-C} h1-region does not affect ER membrane insertion of pGP-C. For GP-C maturation, however, a negatively charged amino acid residue is required. Thus, the negative-charge character of the LCMV SP^{GP-C} n-region seems to be needed for the post-targeting functions of SP^{GP-C}. The unexpected requirement for a negatively charged amino acid residue in the n-region of SP^{GP-C} might also be related to the fact that the LCMV SP^{GP-C} contains two h-regions, separated by a lysine residue, of which only one might function as signal sequence for ER targeting.

The myristoylation consensus sequence at the N-terminus of the LCMV SP^{GP-C} is conserved among all signal sequences of arenavirus pGP-Cs (York et al., 2004). Myristoylation of LCMV SP^{GP-C} at its N-terminal glycine residue was shown by M. Fröschke (published in Schrempf et al. (2007)). To prevent SP^{GP-C} myristoylation, the conserved

Gly-2 was replaced by alanine (G2A mutant). This unmyristoylated SP^{GP-C} is fully functional in promoting GP-C processing into GP-1 and GP-2, cell surface expression of the GP complex, and is still able to interact with GP-C (Figure 4.2). For the Junín virus pGP-C signal sequence, myristoylation was shown by York et al. (2004). Myristoylation of the Junín SP^{GP-C} was also not required for GP-C maturation, complex assembly and intracellular transport.

	ER insertion of pGP-C	interaction	GP-C processing	cell surface expression	amount of GP-2 in virus	infectivity
wt	+++	+++	+++	+++	+++	+++
ΔnME	+++	+++	+++	+++	+	-
ΔnMK	+++	++	-	+	n.d.	n.d.
Δh1	++	-	-	-	n.d.	n.d.
Δh2	+	-	-	-	n.d.	n.d.
G2A	+++	+++	+++	+++	+++	-
I4N	+++	+++	+++	+++	+	-
G2A/I4N	+++	+++	+++	+++	+	-
V22T	+++	+++	+++	+++	++	+++
I29N	++	+++	-	+	n.d.	n.d.
A39T	+++	+++	+++	+++	++	+++
L46N	+	+++	-	+	n.d.	n.d.
G54N	++	+++	-	+	n.d.	n.d.

Figure 4.2: Summarized results of LCMV SP^{GP-C} deletion and point mutants
Functions of LCMV SP^{GP-C} and steps in GP-C maturation are indicated on top of the figure. LCMV pGP-C with the authentic signal sequence (wt) and pGP-Cs with mutant signal sequences are listed vertically. Results are given in comparison to the wt: +++ as wt, ++ less, + drastically reduced, - lacking; n.d. not determined.

4.1.3 Functional significance of the SP^{GP-C} h-regions for GP-C maturation

The most characteristic feature of N-terminal signal sequences for ER targeting is a central hydrophobic core required for SRP binding and ER membrane insertion (von Heijne, 1985; Martoglio and Dobberstein, 1995). The signal sequences of arenaviral pGP-Cs contain two h-regions of which each could be used for ER targeting. The LCMV SP^{GP-C} with either the h1- or h2-region deleted is able to mediate ER membrane insertion of pGP-C, although the h2-region is more efficient in mediating this process (Figure 4.2). The h2-region with the positively charged lysine residue at its N-terminal side and its proximity to the SPase cleavage site at its C-terminal side shows all characteristics of a minimal signal sequence for ER targeting (Martoglio and Dobberstein, 1998). Therefore, the h2-region may function in ER targeting and, in this function, may span the membrane

during insertion and signal sequence cleavage (Figure 4.3). The orientation of signal sequences upon entering the translocon is determined, amongst others, by the distribution of charged residues flanking the hydrophobic core, whereby the more positive segment is predominantly localized on the cytoplasmic side of the membrane ("positive-inside rule") (Goder et al., 2004; Sipos and von Heijne, 1993).
The positively charged lysine residue in front of the LCMV SP^{GP-C} h2-region is conserved among all arenaviruses. The charge requirements in this position concerning GP-C maturation were recently investigated by Saunders et al. (2007). They showed that the exchange of the lysine residue for a negatively charged amino acid strongly reduced accumulation of LCMV GP-C, whereas the exchange for a different positive residue had no negative effect. The reduced accumulation of GP-C might be caused be a lower insertion efficiency and degradation of the protein. The positively charged lysine residue between the h-regions might therefore be important for the function of the LCMV h2-region as signal sequence.

Mutant LCMV SPs^{GP-C} with one of the h-regions deleted neither mediate processing of GP-C into GP-1 and GP-2 nor their cell surface expression (Figure 4.2). A similar result was found previously for the Lassa virus SP^{GP-C}. Eichler et al. (2004) showed that an N-terminal deletion of the Lassa SP^{GP-C} including the h1-region abolished processing of GP-C by SKI-1/S1P. For the LCMV SP^{GP-C} even single point mutations in either the h1- or h2-region (I29N or L46N) prevent processing of GP-C and transport to the cell surface, although they were still able to mediate ER membrane insertion of pGP-C (Figure 4.2). As these mutant SPs^{GP-C} are cleaved from the preprotein but do not accumulate, one can speculate that the destabilization of the mutant SPs^{GP-C} cause the block in GP-C transport. It appears that the two h-regions of the LCMV SP^{GP-C} are important structural elements for intracellular transport of GP-C and its processing into GP-1 and GP-2.

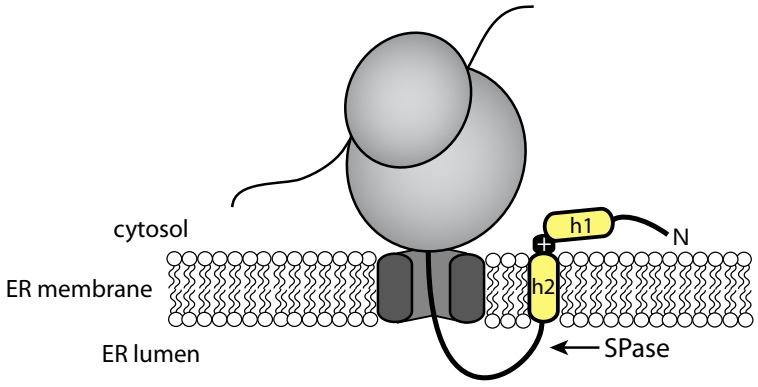

Figure 4.3: Postulated topology of LCMV SP^{GP-C} during ER membrane insertion
During insertion of the nascent chain of LCMV pGP-C into the translocon, the SP^{GP-C} h2-region most likely spans the membrane with the N-terminus facing the cytosol and the SP^{GP-C} c-region with the SPase cleavage site facing the ER lumen. The positively charged lysine residue that N-terminally flanks the h2-region is indicated by a filled circle (+).

4.2 Membrane topology of LCMV SP^{GP-C}

To understand the role of LCMV SP^{GP-C} in GP-C complex maturation and LCMV infectivity, the analysis of the SP^{GP-C} topology in the membrane becomes of central importance. As SP^{GP-C} has two h-regions it is unclear whether one or both of them span the membrane and to which side of the membrane the N- and C-terminus are exposed.

Membrane topology of LCMV SP^{GP-C} was investigated by making use of N-glycosylation sites introduced at different positions along SP^{GP-C}. It was found that the n-region of SP^{GP-C} can be glycosylated when myristoylation is prevented (Figure 3.14). This clearly shows that the n-region of SP^{GP-C} has an intrinsic property to translocate to the exoplasmic side of the ER membrane with one or both h-regions spanning the membrane (Figure 4.4). Glycosylated SP^{GP-C} with an $N_{exo}/C_{cyt/exo}$ (exoplasmic N- and cytoplasmic or exoplasmic C-terminus) topology can still interact with GP-C and is able to promote processing of GP-C into GP-1 and GP-2 and cell surface expression of the GP complex. Thus, SP^{GP-C} with an $N_{exo}/C_{cyt/exo}$ topology has all the functional properties required to promote maturation and intracellular transport of GP-C. This topology, however, does not promote infection of target cells (Figure 4.2). One possible explanation is that myristoylation, a co-translational event occurring in the cytosol, prevents N-terminal membrane translocation of SP^{GP-C} and that it is the topological change in the unmyristoylated SP^{GP-C} that prevents infection. An argument against this explanation is that unmyristoylated and glycosylated SP^{GP-C} with an $N_{exo}/C_{cyt/exo}$ topology is fully functional in promoting GP-C maturation and cell surface expression. Thus, another reason why unmyristoylated SP^{GP-C} is defective in viral infection might be that the myristoylated n-region of SP^{GP-C} has to be exposed on the exoplasmic side of the membrane. In this case, myristoylation might then directly be required for GP-mediated infection of target cells.

The fact that the glycosylation of the SP^{GP-C} I4N mutant is seen only when myristoylation is inhibited (M. Fröschke; published in Schrempf et al. (2007)) or prevented by the G2A mutation does not necessarily mean that myristoylation prevents translocation of the SP^{GP-C} n-region to the exoplasmic side of the membrane. It is conceivable that myristoylation does not allow access of the oligosaccharyl transferase to the Asn-4 glycosylation site (Nilsson and von Heijne, 2000; Silberstein and Gilmore, 1996). It should, however, be mentioned that there is a precedent for glycosylation of an Asn-4 position when the Gly-2 position is myristoylated (Utsumi et al., 2005).

As proteins that expose their myristoylated N-terminal regions on the exoplasmic side of the membrane have been reported previously, myristoylation does not principally prevent the N-terminal translocation of membrane proteins. Examples are the fusion-associated small transmembrane (FAST) proteins of some reoviruses (Corcoran and Duncan, 2004; Dawe et al., 2005) and the large envelope protein of the hepatitis B virus (HBV) (Gripon

et al., 1995; Lambert and Prange, 2001; Urban and Gripon, 2002). Unfortunately, it was not possible to directly determine the membrane topology of the myristoylated LCMV SP^{GP-C}.

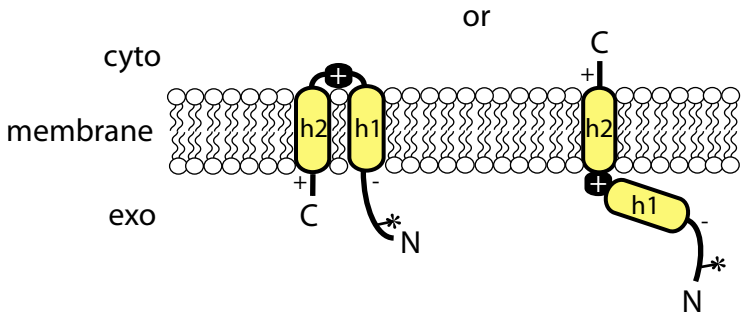

Figure 4.4: Proposed membrane topologies of the unmyristoylated LCMV SP^{GP-C}
The n-region of the LCMV SP^{GP-C} can get N-glycosylated and thus can translocate to the exoplasmic (exo) side of the membrane when myristoylation is prevented. As SP^{GP-C} contains two h-regions one or both might span the membrane. The SP^{GP-C} h-regions (h1 and h2), the lysine residue that separates the two h-regions (filled circle), and the glycosylation in the SP^{GP-C} n-region (*) are indicated. Positive charged as well as negative charged amino acid residues respectively regions are marked.

The fact that the n-region of LCMV SP^{GP-C} is able to translocate to the exoplasmic side of the membrane is certainly unusual, as signal sequences usually insert into the ER membrane in a loop like fashion, exposing the N-terminal region to the cytoplasmic side and the C-terminal region to the lumenal side of the ER membrane. Major determinants for such an N_{cyt}/C_{exo} topology are the positively charged amino acid residues usually found in the n-region of simple signal sequences (von Heijne, 1985; Sipos and von Heijne, 1993). The LCMV SP^{GP-C}, however, can be considered as a complex signal sequence that performs additional functions besides ER targeting and membrane insertion. Consistent with an N-terminal translocation is the overall negative charge of the SP^{GP-C} n-region and the finding that a negatively charged amino acid residue in front of the h1-region is required for post-targeting functions of SP^{GP-C}, whereas a positive charge is not allowed. Positively charged amino acids are indicators for a cytoplasmic localization of segments in membrane proteins, a phenomenon known as "positive-inside rule" (Sipos and von Heijne, 1993). It is also conceivable that SP^{GP-C} does not exclusively adopt one topology across the membrane. Examples for alternative topologies across membranes are well established. The myristoylated N-terminus of the HBV large envelope protein is e.g. post-translationally translocated across the membrane during HBV morphogenesis (Lambert and Prange, 2001; Ostapchuk et al., 1994). Similarly, the internal signal sequences at the C-termini of the transmembrane domains of the HCV (hepatitis C virus) envelope glycoproteins are thought to reorient towards the cytosol after cleavage (Cocquerel et al.,

2002). A further example for alternative topologies across membranes is the prion protein, which is synthesized in multiple topological forms (Kim and Hegde, 2002; Ott et al., 2007).

Previously, the membrane topology of the Lassa virus SP^{GP-C} has been analyzed by introducing epitopes of different length containing N-glycosylation acceptor sites (Eichler et al., 2004). The cytoplasmic or exoplasmic localization of these epitopes was determined either by immunofluorescence analysis of permeabilized cells or by glycosylation within the epitopes. For the modified Lassa SP^{GP-C}, it was found that the N-terminus is localized on the cytoplasmic side of the membrane and that only the h1-region is used as membrane anchor. For several reasons, this topological analysis may not be transferable to the authentic SP^{GP-C} of the Lassa virus or generally to SPs^{GP-C} of arenavirus glycoproteins. The introduced epitopes are between 9 and 25 amino acid residues in length. Such insertions could drastically affect the topology of SP^{GP-C}. Even more serious is the fact that only the mutated SP^{GP-C} without its glycoprotein portion was investigated in this topological analysis (Eichler et al., 2004). Therefore, not only were possible topological determinants added, but also the entire pathway for ER membrane insertion might be different from that of the authentic pGP-C.

A recent study of the pGP-C signal sequence in the New World Junín arenavirus reported a bitopic membrane topology of Junín SP^{GP-C} with both the N- and the C-terminus residing in the cytosol (Agnihothram et al., 2007). As tagged versions of the Junín SP^{GP-C} were used and SP^{GP-C} was expressed in *trans*, it is questionable whether such a topology holds true for the authentic SP^{GP-C} cleaved from pGP-C. The different topology models for the Junín virus and the LCMV SP^{GP-C} may also reflect the differences between the New World and Old World arenaviruses (Clegg, 2002). A further possibility is that the SP^{GP-C} can adopt alternative topologies in the membrane. Clearly, further studies are needed to elucidate the topology of the arenaviral SPs^{GP-C} and its functional significance.

4.3 SP^{GP-C} as part of the LCMV GP complex

After cleavage from the preprotein, the LCMV SP^{GP-C} was found to accumulate in cells and virus particles (Froeschke et al., 2003). As it is most likely that SP^{GP-C} assembles into the particles as part of the GP complex the possible interaction between SP^{GP-C} and GP-C was analyzed.

Using co-immunoprecipitation, a stable interaction between the LCMV SP^{GP-C} and GP-C was discovered (Figure 3.17). Similarly, an interaction of the Lassa virus SP^{GP-C} with its glycoprotein was previously detected (Eichler et al., 2003a). The signal peptide of the New World Junín arenavirus was also found to be part of the GP complex (York et al., 2004). The association of the LCMV SP^{GP-C} with GP-C does not involve disulfide bond formation between the interacting partners (Figure 3.23) as it is true for the Junín virus

(York et al., 2004). Furthermore, the interaction of LCMV SP^{GP-C} with GP-C seems to have a stabilizing effect on SP^{GP-C}, as the stability of SP^{GP-C} was reduced when expressed with an unrelated glycoprotein (Figure 3.27). High SP^{GP-C} stability was detected when SP^{GP-C} was expressed together with its authentic glycoprotein and if SP^{GP-C} was expressed alone, without a glycoprotein, now forming disulfide linked dimers. Dimer formation via disulfide bonds was also detected for the Lassa virus SP^{GP-C} (Eichler et al., 2004). For the dimerization of the Lassa virus SP^{GP-C} the cysteine residue Cys-41 between both SP^{GP-C} h-regions seems to be required.

The analysis of the LCMV GP complex using different co-immunoprecipitation conditions revealed a tight association of SP^{GP-C} with GP-C after cell lysis with a digitonin lysis buffer. Under these conditions a high amount of co-immunoprecipitated SP^{GP-C} was detected, whereas no SP^{GP-C} was immunoprecipitated using the anti-SP7 antibody (Figure 3.16). This antibody recognizes an epitope in the SP^{GP-C} n-region in proximity of the h1-region. The inaccessibility of the epitope indicates that this part of the n-region is either buried inside the GP complex or cannot be reached by the antibody due to steric hindrance under the used conditions. Immunoprecipitation of SP^{GP-C} with the anti-SP7 antibody could be increased using Triton X-100 to solubilize the proteins. The higher accessibility of the anti-SP7 epitope and the lower co-immunoprecipitation efficiency in presence of Triton X-100 indicates a weak interaction between SP^{GP-C} and GP-C under these conditions.

Investigation of the requirements for LCMV SP^{GP-C} interaction with GP-C revealed that the SP^{GP-C} interacts with the GP-2 subunit of GP-C and that the cytoplasmic domain and the transmembrane region of GP-2 are not essential for this interaction (Figure 3.21). The n-region of SP^{GP-C} was also found to be dispensable for the interaction with GP-C, whereas the deletion of one of the SP^{GP-C} h-regions completely abolished a specific interaction (Figure 3.18). This suggests an interaction of the LCMV SP^{GP-C} h-regions with the exoplasmic domain of GP-2. Nevertheless, it is possible that the transmembrane region of GP-2 contributes to the interaction with SP^{GP-C}. Assuming an N_{exo}/C_{cyt} topology of SP^{GP-C} with only the h2-region spanning the membrane, the h1-region may be the interacting partner of the exoplasmic domain of GP-2. The proposed model of the LCMV GP complex is shown in Figure 4.5. The GP complex consists of the non-covalently associated receptor-binding subunit (GP-1), the transmembrane-containing subunit (GP-2) and SP^{GP-C}. Together, GP-1, GP-2, and SP^{GP-C} form the trimeric GP spikes on the viral membrane.

For the New World Junín arenavirus, the transmembrane and cytoplasmic domains of GP-2 were shown to be sufficient for the association with Junín SP^{GP-C} (Agnihothram et al., 2006). In contrast to the results obtained for the interaction of the LCMV SP^{GP-C} with GP-C, the cytoplasmic region of Junín virus GP-2 was even found to be essential for

SP^{GP-C} binding. Whether this reflects differences between LCMV and Junín virus GPs or different interactions at different stages of intracellular transport remains to be seen.

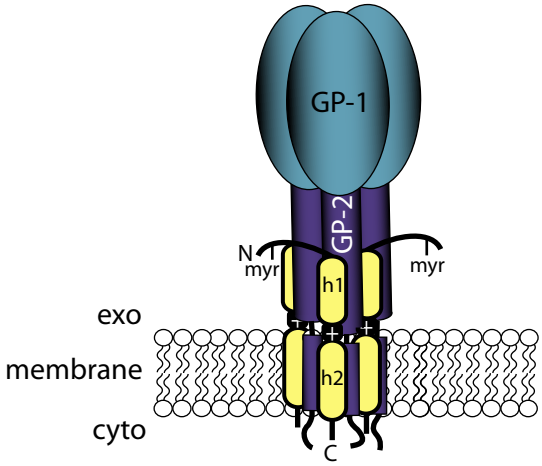

Figure 4.5: Proposed model of the trimeric LCMV GP complex
The trimeric LCMV GP complex is formed by the globular head subunit GP-1, the transmembrane subunit GP-2 and the myristoylated (myr) SP^{GP-C}. Interaction of SP^{GP-C} was observed with GP-2 alone and even with GP-C lacking the transmembrane and cytoplasmic regions. Furthermore, deletion analysis revealed that the SP^{GP-C} h-regions are sufficient and essential for complex formation with the glycoprotein. These findings and the topological consideration in section 4.2, suggest the SP^{GP-C} h1-region and the exoplasmic domain of GP-2 as interacting partners, although an additional interaction between the membrane spanning regions cannot be excluded.

LCMV SP^{GP-C} is an essential component of the GP complex. In absence of SP^{GP-C}, GP-C is neither processed into GP-1 and GP-2 nor expressed on the plasma membrane. The ER retention of LCMV GP-C(WE), containing 12 mutated amino acids, was therefore thought to be due to the inability to associate with SP^{GP-C}. The analysis of pGP-C(WE), however, revealed that the interaction of SP^{GP-C} with GP-C(WE) is not disturbed by the amino acid changes. Hence, the association of SP^{GP-C} with GP-C seems not to be sufficient to promote GP-C transport to the cell surface. Thus, not only the absence of SP^{GP-C} binding but also mutations within GP-C can result in ER retention of GP-C.

As above mentioned, the cytoplasmic domain of LCMV GP-C is dispensable for the interaction with SP^{GP-C}. The deletion of this domain (ΔC), however, was shown to drastically reduce GP-C processing and negatively influence the cell surface expression of GP-C (Figures 3.3 and 3.4). In a previous study, it was shown that the deletion of the last three amino acid residues of the LCMV pGP-C similarly results in a lack of GP-C processing, whereas the cell surface expression was not affected (Kunz et al., 2003). For this to occur, the effects of the C-terminal truncations must be transmitted through the membrane. It is conceivable that truncations in the cytoplasmic domain, for example, affect folding of the extracellular domain of GP-C. A partially misfolded GP-C might not

be processed by SKI-1/S1P but may still get transported to the cell surface as GP-C processing is not a prerequisite for its cell surface expression (Kunz et al., 2003). As misfolding of the glycoprotein might also affect complex formation, the transport of GP-C with the cytoplasmic domain deleted could be impaired by affecting the interaction with SP^{GP-C}. Using digitonin to solubilize the GP complex, however, revealed no obvious difference between the interaction of SP^{GP-C} with GP-C or with GP-C lacking the cytoplasmic domain. In contrast, the co-immunoprecipitation of SP^{GP-C} with the GP-C ΔC mutant was reduced compared to the amounts detected with GP-C in presence of Triton X-100. This reduction suggests a very weak interaction of SP^{GP-C} with GP-C if the cytoplasmic domain is deleted and may thus be the reason for the reduced transport to the cell surface.
The cell surface expression of LCMV GP-C lacking the cytoplasmic domain is still dependent on the presence of the authentic SP^{GP-C} as the substitution with an unrelated signal sequence further decreased the amount of the GPs on the plasma membrane. In contrast, C-terminal truncations in the cytoplasmic domain of the New World Junín arenavirus GP-2 abrogates SP^{GP-C} association yet now permit GP-C processing and transport to the cell surface even in absence of SP^{GP-C} (Agnihothram et al., 2006). Therefore, the Junín SP^{GP-C} is proposed to mask an endogenous ER localization signal within the cytoplasmic domain of GP-2. An SP^{GP-C}-independent transport of LCMV GP-C to the cell surface was only detected for a secretory form of LCMV GP-C, which lacks the cytoplasmic domain and the transmembrane region (ΔTMC). During transport to the cell surface the secretory form was processed into GP-1 and GP-2 even in absence of SP^{GP-C}. Processing of the GP-C ΔTMC mutant indicates correct protein folding of the extracellular domain of GP-C. Although an interaction with SP^{GP-C} is not needed for processing of the secretory form, it was detected when cell lysis was performed with digitonin. This interaction, however, seems to be very weak as it was not detectable in presence of Triton X-100.

4.4 Requirements of SP^{GP-C} for LCMV infection

LCMV infection of target cells is initiated by binding of the GP-1 subunit to its cellular receptor, α-dystroglycan (Cao et al., 1998). After internalization of bound virus into large, smooth-walled, endocytic vesicles, the viral nucleocapsid is delivered into the cell cytoplasm by pH-dependent membrane fusion (Borrow and Oldstone, 1994; Di Simone et al., 1994). At an acidic pH, GP-1 dissociates from GP-2 and upon irreversible conformational rearrangements in GP-2, the hydrophobic N-terminus of GP-2, the putative fusion peptide, gets exposed (Di Simone and Buchmeier, 1995; Di Simone et al., 1994).

To analyze the effects of LCMV SP^{GP-C} mutations on viral infectivity, LCMV pseudoviruses were generated. The pseudovirus system allows easy exchange of the glycoproteins incorporated into the viral membrane by transfection of the appropriate constructs and a quantitative readout of infected cells by measuring the green fluorescence of target cells expressing eGFP (Beyer et al., 2002).
With the exception of the unmyristoylated SP^{GP-C} G2A mutant, all mutants tested (ΔnME, I4N, G2A/I4N, V22T, and A39T) showed a reduction in pseudovirus formation compared to the wt (Figure 4.2). As the mutations are located in the n-region as well as in the h-regions of SP^{GP-C}, this indicates that features of the entire SP^{GP-C} contribute to the efficiency of pseudovirus particle formation. The myristic acid moiety of the SP^{GP-C} (G2A mutant) seems not to be required for particle assembly unlike it is e.g. for the retrovirus matrix protein and the poliovirus capsid protein (Ansardi et al., 1992; Bryant and Ratner, 1990; Chow et al., 1987).
Analysis of pseudovirus infectivity revealed that pseudoviruses produced with one of the two h-region mutants, V22T and A39T, were still able to infect target cells, whereas mutations in the SP^{GP-C} n-region completely inhibit the infection (Figure 4.2). This strongly suggests that the n-region of SP^{GP-C} and, specifically, the myristoylation are crucial for viral infection. The contribution of the LCMV SP^{GP-C} to viral infectivity could be indirect via modulating the conformation of the GP complex or a direct involvement of the SP^{GP-C} in viral entry or fusion. A role for SP^{GP-C} in viral fusion is supported by the finding that the SP^{GP-C} of the New World Junín arenavirus is essential for pH-dependent membrane fusion, which was tested by syncytium formation (York and Nunberg, 2006; York et al., 2004). Furthermore, a recent study of the LCMV SP^{GP-C} showed that the reduced infectivity of virus-like particles (VLPs) produced with a G2A mutant of LCMV pGP-C could be explained by the block of GP-C-mediated cell-cell fusion (Saunders et al., 2007).
Participation of a small myristoylated peptide in membrane fusion is not without precedent. Considering size, topology, myristoylation, and sequence specific effects on viral infectivity, the arenavirus SPs^{GP-C} share striking similarities with the fusion-associated small transmembrane (FAST) proteins. The FAST proteins are encoded by a subgroup of the orthoreoviruses which are nonenveloped viruses that induce cell-cell fusion and syncytium formation (Duncan, 1999; Shmulevitz and Duncan, 2000). The FAST proteins of the reptilian reovirus and the baboon reovirus are small (14 to 15 kDa) integral membrane fusion proteins that expose their N-terminally-myristoylated region to the exoplasmic side of the plasma membrane (Corcoran and Duncan, 2004; Dawe et al., 2005). The myristoylation of the exoplasmic N-terminus of these proteins is essential for the fusion process. The FAST proteins are proposed to mediate cell-cell fusion in cooperation with cellular adhesion proteins that promote close apposition of the cellular membranes (Dawe et al., 2005). In the case of arenavirus membrane fusion, SP^{GP-C} may similarly

cooperate with GP-2 in the fusion process. Clearly, further work is required to elucidate the functional contribution of SP^{GP-C} to viral infection.

4.5 Towards the analysis of LCMV pseudovirus cell entry using fluorescent labeling

Fluorescent labeling of LCMV pseudoviruses would allow to follow the viral particles during cell entry and to identify the compartments to which they localize within the cell using organellar markers. Furthermore, fluorescent LCMV pseudoviruses could be used to elucidate which step of LCMV pseudovirus entry into target cells is blocked by mutations within the SP^{GP-C}. If, for example, membrane fusion is blocked, mutant LCMV pseudoviruses are assumed to accumulate in intracellular vesicles unable to fuse with the host cell membrane. Fluorescently labeled viral particles were previously used to analyze retroviral replication and virus-cell interaction in living cells (Lampe et al., 2007; Muller et al., 2004; Sherer et al., 2003).
In order to follow the LCMV pseudoviruses during cell entry, a MLV Gag-YFP fusion protein was used to fluorescently label the viral capsid (Sherer et al., 2003). The produced labeled LCMV pseudoviruses could be directly visualized by immunofluorescence microscopy and, by using the wt GP-C, were shown to infect target cells (Figures 3.30 and 3.31). Fluorescent particles produced without a viral glycoprotein were not infectious, however, were able to attach to the cells and most likely were endocytosed. Binding of MLV-based particles to the cell surface was previously reported to be independent of the envelope glycoprotein (Pizzato et al., 1999). Viral particles lacking the glycoprotein in the membrane cannot be distinguished from glycoprotein-containing pseudoviruses by fluorescent microscopy, as both contain the YFP-labeled capsid. Therefore, the fluorescent viral particles detected after incubation with the supernatant of HEK 293T cells producing LCMV pseudoviruses might be a mixture of LCMV pseudoviruses containing the glycoprotein and viral particles devoid of the glycoprotein. To use this system for the localization of LCMV pseudoviruses during cell entry, it is, however, necessary to discriminate both types of viral particles. One possibility to directly identify the glycoprotein-containing pseudoviruses would be to fluorescently label the LCMV glycoprotein in addition to the viral capsid, as it was done for the MLV envelope protein (Sherer et al., 2003). Alternatively, the viral particles could be distinguished by using an antibody against the LCMV glycoprotein and a fluorescently labeled secondary antibody. Future work will determine the applicability of fluorescent LCMV pseudoviruses to study cell entry.

Publications derived from this thesis

Freigang, S., Eschli, B., Harris, N., Geuking, M., Quirin, K., Schrempf, S., Zellweger, R., Weber, J., Hengartner, H., Zinkernagel, R. M., Aug 2007. A lymphocytic choriomeningitis virus glycoprotein variant that is retained in the endoplasmic reticulum efficiently cross-primes CD8(+) T cell responses. Proc Natl Acad Sci U S A 104 (33), 13426–13431.

Schrempf, S., Froeschke, M., Giroglou, T., von Laer, D., Dobberstein, B., Nov 2007. Signal peptide requirements for lymphocytic choriomeningitis virus glycoprotein C maturation and virus infectivity. J Virol 81 (22), 12515–12524.

References

Agnihothram, S. S., York, J., Nunberg, J. H., Jun 2006. Role of the stable signal peptide and cytoplasmic domain of G2 in regulating intracellular transport of the Junín virus envelope glycoprotein complex. J Virol 80 (11), 5189–5198.

Agnihothram, S. S., York, J., Trahey, M., Nunberg, J. H., Apr 2007. Bitopic membrane topology of the stable signal peptide in the tripartite Junín virus GP-C envelope glycoprotein complex. J Virol 81 (8), 4331–4337.

Alberts, B., Johnson, A., Lewis, J., Raff, M., Roberts, K., Walter, P., 2002. Molecular Biology of the Cell. Garland Science.

Ansardi, D. C., Porter, D. C., Morrow, C. D., 1992. Myristylation of poliovirus capsid precursor P1 is required for assembly of subviral particles. J Virol 66 (7), 4556–63.

Auperin, D. D., Romanowski, V., Galinski, M., Bishop, D. H., Dec 1984. Sequencing studies of pichinde arenavirus S RNA indicate a novel coding strategy, an ambisense viral S RNA. J Virol 52 (3), 897–904.

Barlowe, C., Orci, L., Yeung, T., Hosobuchi, M., Hamamoto, S., Salama, N., Rexach, M. F., Ravazzola, M., Amherdt, M., Schekman, R., Jun 1994. COPII: a membrane coat formed by Sec proteins that drive vesicle budding from the endoplasmic reticulum. Cell 77 (6), 895–907.

Barresi, R., Campbell, K. P., Jan 2006. Dystroglycan: from biosynthesis to pathogenesis of human disease. J Cell Sci 119 (Pt 2), 199–207.

Beyer, W. R., Miletic, H., Ostertag, W., von Laer, D., 2001. Recombinant expression of lymphocytic choriomeningitis virus strain WE glycoproteins: a single amino acid makes the difference. J Virol 75 (2), 1061–4.

Beyer, W. R., Popplau, D., Garten, W., von Laer, D., Lenz, O., 2003. Endoproteolytic processing of the lymphocytic choriomeningitis virus glycoprotein by the subtilase SKI-1/S1P. J Virol 77 (5), 2866–72.

Beyer, W. R., Westphal, M., Ostertag, W., von Laer, D., 2002. Oncoretrovirus and lentivirus vectors pseudotyped with lymphocytic choriomeningitis virus glycoprotein: generation, concentration, and broad host range. J Virol 76 (3), 1488–95.

Blobel, G., Mar 1980. Intracellular protein topogenesis. Proc Natl Acad Sci U S A 77 (3), 1496–1500.

Blobel, G., Dobberstein, B., Dec 1975. Transfer of proteins across membranes. I. Presence of proteolytically processed and unprocessed nascent immunoglobulin light chains on membrane-bound ribosomes of murine myeloma. J Cell Biol 67 (3), 835–851.

Bonifacino, J. S., Glick, B. S., Jan 2004. The mechanisms of vesicle budding and fusion. Cell 116 (2), 153–166.

Bonifacino, J. S., Lippincott Schwartz, J., May 2003. Coat proteins: shaping membrane transport. Nat Rev Mol Cell Biol 4 (5), 409–414.

Borrow, P., Oldstone, M. B., 1992. Characterization of lymphocytic choriomeningitis virus-binding protein(s): a candidate cellular receptor for the virus. J Virol 66 (12), 7270–81.

Borrow, P., Oldstone, M. B., 1994. Mechanism of lymphocytic choriomeningitis virus entry into cells. Virology 198 (1), 1–9.

Braud, V., Jones, E. Y., McMichael, A., May 1997. The human major histocompatibility complex class Ib molecule HLA-E binds signal sequence-derived peptides with primary anchor residues at positions 2 and 9. Eur J Immunol 27 (5), 1164–1169.

Braud, V. M., Allan, D. S., O'Callaghan, C. A., Söderström, K., D'Andrea, A., Ogg, G. S., Lazetic, S., Young, N. T., Bell, J. I., Phillips, J. H., Lanier, L. L., McMichael, A. J., Feb 1998. HLA-E binds to natural killer cell receptors CD94/NKG2A, B and C. Nature 391 (6669), 795–799.

Brown, D. A., Rose, J. K., Feb 1992. Sorting of GPI-anchored proteins to glycolipid-enriched membrane subdomains during transport to the apical cell surface. Cell 68 (3), 533–544.

Bruns, M., Cihak, J., Muller, G., Lehmann Grube, F., 1983. Lymphocytic choriomeningitis virus. VI. Isolation of a glycoprotein mediating neutralization. Virology 130 (1), 247–51.

Bryant, M., Ratner, L., 1990. Myristoylation-dependent replication and assembly of human immunodeficiency virus 1. Proc Natl Acad Sci U S A 87 (2), 523–7.

Buchmeier, M. J., 2002. Arenaviruses: protein structure and function. Springer, Berlin, Germany, pp. 159–173.

Buchmeier, M. J., Parekh, B. S., 1987. Protein structure and expression among arenaviruses. Curr Top Microbiol Immunol 133, 41–57.

Bullough, P. A., Hughson, F. M., Skehel, J. J., Wiley, D. C., Sep 1994. Structure of influenza haemagglutinin at the pH of membrane fusion. Nature 371 (6492), 37–43.

Burns, J. W., Buchmeier, M. J., 1991. Protein-protein interactions in lymphocytic choriomeningitis virus. Virology 183 (2), 620–9.

Cao, W., Henry, M. D., Borrow, P., Yamada, H., Elder, J. H., Ravkov, E. V., Nichol, S. T., Compans, R. W., Campbell, K. P., Oldstone, M. B., 1998. Identification of alpha-dystroglycan as a receptor for lymphocytic choriomeningitis virus and Lassa fever virus. Science 282 (5396), 2079–81.

Capul, A. A., Perez, M., Burke, E., Kunz, S., Buchmeier, M. J., Juan C de la Torre, Sep 2007. Arenavirus Z-glycoprotein association requires Z myristoylation but not functional RING or late domains. J Virol 81 (17), 9451–9460.

Carr, C. M., Chaudhry, C., Kim, P. S., Dec 1997. Influenza hemagglutinin is spring-loaded by a metastable native conformation. Proc Natl Acad Sci U S A 94 (26), 14306–14313.

Carr, C. M., Kim, P. S., May 1993. A spring-loaded mechanism for the conformational change of influenza hemagglutinin. Cell 73 (4), 823–832.

Chow, M., Newman, J. F., Filman, D., Hogle, J. M., Rowlands, D. J., Brown, F., 1987. Myristylation of picornavirus capsid protein VP4 and its structural significance. Nature 327 (6122), 482–486.

Clegg, J. C. S., 2002. Molecular phylogeny of the arenaviruses. Curr Top Microbiol Immunol 262, 1–24.

Cocquerel, L., Op de Beeck, A., Lambot, M., Roussel, J., Delgrange, D., Pillez, A., Wychowski, C., Penin, F., Dubuisson, J., 2002. Topological changes in the transmembrane domains of hepatitis C virus envelope glycoproteins. Embo J 21 (12), 2893–902.

Colman, P. M., Lawrence, M. C., Apr 2003. The structural biology of type I viral membrane fusion. Nat Rev Mol Cell Biol 4 (4), 309–319.

Compans, R. W., Cooper, M. D., Honjo, T., Koprowski, H., Melchers, F., Oldstone, M. B. A., Olsnes, S., Potter, M., Vogt, P. K., Wagner H., Marsh M., 2004. Membrane Trafficking in Viral Replication. Springer Berlin Heidelberg.

Connolly, T., Gilmore, R., May 1989. The signal recognition particle receptor mediates the GTP-dependent displacement of SRP from the signal sequence of the nascent polypeptide. Cell 57 (4), 599–610.

Cooper, G. M., 2000. The Cell: A Molecular Approach. Sinauer Associates.

Corcoran, J. A., Duncan, R., Apr 2004. Reptilian reovirus utilizes a small type III protein with an external myristylated amino terminus to mediate cell-cell fusion. J Virol 78 (8), 4342–4351.

Crawshaw, S. G., Martoglio, B., Meacock, S. L., High, S., 2004. A misassembled transmembrane domain of a polytopic protein associates with signal peptide peptidase. Biochem J Pt.

Dalbey, R., von Heijne, G. (Eds.), 2003. Protein Targeting, Transport & Translocation. Academic Press.

Dalbey, R. E., von Heijne, G., Nov 1992. Signal peptidases in prokaryotes and eukaryotes–a new protease family. Trends Biochem Sci 17 (11), 474–478.

Dawe, S., Corcoran, J. A., Clancy, E. K., Salsman, J., Duncan, R., May 2005. Unusual topological arrangement of structural motifs in the baboon reovirus fusion-associated small transmembrane protein. J Virol 79 (10), 6216–6226.

de Zarate, I. B. O., Kaelin, K., Rozenberg, F., Feb 2004. Effects of mutations in the cytoplasmic domain of herpes simplex virus type 1 glycoprotein B on intracellular transport and infectivity. J Virol 78 (3), 1540–1551.

Di Simone, C., Buchmeier, M. J., 1995. Kinetics and pH dependence of acid-induced structural changes in the lymphocytic choriomeningitis virus glycoprotein complex. Virology 209 (1), 3–9.

Di Simone, C., Zandonatti, M. A., Buchmeier, M. J., 1994. Acidic pH triggers LCMV membrane fusion activity and conformational change in the glycoprotein spike. Virology 198 (2), 455–65.

Doms, R. W., Lamb, R. A., Rose, J. K., Helenius, A., Apr 1993. Folding and assembly of viral membrane proteins. Virology 193 (2), 545–562.

Dultz, E., Hildenbeutel, M., Martoglio, B., Hochman, J., Dobberstein, B., Kapp, K., Feb 2008. The signal peptide of the mouse mammary tumor virus rem protein is released from the ER membrane and accumulates in nucleoli. J Biol Chem.

Duncan, R., Aug 1999. Extensive sequence divergence and phylogenetic relationships between the fusogenic and nonfusogenic orthoreoviruses: a species proposal. Virology 260 (2), 316–328.

Earp, L. J., Delos, S. E., Park, H. E., White, J. M., 2005. The many mechanisms of viral membrane fusion proteins. Curr Top Microbiol Immunol 285, 25–66.

Eckert, D. M., Kim, P. S., 2001. Mechanisms of viral membrane fusion and its inhibition. Annu Rev Biochem 70, 777–810.

Edwards, T. G., Wyss, S., Reeves, J. D., Zolla Pazner, S., Hoxie, J. A., Doms, R. W., Baribaud, F., 2002. Truncation of the cytoplasmic domain induces exposure of conserved regions in the ectodomain of human immunodeficiency virus type 1 envelope protein. J Virol 76 (6), 2683–91.

Eichler, R., Lenz, O., Strecker, T., Eickmann, M., Klenk, H. D., Garten, W., Oct. 2003a. Identification of Lassa virus glycoprotein signal peptide as a trans-acting maturation factor. EMBO Rep 4 (11), 1084–8.

Eichler, R., Lenz, O., Strecker, T., Eickmann, M., Klenk, H. D., Garten, W., 2004. Lassa virus glycoprotein signal peptide displays a novel topology with an extended endoplasmic reticulum luminal region. J Biol Chem 279 (13), 12293–9.

Eichler, R., Lenz, O., Strecker, T., Garten, W., Feb. 2003b. Signal peptide of Lassa virus glycoprotein GP-C exhibits an unusual length. FEBS Lett 538 (1-3), 203–6.

Ellgaard, L., Helenius, A., Mar 2003. Quality control in the endoplasmic reticulum. Nat Rev Mol Cell Biol 4 (3), 181–191.

Epand, R. M., Jul 2003. Fusion peptides and the mechanism of viral fusion. Biochim Biophys Acta 1614 (1), 116–121.

Eschli, B., Quirin, K., Wepf, A., Weber, J., Zinkernagel, R., Hans Hengartner, Jun 2006. Identification of an N-terminal trimeric coiled-coil core within arenavirus glycoprotein 2 permits assignment to class I viral fusion proteins. J Virol 80 (12), 5897–5907.

Fenteany, G., Schreiber, S. L., Apr 1998. Lactacystin, proteasome function, and cell fate. J Biol Chem 273 (15), 8545–8548.

Froeschke, M., Basler, M., Groettrup, M., Dobberstein, B., 2003. Long-lived signal peptide of lymphocytic choriomeningitis virus glycoprotein pGP-C. J Biol Chem 278 (43), 41914–20.

Gallaher, W. R., DiSimone, C., Buchmeier, M. J., 2001. The viral transmembrane superfamily: possible divergence of Arenavirus and Filovirus glycoproteins from a common RNA virus ancestor. BMC Microbiol 1 (1), 1.

Garoff, H., Hewson, R., Opstelten, D. J., Dec 1998. Virus maturation by budding. Microbiol Mol Biol Rev 62 (4), 1171–1190.

Gierasch, L. M., Feb 1989. Signal sequences. Biochemistry 28 (3), 923–930.

Gilmore, R., Blobel, G., Walter, P., Nov 1982. Protein translocation across the endoplasmic reticulum. I. Detection in the microsomal membrane of a receptor for the signal recognition particle. J Cell Biol 95 (2 Pt 1), 463–469.

Glushakova, S. E., Lukashevich, I. S., Baratova, L. A., 1990. Prediction of arenavirus fusion peptides on the basis of computer analysis of envelope protein sequences. FEBS Lett 269 (1), 145–7.

Goder, V., Junne, T., Spiess, M., 2004. Sec61p contributes to signal sequence orientation according to the positive-inside rule. Mol Biol Cell 15 (3), 1470–8.

Gripon, P., Le Seyec, J., Rumin, S., Guguen Guillouzo, C., 1995. Myristylation of the hepatitis B virus large surface protein is essential for viral infectivity. Virology 213 (2), 292–9.

Görlich, D., Kutay, U., 1999. Transport between the cell nucleus and the cytoplasm. Annu Rev Cell Dev Biol 15, 607–660.

Harrison, S. C., 2005. Mechanism of membrane fusion by viral envelope proteins. Adv Virus Res 64, 231–261.

Hegde, R. S., Bernstein, H. D., Oct 2006. The surprising complexity of signal sequences. Trends Biochem Sci 31 (10), 563–571.

High, S., Dobberstein, B., Aug 1992. Mechanisms that determine the transmembrane disposition of proteins. Curr Opin Cell Biol 4 (4), 581–586.

Higy, M., Junne, T., Spiess, M., 2004. Topogenesis of membrane proteins at the endoplasmic reticulum. Biochemistry 43 (40), 12716–22.

Hoch Marchaim, H., Weiss, A. M., Bar Sinai, A., Fromer, M., Adermann, K., Hochman, J., 2003. The leader peptide of MMTV Env precursor localizes to the nucleoli in MMTV-derived T cell lymphomas and interacts with nucleolar protein B23. Virology 313 (1), 22–32.

Hurtley, S. M., Helenius, A., 1989. Protein oligomerization in the endoplasmic reticulum. Annu Rev Cell Biol 5, 277–307.

Iapalucci, S., López, N., Rey, O., Zakin, M. M., Cohen, G. N., Franze Fernández, M. T., Nov 1989. The 5' region of Tacaribe virus L RNA encodes a protein with a potential metal binding domain. Virology 173 (1), 357–361.

Jahn, R., Lang, T., Südhof, T. C., Feb 2003. Membrane fusion. Cell 112 (4), 519–533.

Johnson, A. E., van Waes, M. A., 1999. The translocon: a dynamic gateway at the ER membrane. Annu Rev Cell Dev Biol 15, 799–842.

Kalderon, D., Roberts, B. L., Richardson, W. D., Smith, A. E., Dec 1984. A short amino acid sequence able to specify nuclear location. Cell 39 (3 Pt 2), 499–509.

Keenan, R. J., Freymann, D. M., Stroud, R. M., Walter, P., 2001. The signal recognition particle. Annu Rev Biochem 70, 755–75.

Keller, P., Simons, K., Dec 1997. Post-Golgi biosynthetic trafficking. J Cell Sci 110 (Pt 24), 3001–3009.

Kido, H., Niwa, Y., Beppu, Y., Towatari, T., 1996. Cellular proteases involved in the pathogenicity of enveloped animal viruses, human immunodeficiency virus, influenza virus A and Sendai virus. Adv Enzyme Regul 36, 325–347.

Kielian, M., Jan 2006. Class II virus membrane fusion proteins. Virology 344 (1), 38–47.

Kielian, M., Rey, F. A., Jan 2006. Virus membrane-fusion proteins: more than one way to make a hairpin. Nat Rev Microbiol 4 (1), 67–76.

Kim, S. J., Hegde, R. S., Nov 2002. Cotranslational partitioning of nascent prion protein into multiple populations at the translocation channel. Mol Biol Cell 13 (11), 3775–3786.

Kirchhausen, T., Dec 2000. Three ways to make a vesicle. Nat Rev Mol Cell Biol 1 (3), 187–198.

Klein, K. C., Reed, J. C., Lingappa, J. R., 2007. Intracellular destinies: degradation, targeting, assembly, and endocytosis of HIV Gag. AIDS Rev 9 (3), 150–161.

Knipe, D. M., Howley, P. M. (Eds.), 2001. Fields Virology, 4th Edition. Lippincott Williams & Wilkins.

Krzyzaniak, M., Mach, M., Britt, W. J., Oct 2007. The cytoplasmic tail of glycoprotein M (gpUL100) expresses trafficking signals required for human cytomegalovirus assembly and replication. J Virol 81 (19), 10316–10328.

Kunz, S., Edelmann, K. H., de la Torre, J. C., Gorney, R., Oldstone, M. B., 2003. Mechanisms for lymphocytic choriomeningitis virus glycoprotein cleavage, transport, and incorporation into virions. Virology 314 (1), 168–78.

Lambert, C., Prange, R., 2001. Dual topology of the hepatitis B virus large envelope protein: determinants influencing post-translational pre-S translocation. J Biol Chem 276 (25), 22265–72.

Lampe, M., Briggs, J. A. G., Endress, T., Glass, B., Riegelsberger, S., Kräusslich, H. G., Lamb, D. C., Bräuchle, C., Müller, B., Mar 2007. Double-labelled HIV-1 particles for study of virus-cell interaction. Virology 360 (1), 92–104.

Lanford, R. E., Butel, J. S., Jul 1984. Construction and characterization of an SV40 mutant defective in nuclear transport of T antigen. Cell 37 (3), 801–813.

Lee, K. J., Perez, M., Pinschewer, D. D., de la Torre, J. C., 2002. Identification of the lymphocytic choriomeningitis virus (LCMV) proteins required to rescue LCMV RNA analogs into LCMV-like particles. J Virol 76 (12), 6393–7.

Lemberg, M. K., Bland, F. A., Weihofen, A., Braud, V. M., Martoglio, B., 2001. Intramembrane proteolysis of signal peptides: an essential step in the generation of HLA-E epitopes. J Immunol 167 (11), 6441–6.

Lemberg, M. K., Martoglio, B., 2002. Requirements for signal peptide peptidase-catalyzed intramembrane proteolysis. Mol Cell 10 (4), 735–44.

Lenz, O., ter Meulen, J., Klenk, H. D., Seidah, N. G., Garten, W., 2001. The Lassa virus glycoprotein precursor GP-C is proteolytically processed by subtilase SKI-1/S1P. Proc Natl Acad Sci U S A 98 (22), 12701–5.

Letourneur, F., Gaynor, E. C., Hennecke, S., Démollière, C., Duden, R., Emr, S. D., Riezman, H., Cosson, P., Dec 1994. Coatomer is essential for retrieval of dilysine-tagged proteins to the endoplasmic reticulum. Cell 79 (7), 1199–1207.

Lindemann, D., Pietschmann, T., Picard Maureau, M., Berg, A., Heinkelein, M., Thurow, J., Knaus, P., Zentgraf, H., Rethwilm, A., 2001. A particle-associated glycoprotein signal peptide essential for virus maturation and infectivity. J Virol 75 (13), 5762–71.

Loureiro, J., Lilley, B. N., Spooner, E., Noriega, V., Tortorella, D., Ploegh, H. L., Jun 2006. Signal peptide peptidase is required for dislocation from the endoplasmic reticulum. Nature 441 (7095), 894–897.

Luirink, J., Sinning, I., Nov 2004. SRP-mediated protein targeting: structure and function revisited. Biochim Biophys Acta 1694 (1-3), 17–35.

Lyko, F., Martoglio, B., Jungnickel, B., Rapoport, T. A., Dobberstein, B., 1995. Signal sequence processing in rough microsomes. J Biol Chem 270 (34), 19873–8.

Lyman, S. K., Schekman, R., Jan 1997. Binding of secretory precursor polypeptides to a translocon subcomplex is regulated by BiP. Cell 88 (1), 85–96.

Marsh, M., Helenius, A., Feb 2006. Virus entry: open sesame. Cell 124 (4), 729–740.

Martoglio, B., 2003. Intramembrane proteolysis and post-targeting functions of signal peptides. Biochem Soc Trans 31 (Pt 6), 1243–7.

Martoglio, B., Dobberstein, B., 1995. Protein insertion into the membrane of the endoplasmic reticulum: the architecture of the translocation site. Cold Spring Harb Symp Quant Biol 60, 41–5.

Martoglio, B., Dobberstein, B., 1998. Signal sequences: more than just greasy peptides. Trends Cell Biol 8 (10), 410–5.

Martoglio, B., Graf, R., Dobberstein, B., 1997. Signal peptide fragments of preprolactin and HIV-1 p-gp160 interact with calmodulin. Embo J 16 (22), 6636–45.

Martoglio, B., Hofmann, M. W., Brunner, J., Dobberstein, B., 1995. The protein-conducting channel in the membrane of the endoplasmic reticulum is open laterally toward the lipid bilayer. Cell 81 (2), 207–14.

Matlack, K. E., Misselwitz, B., Plath, K., Rapoport, T. A., May 1999. BiP acts as a molecular ratchet during posttranslational transport of prepro-alpha factor across the ER membrane. Cell 97 (5), 553–564.

Matsuura Tokita, K., Takeuchi, M., Ichihara, A., Mikuriya, K., Nakano, A., Jun 2006. Live imaging of yeast Golgi cisternal maturation. Nature 441 (7096), 1007–1010.

McLauchlan, J., Lemberg, M. K., Hope, G., Martoglio, B., 2002. Intramembrane proteolysis promotes trafficking of hepatitis C virus core protein to lipid droplets. Embo J 21 (15), 3980–8.

Mertz, J. A., Simper, M. S., Lozano, M. M., Payne, S. M., Jaquelin P Dudley, Dec 2005. Mouse mammary tumor virus encodes a self-regulatory RNA export protein and is a complex retrovirus. J Virol 79 (23), 14737–14747.

Meyer, D. I., Dobberstein, B., Nov 1980. Identification and characterization of a membrane component essential for the translocation of nascent proteins across the membrane of the endoplasmic reticulum. J Cell Biol 87 (2 Pt 1), 503–508.

Meyer, H. A., Grau, H., Kraft, R., Kostka, S., Prehn, S., Kalies, K. U., Hartmann, E., May 2000. Mammalian Sec61 is associated with Sec62 and Sec63. J Biol Chem 275 (19), 14550–14557.

Michelsen, K., Yuan, H., Schwappach, B., 2005. Hide and run. EMBO Rep 6 (8), 717–22.

Muller, B., Daecke, J., Fackler, O. T., Dittmar, M. T., Zentgraf, H., Krausslich, H. G., 2004. Construction and characterization of a fluorescently labeled infectious human immunodeficiency virus type 1 derivative. J Virol 78 (19), 10803–13.

Neuman, B. W., Adair, B. D., Burns, J. W., Milligan, R. A., Buchmeier, M. J., Yeager, M., Mar 2005. Complementarity in the supramolecular design of arenaviruses and retroviruses revealed by electron cryomicroscopy and image analysis. J Virol 79 (6), 3822–3830.

Nieva, J. L., Agirre, A., Jul 2003. Are fusion peptides a good model to study viral cell fusion? Biochim Biophys Acta 1614 (1), 104–115.

Nilsson, I., von Heijne, G., Jun 2000. Glycosylation efficiency of Asn-Xaa-Thr sequons depends both on the distance from the C terminus and on the presence of a downstream transmembrane segment. J Biol Chem 275 (23), 17338–17343.

Nilsson, T., Warren, G., Aug 1994. Retention and retrieval in the endoplasmic reticulum and the Golgi apparatus. Curr Opin Cell Biol 6 (4), 517–521.

Ostapchuk, P., Hearing, P., Ganem, D., 1994. A dramatic shift in the transmembrane topology of a viral envelope glycoprotein accompanies hepatitis B viral morphogenesis. Embo J 13 (5), 1048–57.

Ott, C. M., Akhavan, A., Lingappa, V. R., Apr 2007. Specific features of the prion protein transmembrane domain regulate nascent chain orientation. J Biol Chem 282 (15), 11163–11171.

Paetzel, M., Karla, A., Strynadka, N. C., Dalbey, R. E., 2002. Signal peptidases. Chem Rev 102 (12), 4549–80.

Pelham, H. R., Dec 2001. Traffic through the Golgi apparatus. J Cell Biol 155 (7), 1099–1101.

Perez, M., Craven, R. C., de la Torre, J. C., 2003. The small RING finger protein Z drives arenavirus budding: implications for antiviral strategies. Proc Natl Acad Sci U S A 100 (22), 12978–83.

Perez, M., Greenwald, D. L., De La Torre, J. C., 2004. Myristoylation of the RING Finger Z Protein Is Essential for Arenavirus Budding. J Virol 78 (20), 11443–8.

Pizzato, M., Marlow, S. A., Blair, E. D., Takeuchi, Y., Oct 1999. Initial binding of murine leukemia virus particles to cells does not require specific Env-receptor interaction. J Virol 73 (10), 8599–8611.

Pool, M. R., Dec 2003. Getting to the membrane: how is co-translational protein targeting to the endoplasmic reticulum regulated? Biochem Soc Trans 31 (Pt 6), 1232–1237.

Pool, M. R., Stumm, J., Fulga, T. A., Sinning, I., Dobberstein, B., Aug 2002. Distinct modes of signal recognition particle interaction with the ribosome. Science 297 (5585), 1345–1348.

Rapoport, T. A., Nov 2007. Protein translocation across the eukaryotic endoplasmic reticulum and bacterial plasma membranes. Nature 450 (7170), 663–669.

Rapoport, T. A., Goder, V., Heinrich, S. U., Matlack, K. E., 2004. Membrane-protein integration and the role of the translocation channel. Trends Cell Biol 14 (10), 568–75.

Rapoport, T. A., Matlack, K. E., Plath, K., Misselwitz, B., Staeck, O., Oct 1999. Post-translational protein translocation across the membrane of the endoplasmic reticulum. Biol Chem 380 (10), 1143–1150.

Resh, M. D., 1999. Fatty acylation of proteins: new insights into membrane targeting of myristoylated and palmitoylated proteins. Biochim Biophys Acta 1451 (1), 1–16.

Resh, M. D., 2005. Intracellular trafficking of HIV-1 Gag: how Gag interacts with cell membranes and makes viral particles. AIDS Rev 7 (2), 84–91.

Robinson, M. S., Mar 1987. Coated vesicles and protein sorting. J Cell Sci 87 (Pt 2), 203–204.

Rojek, J. M., Kunz, S., Jan 2008. Cell entry by human pathogenic arenaviruses. Cell Microbiol.

Rojek, J. M., Perez, M., Kunz, S., Feb 2008. Cellular entry of lymphocytic choriomeningitis virus. J Virol 82 (3), 1505–1517.

Romanowski, V., Matsuura, Y., Bishop, D. H., 1985. Complete sequence of the S RNA of lymphocytic choriomeningitis virus (WE strain) compared to that of Pichinde arenavirus. Virus Res 3 (2), 101–14.

Salvato, M., Shimomaye, E., Oldstone, M. B., Apr 1989. The primary structure of the lymphocytic choriomeningitis virus L gene encodes a putative RNA polymerase. Virology 169 (2), 377–384.

Sanders, S. L., Whitfield, K. M., Vogel, J. P., Rose, M. D., Schekman, R. W., Apr 1992. Sec61p and BiP directly facilitate polypeptide translocation into the ER. Cell 69 (2), 353–365.

Saunders, A. A., Ting, J. P. C., Meisner, J., Neuman, B. W., Perez, M., de la Torre, J. C., Buchmeier, M. J., Jun 2007. Mapping the landscape of the lymphocytic choriomeningitis virus stable signal peptide reveals novel functional domains. J Virol 81 (11), 5649–5657.

Schatz, G., Dobberstein, B., Mar 1996. Common principles of protein translocation across membranes. Science 271 (5255), 1519–1526.

Schrempf, S., Froeschke, M., Giroglou, T., von Laer, D., Dobberstein, B., Nov 2007. Signal peptide requirements for lymphocytic choriomeningitis virus glycoprotein C maturation and virus infectivity. J Virol 81 (22), 12515–12524.

Shah, W. A., Peng, H., Carbonetto, S., 2006. Role of non-raft cholesterol in lymphocytic choriomeningitis virus infection via alpha-dystroglycan. J Gen Virol 87 (Pt 3), 673–8.

Sherer, N. M., Lehmann, M. J., Jimenez Soto, L. F., Ingmundson, A., Horner, S. M., Cicchetti, G., Allen, P. G., Pypaert, M., Cunningham, J. M., Mothes, W., 2003. Visualization of retroviral replication in living cells reveals budding into multivesicular bodies. Traffic 4 (11), 785–801.

Shmulevitz, M., Duncan, R., Mar 2000. A new class of fusion-associated small transmembrane (FAST) proteins encoded by the non-enveloped fusogenic reoviruses. EMBO J 19 (5), 902–912.

Silberstein, S., Gilmore, R., Jun 1996. Biochemistry, molecular biology, and genetics of the oligosaccharyltransferase. FASEB J 10 (8), 849–858.

Sipos, L., von Heijne, G., May 1993. Predicting the topology of eukaryotic membrane proteins. Eur J Biochem 213 (3), 1333–1340.

Söllner, T. H., Aug 2004. Intracellular and viral membrane fusion: a uniting mechanism. Curr Opin Cell Biol 16 (4), 429–435.

Southern, P. J., Singh, M. K., Riviere, Y., Jacoby, D. R., Buchmeier, M. J., Oldstone, M. B., Mar 1987. Molecular characterization of the genomic S RNA segment from lymphocytic choriomeningitis virus. Virology 157 (1), 145–155.

Stiasny, K., Allison, S. L., Mandl, C. W., Heinz, F. X., Aug 2001. Role of metastability and acidic pH in membrane fusion by tick-borne encephalitis virus. J Virol 75 (16), 7392–7398.

Tajima, S., Lauffer, L., Rath, V. L., Walter, P., Oct 1986. The signal recognition particle receptor is a complex that contains two distinct polypeptide chains. J Cell Biol 103 (4), 1167–1178.

Tamm, L. K., Han, X., Dec 2000. Viral fusion peptides: a tool set to disrupt and connect biological membranes. Biosci Rep 20 (6), 501–518.

Teasdale, R. D., Jackson, M. R., 1996. Signal-mediated sorting of membrane proteins between the endoplasmic reticulum and the golgi apparatus. Annu Rev Cell Dev Biol 12, 27–54.

Terzi, L., Pool, M. R., Dobberstein, B., Strub, K., Jan 2004. Signal recognition particle Alu domain occupies a defined site at the ribosomal subunit interface upon signal sequence recognition. Biochemistry 43 (1), 107–117.

Urban, S., Gripon, P., 2002. Inhibition of duck hepatitis B virus infection by a myristoylated pre-S peptide of the large viral surface protein. J Virol 76 (4), 1986–90.

Utsumi, T., Ohta, H., Kayano, Y., Sakurai, N., Ozoe, Y., 2005. The N-terminus of B96Bom, a Bombyx mori G-protein-coupled receptor, is N-myristoylated and translocated across the membrane. Febs J 272 (2), 472–81.

Verner, K., Schatz, G., Sep 1988. Protein translocation across membranes. Science 241 (4871), 1307–1313.

von Heijne, G., Jun 1983. Patterns of amino acids near signal-sequence cleavage sites. Eur J Biochem 133 (1), 17–21.

von Heijne, G., 1985. Signal sequences. The limits of variation. J Mol Biol 184 (1), 99–105.

von Heijne, G., Oct 1989. Control of topology and mode of assembly of a polytopic membrane protein by positively charged residues. Nature 341 (6241), 456–458.

von Heijne, G., Aug 1990. Protein targeting signals. Curr Opin Cell Biol 2 (4), 604–608.

Walter, P., Blobel, G., Nov 1981. Translocation of proteins across the endoplasmic reticulum III. Signal recognition protein (SRP) causes signal sequence-dependent and site-specific arrest of chain elongation that is released by microsomal membranes. J Cell Biol 91 (2 Pt 1), 557–561.

Walter, P., Blobel, G., Oct 1982. Signal recognition particle contains a 7S RNA essential for protein translocation across the endoplasmic reticulum. Nature 299 (5885), 691–698.

Walter, P., Gilmore, R., Blobel, G., Aug 1984. Protein translocation across the endoplasmic reticulum. Cell 38 (1), 5–8.

Walter, P., Johnson, A. E., 1994. Signal sequence recognition and protein targeting to the endoplasmic reticulum membrane. Annu Rev Cell Biol 10, 87–119.

Weihofen, A., Binns, K., Lemberg, M. K., Ashman, K., Martoglio, B., 2002. Identification of signal peptide peptidase, a presenilin-type aspartic protease. Science 296 (5576), 2215–8.

Weihofen, A., Martoglio, B., 2003. Intramembrane-cleaving proteases: controlled liberation of proteins and bioactive peptides. Trends Cell Biol 13 (2), 71–8.

Wilk, T., Geiselhart, V., Frech, M., Fuller, S. D., Flugel, R. M., Lochelt, M., 2001. Specific interaction of a novel foamy virus Env leader protein with the N-terminal Gag domain. J Virol 75 (17), 7995–8007.

Wright, K. E., Spiro, R. C., Burns, J. W., Buchmeier, M. J., 1990. Post-translational processing of the glycoproteins of lymphocytic choriomeningitis virus. Virology 177 (1), 175–83.

Yee, J. K., Miyanohara, A., LaPorte, P., Bouic, K., Burns, J. C., Friedmann, T., 1994. A general method for the generation of high-titer, pantropic retroviral vectors: highly efficient infection of primary hepatocytes. Proc Natl Acad Sci U S A 91 (20), 9564–8, department of Pediatrics, University of California, San Diego, La Jolla 92093.

York, J., Nunberg, J. H., 2006. Role of the Stable Signal Peptide of Junin Arenavirus Envelope Glycoprotein in pH-Dependent Membrane Fusion. J Virol 80 (15), 7775–80.

York, J., Romanowski, V., Lu, M., Nunberg, J. H., 2004. The signal peptide of the Junin arenavirus envelope glycoprotein is myristoylated and forms an essential subunit of the mature G1-G2 complex. J Virol 78 (19), 10783–92.

List of Figures

List of Abbreviations

aa	amino acid
Ala	alanine (A)
APS	ammonium persulfate
Arg	arginine (R)
Asn	asparagine (N)
Asp	aspartic acid (D)
ATP	adenosine triphosphate
bp	base pair
CIP	calf intestine phosphatase
cryo-EM	electron cryomicroscopy
COP	coat protein
Co-IP	co-immunoprecipitation
CTP	cytosine triphosphate
Cys	cysteine (C)
DAPI	4′,6′-diamidino-2-phenylindole
DMEM	Dulbecco's Modified Eagle's Medium
DMSO	dimethylsulphoxide
DNA	deoxyribonucleic acid
dNTP	deoxyribonucleotide triphosphate (dATP, dCTP, dGTP, dTTP)
DTT	dithiothreitol
E.coli	*Escherichia coli*
EDTA	ethylenediaminetetraacetic acid
eGFP	enhanced green fluorescent protein
Endo H	Endoglycosidase H
ER	endoplasmic reticulum
FACS	fluorescence-activated cell sorter
FAST	fusion-associated small transmembrane (FAST) proteins
FCS	fetal calf serum
Gag	group specific antigen
GFP	green fluorescent protein
Gln	glutamine (Q)
Glu	glutamic acid (E)
Gly	glycine (G)
GP	glycoprotein
GTP	guanosine triphosphate

HA	hemagglutinin
HBV	hepatitis B virus
HCV	hepatitis C virus
HeBS	HEPES buffered saline
HEPES	4-(2-Hydroxyethyl)piperazine-1-ethanesulfonic acid
His	histidine (H)
HIV	human immunodeficiency virus
HLA	human lymphocyte antigen
HRPO	horseradish peroxidase
I-Clip	intramembrane cleaving protease
IgG	immunoglobulin G
IGR	intergenic region
Ile	isoleucine (I)
IP	immunoprecipitation
kDa	kilodalton
LB	Luria-Bertani
LCMV	lymphocytic choriomeningitis virus
Leu	leucine (L)
Lys	lysine (K)
Met	methionine (M)
MHC	major histocompatibility complex
MLV	murine leukemia virus
MMTV	mouse mammary tumor virus
ODG	Octyl-β-D-glucopyranoside
PAGE	polyacrylamide gel electrophoresis
PBS	phosphate buffered saline
PCR	polymerase chain reaction
PE	phycoerythrin
pGP	precursor glycoprotein
Phe	phenylalanine (F)
PMSF	phenylmethanesulphonylfluoride
PNGase F	peptide-N-glycosidase F
Pro	proline (P)
Pol	polymerase
RIPA buffer	Radio-Immunoprecipitation Assay buffer
RNA	ribonucleic acid
RNP	ribonucleoprotein
RT	room temperature
SDS	sodium dodecyl sulfate

Ser	serine (S)
SKI1/S1P	subtilisin-kexin isoenzyme 1/site 1 protease
SP	signal peptide
SPase	signal peptidase
SPP	signal peptide peptidase
SR	SRP receptor
SRP	signal recognition particle
TAE	Tris-acetate/EDTA
TAP	transporter associated with antigen presentation
TBS	Tris buffered saline
TEMED	Tetramethylethylendiamin
Thr	threonine (T)
TM	transmembrane
Tris	Trishydroxymethylaminomethan
Trp	tryptophane (W)
TTP	thymidine triphosphate
Tyr	tyrosine (Y)
UTR	untranslated region
Val	valine (V)
VLP	virus-like particle
VSV	vesicular stomatitis virus
VSV-G	VSV glycoprotein
wt	wild type
YFP	yellow fluorescent protein

Danksagung

Ich danke all denen, die mir mit Rat und Tat zur Seite standen und somit zum Gelingen dieser Arbeit beigetragen haben.

Allen voran geht mein Dank an Prof. Dr. Bernhard Dobberstein für die Bereitstellung des Themas und die gute wissenschaftliche Betreuung meiner Arbeit. Er hat mich stets unterstützt und war immer bereit auf Fragen und Probleme einzugehen.

Prof. Dr. Irmgard Sinning danke ich für die Bereitschaft, meine Arbeit zu bewerten und sie als Zweitgutachter vor der Fakultät zu vertreten.

Prof. Dr. med. Dorothee von Laer und Dr. Tsanan Giroglou vom Georg-Speyer-Haus in Frankfurt a.M. möchte ich für die gute Zusammenarbeit und die Analyse der LCMV Pseudoviren danken.

Des Weiteren gilt mein Dank all meinen Kollegen in den Arbeitsgruppen Dobberstein und Seedorf für das angenehme und nie langweilig werdende Arbeitsklima, für die vielen wertvollen Diskussionen und Ratschläge und für all die großen und kleinen Hilfestellungen.